Master Thesis, Department of Geosciences

A shallow marine storm-dominated shelf: Sælabonn Formation, Oslo Region (Lower Silurian)

The transition from an epicontinental sea to the Caledonian foreland basin in the Oslo Region.

Andreas Garten

UiO **:** Natural History Museum

UNIVERSITY OF OSLO
FACULTY OF MATHEMATICS AND NATURAL SCIENCES

A shallow marine storm-dominated shelf: Sælabonn Formation, Oslo Region (Lower Silurian)

The transition from an epicontinental sea to the Caledonian foreland basin in the Oslo Region.

Andreas Garten

Master Thesis in Geosciences

Discipline: Geology

Department of Geosciences

Faculty of Mathematics and Natural Sciences

University of Oslo

October 9th, 2012

© Andreas Garten, 2012

Tutors: Professor Hans Arne Nakrem (UiO), Professor emeritus Johan Petter Nystuen (UiO) and Bjørn Tore Larsen (Det norske oljeselskap ASA)

This work is published digitally through DUO – Digitale Utgivelser ved UiO

http://www.duo.uio.no

It is also catalogued in BIBSYS (http://www.bibsys.no/english)

Abstract

The Sælabonn Formation belongs to the Bærum Group, and is recognized in the western part of the Oslo Region, from Mjøsa in the north to Skien in the south. The Sælabonn Formation is the lowermost unit in the Silurian succession in the Western Districts of the Oslo Region bound to an erosional surface, the Ordovician-Silurian boundary. In the Central Oslo Region the Solvik Formation is the eastern equivalent, displaying deeper marine conditions. Overlying the Sælabonn and Solvik formations is the carbonate dominated Rytteråker Formation. The Sælabonn Formation represents a shallow shelf environment dominated by storm processes. The relationship between the epicontinental sea and the advancement of the Caledonian orogeny, during the time of deposition, has previously been vaguely defined.

Outcrops in the Ringerike District and the Modum District have been logged during the summer and autumn of 2011. Samples of both siliciclastic and carbonate material have been collected, and various laboratory and microscope techniques, including point counting analyses have been performed.

The sedimentary logs display three units of the Sælabonn Formation. The laterally equivalent lower units, Store Svartøya Member and Sylling Member, are dominated by mudstone occasionally interbedded by sandstone and biosparitic limestone beds. The middle unit (Djupvarp Member) is the sandiest, and represents isolated sand shoals in the Ringerike District, and tempestites in the Modum District. The upper unit (Limovnstangen Member) has a decreasing content of siliciclastic material with mudstones interbedded with tempestites containing sand and bioclastic material, occasionally occurring in couplets. The sedimentary structures and lithology indicate a sedimentary environment dominated by storm processes where siliciclastic material is brought out into the basin and deposited together with winnowed bioclastic material. Results from tidal processes have not been recorded. The members belonging to the Sælabonn Formation are all positioned in the offshore-transitional environment on the shelf. Palaeocurrent measurements from the Djupvarp and Limovnstangen members suggest a stable palaeoshoreline, with a SW to NE strike.

Grain size of the tempestites range from silt to very fine sand. Mineralogical composition suggests a quartz rich source, "Telemark land" or possibly Valdres Thrust Sheet. The development of the Sælabonn Formation represents an overall transgressive setting, where the Djupvarp Member represents a progradation. In the developing Caledonian foreland basin, the Sælabonn Formation is suggested to have been formed in the back-bulge depozone.

II

Acknowledgements

Contents

VI

1 Introduction

The Sælabonn Formation is a lithostratigraphic unit dominated by siliciclastic material composed of mudstone and fine sand. It is the lowermost formation in the Silurian succession in the western districts of the Oslo Region (Fig. 2.1) belonging to the Bærum Group. The purpose of this study is to get a more complete understanding of the transition from an epicontinental sea to a foreland basin and the sedimentological development of the Sælabonn Formation. Questions surrounding this formation are the position of deposition in relation to the advancing Caledonian orogeny in the north-west, the epicontinental shelf to the south-east, and the source of the siliciclastic input.

The Sælabonn Formation is the western equivalent to the Solvik Formation, which has its distribution in the Oslo and Asker districts. The Solvik Formation displays a more distal position than the Sælabonn Formation. The stable epicontinental shelf was dominated by deposits of mudstone during the Cambrian and Ordovician, with increased carbonate content during the Ordovician. Through the Silurian several rapid shifts in deposition occurred. Fine siliciclastic sediments were introduced which then shifted to a dominance of carbonate sediments and then back again to siliciclastic sediments. The Silurian succession ends with the fluvial sediments of the Ringerike Group, and is a clear indicator of a palaeoenvironment situated in the foreland basin.

There has been done some previous work on other clastic input in the Oslo Region such as the Bruflat Formation (Worsley et al., 2011), the Vik Formation (Baarli, 1990a) and the Ringerike Group (e.g. Halvorsen, 2003, Davies et al., 2005a), in which the palaeogeographic position of the basin sands and a regional development have been proposed in relation to the Caledonian foreland basin.

Data for this work has been collected from the Ringerike District and the Modum District, and has been processed at the Natural History Museum (Geology) in Oslo.

2 Previous work at Ringerike

2.1 The Oslo Region – an historical introduction

Theodor Kjerulf (1825-1888) is, for most geologists, known as the founder of modern geology in Norway, as he was the first to publish relevant work about the Oslo Region (Larsen and Olaussen, 2005). In "Das Christiania Silurbecken" he wrote about the Lower Palaeozoic sediments and also the igneous Permian rocks. His work on the stratigraphy in the Oslo Region eventually enabled him to make a system consisting of ten stages ("Etagen"). Kjerulf was a teacher to both Waldemar C. Brøgger (1851-1940) and Johan Kiær (1869-1931), who became important contributors to the understanding of the Oslo Region after Kjerulf (Larsen and Olaussen, 2005). Brøgger had three main scientific areas he contributed to during his work: 1) Paleontology, stratigraphy and tectonics of the "Cambro-Silurian" sediments, 2) Mineralogy of the rare minerals of the Oslo Igneous province, and 3) Petrography and geology of the igneous rocks of the Oslo Region (Larsen and Olaussen, 2005, Larsen et al., 2008). Kiær devoted most of his work to the uppermost Ordovician and the Silurian, where one of his key areas was the Ringerike District (Larsen and Olaussen, 2005, Larsen et al., 2008). Kiær (1908) did a thorough description of the stages 6 to 9 in the Oslo Region from 1908 to 1922. He did a further subdivision of the stages based on both litho- and biostratigraphy (e.g. 6bβ). Because of his thorough work, the Silurian succession was left alone until the 1970s when Worsley et al. (1982) started a major revision of Kiær's earlier work.

As more data were collected and analysed it became possible to make a reasonable correlation between units in the Oslo Region.

The distribution of Silurian outcrops in the Oslo Region

1a Oslo
1b Asker
2 Holmestrand
3 Skien
4 Eiker
5 Modum
6 Ringerike
7 Hadeland
8 Feiring
9 Toten
10 Hamar
11 Ringsaker

N

0 10 20 km

Figure 2.1: Districts in the Oslo Region, where the Silurian outcrops are marked in black. Figure from Worsley et al. (1983).
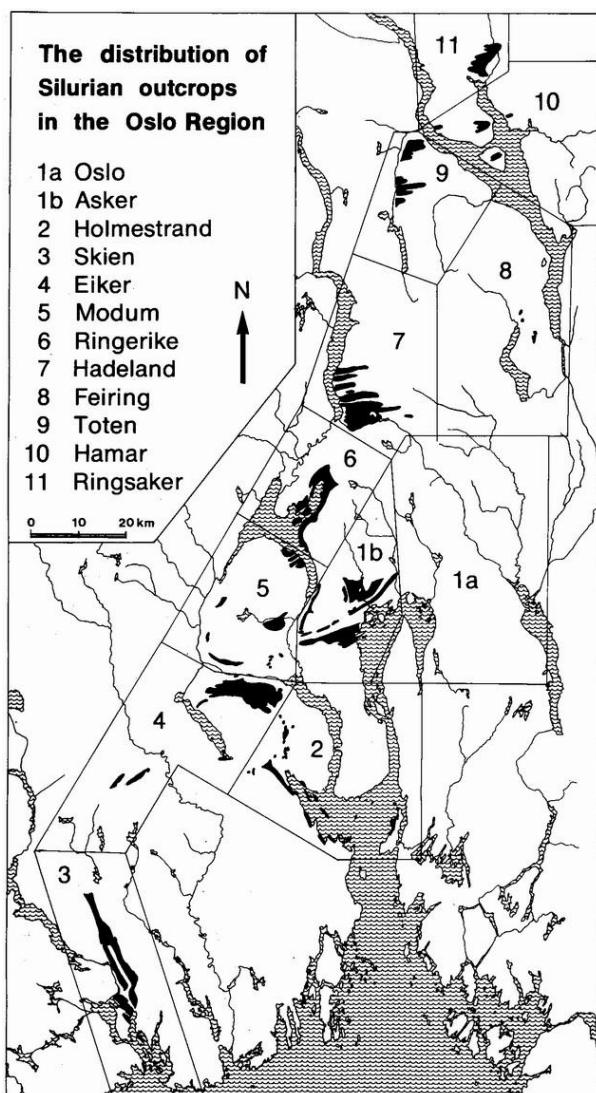
Worsley et al. (1983) stated that the numerical system by Kiær (1908) had to be modernised, since it is diachronous in the Oslo Region. They suggested further to use lithostratigraphical units with designated stratotypes for each unit. The new system was presented for the Silurian succession in the paper by Worsley et al. (1983). It is the most widely used system in the Oslo Region today. Worsley et al. (1983) also divided the Oslo Region into districts (Fig. 2.1), based on the division Størmer et al. (1953) published regarding the Ordovician stratigraphy. Owen et al. (1990) presented an equal division for the Ordovician system.

2.2 The Oslo region

In the 1980's and in the 1990's articles were published regarding basin evolution, fauna distribution and depositional environment. Möller (1987, 1989) studied the Rytteråker Formation. Thomsen (1982), Thomsen and Baarli (1982) and Thomsen et al. (2006) did work on the Sælabonn Formation. Baarli (1988) also published a paper regarding the Sælabonn Formation, but she also focused on the eastern equivalent, the Solvik Formation (Baarli, 1985). Postulation regarding the palaeogeographic setting was also presented by Baarli (1990b) and Baarli (1990a). Brenchley and Newall presented a major work regarding the understanding of the Langøyene Formation and its development (e.g. Brenchley and Newall, 1975, Brenchley et al., 1979, Brenchley and Newall, 1980). Braithwaite et al. (1995) presented a work that dealt with the Hadeland District, where they focused on the Ordovician-Silurian boundary and the underlying and overlying units. Skjeseth (1963) did work in the Toten, Hamar and Ringsaker districts, regarding the tectonic and stratigraphy of the area. A guide book, published by Whitaker (1977), addresses important geological localities around the Steinsfjord lake, in the Ringerike District (Fig. 2.1).

Whitaker (1973) and Broadhurst (1968) did work on sedimentary structures in the Silurian succession of the Oslo Region (e.g. gutter casts by Whitaker and large scale ripples by Broadhurst).

In the last decade three University theses have been devoted to the Ringerike District. Halvorsen (2003) wrote about the Ringerike Group, and the dynamics of the sediment infill of the foreland basin. Hjelseth (2010) and Kleven (2010) studied Caledonian structures in Ringerike area, respectively.

3 Dynamics in a foreland basin

In the paper by DeCelles and Giles (1996, p. 107) three criteria are emphasized in how a foreland basin should be defined:

> *"(I) Foreland basin systems are elongated regions of potential sediment accommodation that form on continental crust between contractional orogenic belts and cratons in response to geodynamic processes related to orogenic belt and its associated subduction system. (II) Foreland basin systems may be divided into four depozones, which we refer to as wedge-top, foredeep, forebulge and back-bulge depozones. Which of these depozones a sediment particle occupies depends on its location at the time of deposition. Boundaries between depozones may shift laterally through time. In some foreland basin systems, the forebulge and back-bulge depozones may be poorly developed or absent. (III) The longitudinal dimension of the foreland basin system is roughly equal to the length of the adjacent fold-thrust belt."*

3.1 Foreland basin evolution

Dickinson (1974) was the first to distinguish between two different types of foreland basins, *retroarc-* and *peripheral basins*. A retroarc basin is formed in proximity to the creation of a magmatic arc along a continental margin, caused by subduction of oceanic lithosphere under continental lithosphere (Fig. 3.1). Sediments are accumulated behind the magmatic arc, where the source area could be the magmatic arc but are most commonly sediments from the fold-and-thrust belt. A peripheral foreland basin is formed when two continental plates collide (Fig. 3.1). The mountain belt causes tectonic loading on the subducting continental
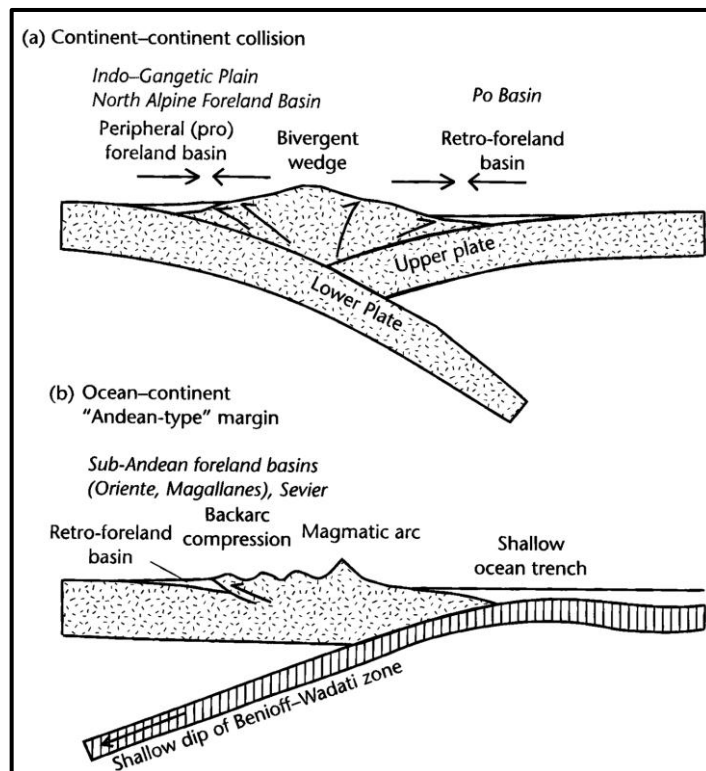
Figure 3.1: a) Peripheral foreland basin. b) Retroarc foreland basin. Figure from Allen and Allen (2005).

plate adjacent to the advancing thrust front (Dickinson, 1974). The crustal thickening causes flexuring of the cratonic crust with the result that the peripheral depression stretches further on to the craton than the advancing thrusts (Kearey et al., 2009). The fold-and-thrust belt is the main source of siliciclastic input to the foreland basin. If the depression is large and deep enough, deep-marine deposits (e.g. turbidites) termed *flysch* can be formed in a stage when the basin is underfilled. Cratonward of the peripheral foreland basin an uplifted flexural peripheral bulge can be formed, separating the deep foreland basin *sensu stricto* from a shallow marine or continental back-bulge basin further onto the craton (Fig. 3.2). Deposits of the foreland bulge are usually shallow-marine siliciclastic and/or carbonate facies. In turn, these sediments can be succeeded by coarser grained, usually fluvial or alluvial sandstones and conglomerates derived from the erosion and break-down of the thrust wedge. This occurs in the overfilled stage of the foreland basin system. Such late to post-orogenic deposits have been termed *molasse* (Dickinson, 1974, DeCelles and Giles, 1996).

According to Jordan and Watts (2005) the geometry of a foreland basin is controlled by the type of lithosphere. A wide basin will develop if the lithosphere is old, cool and strong. If the lithosphere is young, hot and weak a deep narrow basin will develop.

Since the Caledonian foreland basin is a peripheral foreland basin, only this subject will be treated here.

3.2 Sedimentation control

3.2.1 Depozones in a peripheral foreland basin

In Figure 3.2 a schematic view of the foreland basin system is presented, where it is divided into four different regions of deposition; wedge-top, foredeep, forebulge and back-bulge (DeCelles and Giles, 1996).

The wedge-top depozone is a part of the orogenic wedge (Fig. 3.2), and is the place where sediments of the frontal part of the orogenic belt are deposited. This area extends parallel to the orogeny, for tens of kilometres (DeCelles and Giles, 1996). In this area structures like blind thrusts tipping out in fault propagation anticlines develop (Yeats and Lillie, 1991), and passive roof duplexes in the subsurface (Skuce et al., 1992). Closer to the hinterland, development of trailing fault-bend and fault-propagation folds develop above major structural ramps and duplexes. This structural development of the fold-and-thrust belt can also hinder sediments entering the foredeep by acting as a barrier and directing sediments other places

(DeCelles and Giles, 1996). A wedge-top depozone can be recognized by local and regional unconformities, immaturity of sediments, and by the strong structural influence (DeCelles and Giles, 1996). In areas where there is subaerial exposer fluvial and alluvial deposits accumulates, creating the area with the coarsest sediments in the foreland basin. Several authors have according to DeCelles and Giles (1996) recognized a dominance of mass-flows in subaqueous settings; this includes fine grained shelf sediments.

The foredeep depozone (Fig. 3.2) is the area between the orogenic wedge and the forebulge depozone. It can extend 100-300 km across the basin and can accommodate sediment successions 2-8 km thick (DeCelles and Giles, 1996). DeCelles and Giles (1996) stated that subaerial foredeep depozones can receive sediments from alluvial and fluvial systems both longitudinally and transversely. In subaqueous areas, deltaic, shallow shelf and turbidity fan environments dominate. The main source of the sediments in the foredeep is the fold-and-thrust belt, but sediments from the forebulge and craton also contribute; however, to a lesser degree (DeCelles and Hertel, 1989). Since the main source in the depozone is the fold-and-thrust belt, the rate of accumulation is highest closest to the orogenic wedge (Sinclair et al., 1991). The sedimentary environments in the forebulge show a transition from early deep-marine sedimentation ("flysch") to shallow-marine and non-marine sedimentation ("molasse") (Sinclair and Allen, 1992).

The forebulge depozone (Fig. 3.2) is created by a flexural uplift of the craton along the orogenic belt, caused by the load of the converging plate on the subducting plate (DeCelles and Giles, 1996). The size of the forebulge has the potential to be up to 60-470 km wide and a few tens to a few hundred meters high (DeCelles and Giles, 1996). The movement of the forebulge may also be stationary over longer periods of time before it "jumps" toward or away from the orogenic belt. The foreland bulge is an elevated feature, and tends to be characterized by non-deposition or erosion. This can be used to track the movement over time in the foreland basin (Jacobi, 1981). According to Crampton and Allen (1995) the unconformity produces features as the forebulge moves. These are progressive onlap in a cratonward direction by deposition from the foredeep on to the unconformity, an increased stratigraphic gap in the foredeep towards the craton, and an angular difference ($<<1°$) between the pre-existing and newly deposited layers. The forebulge may also be buried, due to sediment load prograding from the thrust-and-fold belt (Patton and O'Connor, 1988). In cases where the foreland basin is submarine and the foredeep is not filled up to the crest of the forebulge development of forebulge carbonate platforms may occur. According to Giles and

6

Dickinson (1995) carbonate platforms can grow and extend over large regions from the foredeep to the craton. If the foreland basin is subaerially exposed, and the foredeep is not filled up to the crest of the forebulge, a zone of erosion will develop on the forebulge with a drainage system towards and away from the orogenic belt (Crampton and Allen, 1995).
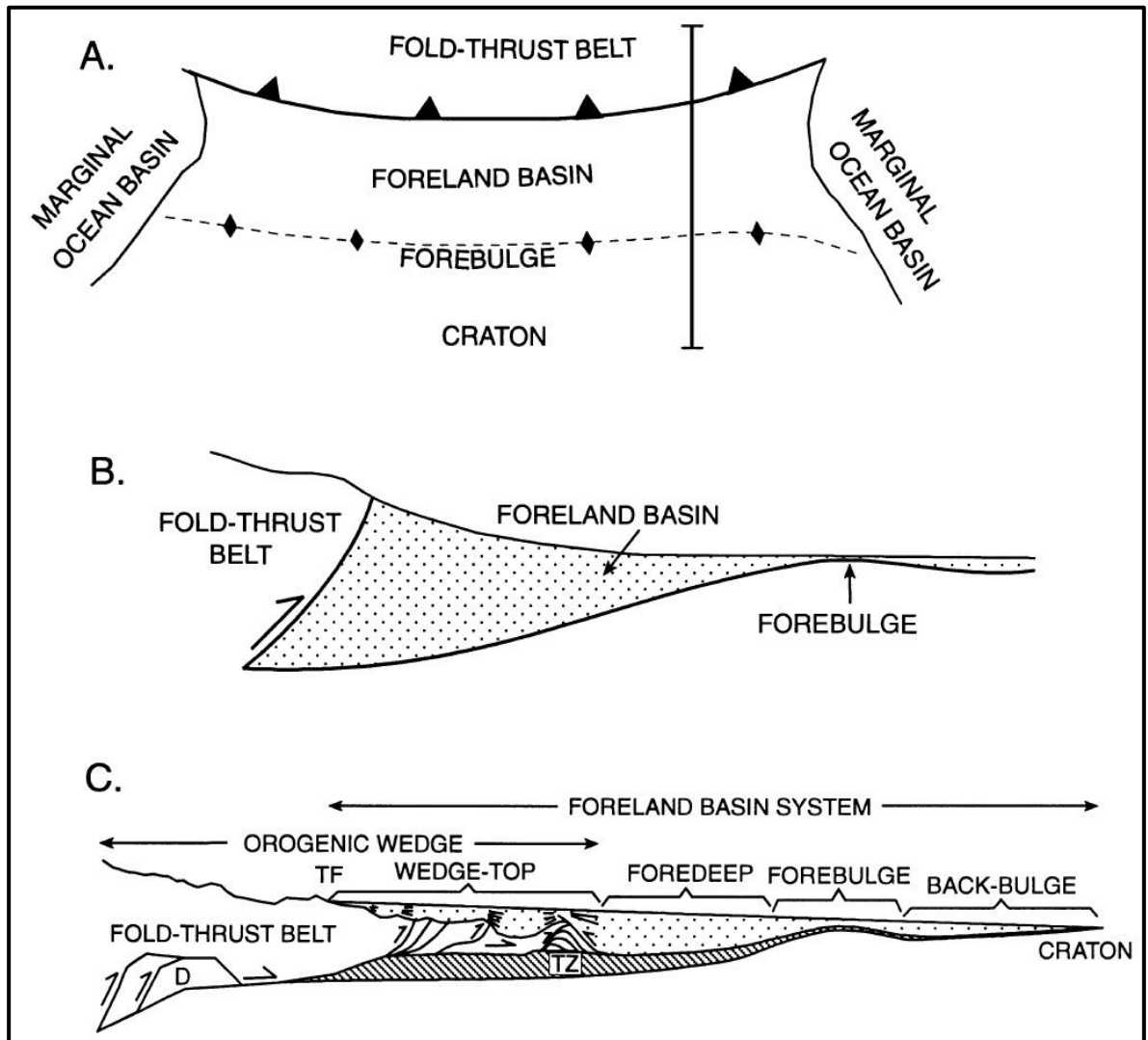
Figure 3.2: A.) A schematic map view of a "typical" foreland basin, bounded longitudinally by a pair of marginal ocean basin. The scale is not specific but would be in the order of 102-103 km. Vertical line at right indicates the orientation of a cross-section what would resemble what is shown in part B. B.) The generally accepted notion of foreland-basin geometry in transverse cross-section. Note the unrealistic geometry of the boundary between the basin and the thrust belt. Vertical exaggeration is of the order of 10 times. C.) Schematic cross-section depicting a revised concept of a foreland basin system, with the wedge-top, foredeep, forebulge and back-bulge depozones shown at approximately true scale. D: Duplex structures situated in the hinterland. TF: Topographic front of the thrust belt. TZ: Frontal triangle zone. Figure and text from DeCelles and Giles (1996).

The back-bulge depozone (Fig. 3.2) is the area furthest away from the orogenic wedge. The sources for this area are, according to DeCelles and Giles (1996), sediments from the orogenic wedge as well as sediments from the craton and development of carbonate platforms in deep marine systems. Subsidence has been recorded in the back-bulge area towards the craton, but

it is too low to create large accommodation spaces (DeCelles and Giles, 1996). Therefore the stratigraphic units at this depozone are thin, but can extend several hundred kilometres perpendicular to the orogenic belt. According to Holt and Stern (1994), the depositional system is less than 200m deep, which represent a shallow marine or non-marine environment. However, the large distance from the orogenic belt causes only fine grained sediments to be deposited in the back-bulge depozone.

3.2.2 Accommodation space

The main control of accommodation space in a peripheral foreland basin is the subsidence caused by the subduction load and topographic load. According to Royden (1993) the largest subsidence takes place when ocean crust is subducted under a continental plate and causes a subduction drag. When continents collide the degree of subduction is less because of partial subduction of transitional or continental lithosphere. Topographic load becomes the main contributor to subsidence in the basin (Royden, 1993).

Other factors controlling the accommodation space are the variation in sea-level or base-level and structural damming.

Each of the depozones has different controls influencing the accommodation space. In the **wedge-top depozone** there is a competition between the subsidence and uplift of the orogenic wedge which is caused by crustal thickening and isostatic rebound (DeCelles and Giles, 1996). Structural damming by uplift of anticlinal ridges can cause local accommodation of sediments. In the front of the depozone eustatic changes in sea-level can cause destruction or creation of accommodation spaces (DeCelles and Giles, 1996). In periods of shortening a syndeposistional, thrust-related deformation and development of unconformities can be observed in the wedge-top depozone (DeCelles and Giles, 1996). During periods of non-shortening the wedge-top depozone has a continued development of unconformities followed by regional onlap of sediments that is not syndepositionally deformed (DeCelles, 1994). In the **foredeep depozone** the relative sea-level can cause an increase or decrease in the accommodation space (DeCelles and Giles, 1996). Other factors controlling the accommodation space are the regional isostatic uplift caused by erosion of the orogenic load, advances of orogenic thrust wedge, and retrograde migration of the forebulge (Sinclair et al., 1991, Bertog, 2010). The **forebulge depozone** can be an area of subaerial erosion (Crampton and Allen, 1995) or buried by synorogenic sediments (DeCelles and Giles, 1996). Accumulation of sediments can either happen by drainage systems prograding out to the

forebulge or by deposition during high sea-level. In a **back-bulge depozone** it is thought that the main controls of the accommodation space are the elevation of the forebulge, relative sea-level, and availability of sediments (DeCelles and Giles, 1996).

Underfilled to overfilled basin

An underfilled situation of the basin occurs during rapid advances in the thrust belt, where the creation of accommodation space is larger than the infilling of sediments (Allen and Allen, 2005). In an overfilled situation the advances of the thrust belt have a decreased rate, and the infilling of sediments manage to keep up with the creation of accommodation space (Allen and Allen, 2005). The degree of filling in the basin can be interpreted by the long-term trends in facies found there. Deep-marine facies are associated with underfilling, shallow marine-distal continental facies are associated with a filled basin and fully continental facies are associated with an overfilled basin (Sinclair and Allen, 1992). According to Sinclair (1997) modelling done by different authors suggested three factors encouraging a transition from an underfilled to overfilled basin: 1) slowing thrust wedge advance 2) increasing exhumation and sediment production from the thrust wedge 3) increasing flexural rigidity of the underlying cratonic plate.

3.3 Epicontinental shelf
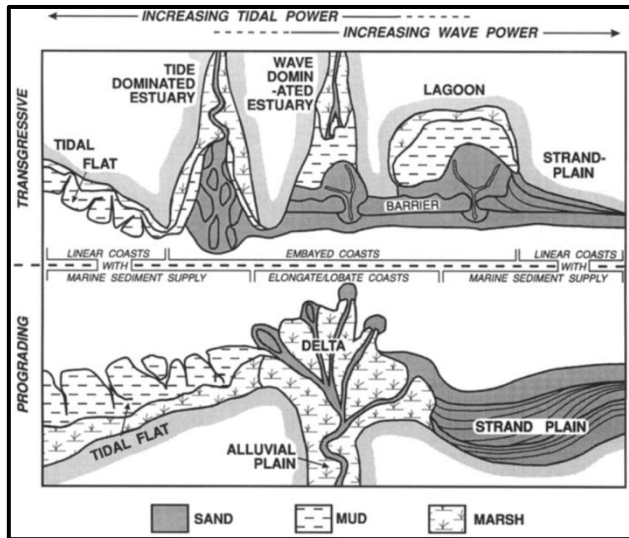
Figure 3.3: Coastal depositional features, in relationship to prograding or transgressive coast, and tide or wave dominated coast. Figure from Boyd et al. (1992).

On an epicontinental shelf depositional features can generally be distinguished based on a prograding or a transgressive setting and an increasing tide or wave power influence on the shelf (Fig. 3.3) (Boyd et al., 1992). Progradation takes place when the rate of sediment supply exceeds the rate of relative sea-level rise, or when sea-level falls and accumulation of sediments occur. During such an event; development of tidal flat, delta or strand plains occur (Fig. 3.3) (Boyd et al., 1992).

During a transgression the opposite happen and sea-level exceeds the sediment supply. As the sea level rises, formation of tidal flats, estuaries, lagoons or strand plains takes place (Fig. 3.3) (Boyd et al., 1992).
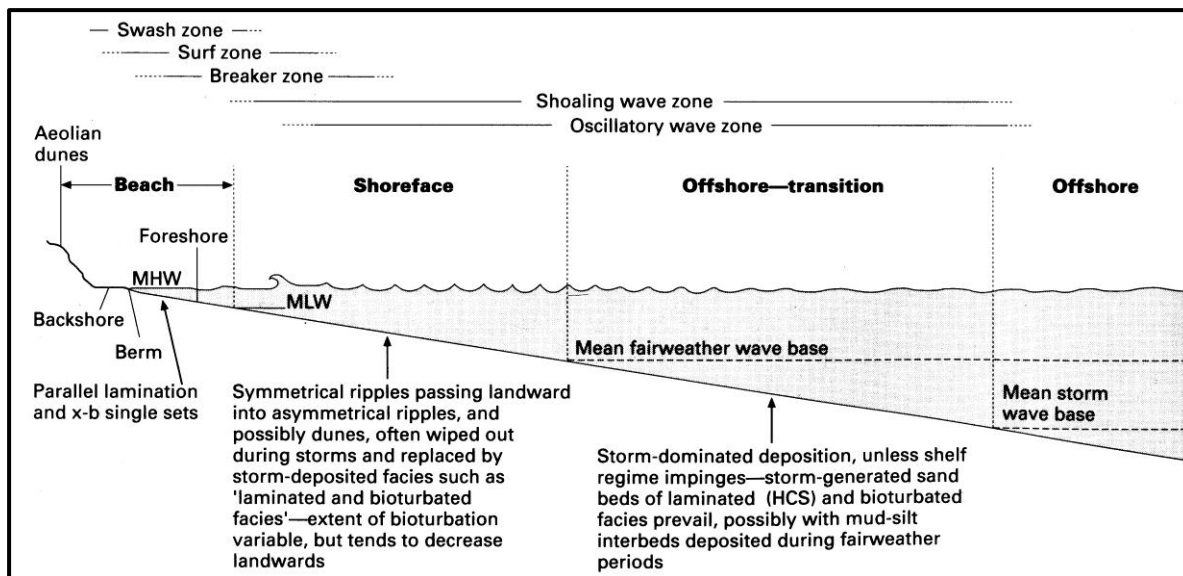
Figure 3.4: Generalized shoreline profile showing subenvironments. Figure and text from Reading and Collinson (1996).

The shelf can be divided into zones based on types of energy that affect the different depths (Fig. 3.4). The foreshore is mostly subjected to tidal processes where the backshore is the supratidal area, affected by high tides and storms (Reading and Collinson, 1996). The shoreface is subjected to the daily fairweather, where the oscillatory and shoaling wave processes operate in the lower part. The breaker zone of the waves operates in the upper

shoreface. The littoral energy fence is situated in the shoreface area, trapping sediments from reaching further out on the shelf during normal conditions (Reading and Collinson, 1996). The Offshore–transition zone is characterized by both high and low energy conditions and is situated between the mean fairweather wave base and mean storm wave base (Fig. 3.4). The zone is characterized by fine sediments settling from suspension during fairweather. During storms it becomes an extension of the shoreface as oscillatory and shoaling waves also affect the sea-bottom in this deeper area (Reading and Collinson, 1996). During storms different processes affect the deposition at different stages. The main processes are geostrophic flow, wave oscillation and density-induced flow (Myrow and Southard, 1996).

4 Regional setting

4.1 A shift from an Epicontinental sea to a Foreland basin

The Lower Palaeozoic succession of the Oslo Region has been divided into four events by Larsen and Olaussen (2005). The first event, which is situated on the eroded Archean crustal rocks ("Sub-Cambrian peneplain"), range from Early Cambrian to Middle Cambrian in age and is characterized by a shallow southward transgressing sea. The second event range from Late Cambrian to Middle Ordovician in age and is characterized by a basin with low sedimentation rate of typical epicontinental sea. The third event range in age from Late Ordovician into the early part of Late Silurian in age and is characterized by the onset of foreland basin silt- and sandstone and shallow marine warm water carbonates. The fourth event is of Late Silurian age and is characterized by the foreland alluvial and fluvial basin fill (The Ringerike Group).

From the Middle Cambrian to Early Ordovician the succession is characterized by the deposition of black shales ("Alum shale") (Bjørlykke, 1974, Bockelie and Nystuen, 1985). In the Lower to Middle Ordovician carbonate and mud dominated, with a low siliciclastic input of coarser material (Bjørlykke, 1974, Owen et al., 1990). In the Upper Ordovician coarser siliciclastic material was introduced, however, shales and limestone were still dominant (Bjørlykke, 1974).

The oblique collision between the Baltica and the Laurentia plate eventually led to the convergence of the two continents. The margin of Baltica was subducted under the Laurentia plate (Roberts, 2003). This lasted from the Silurian to Early Devonian. The earliest collision within the Baltoscandian segment of the Caledonian orogen occurred in the Tremadocian Stage (c. 485 Ma) with initial closing of the Iapetus Ocean in the Ludlow Epoch (c. 420 Ma) (Fig. 4.1) (Pedersen et al., 1988, Pedersen et al., 1992). The on-going collision was also observed by the increased clastic input in the Oslo Region from late Ordovician and onwards. Erosion was indicated from the growing Caledonian orogeny in the west and north-west (Bruton et al., 2010). To get a proper understanding of the tectonic evolution and timing of the Oslo Region, observations of the interaction between faulting and folding, and sedimentary processes must be documented. These observations are sparse in the Oslo Region as even the youngest sediments (Ringerike Group) were deposited before the main episode of

folding and faulting (Bruton et al., 2010). However, Halvorsen (2003) indicated an interaction between sedimentation and tectonics, suggesting that the Ringerike Group was formed contemporaneously with thrust movements within a major synclinal piggy-back basin. The depositional basin in the north has shown to be very narrow in the early Silurian (Llandovery) with sediment sources in the west and east (Worsley et al., 2011). The shortening of the Lower Palaeozoic rocks in the Oslo Region has been greatest in the northernmost districts (Worsley et al., 2011). Morley (1986a) suggested a shortening of at least 130 km in the Mjøsa area, while the shortening at Langesund has been close to zero. The shortening also depends on the change in deformation style and lithology, where the shortening decreases upwards in the sequence (Morley, 1986a, 1986b). The Lower Palaeozoic in the Oslo Region is part of a décollement unit, which is considered to be a southward continuation of the Osen-Røa Nappe complex (Nystuen, 1981). The Osen-Røa detachment lies within the late Cambrian Alum Shale, which underlies the entire Oslo Region (Bruton et al., 2010). The thrust sheet is suggested to be 280 km long and to have a undeformed thickness of about 2 to 4 km (Morley, 1986a).
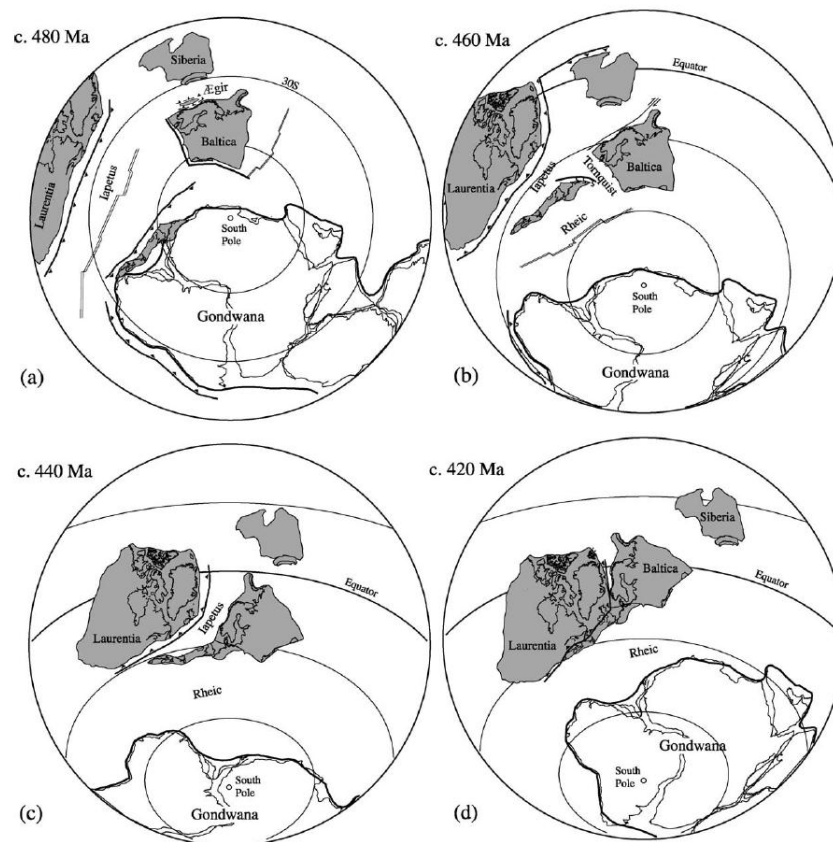

Figure 4.1: The paleogeographic movement of the continents from Early Ordovician to Late Silurian, where Avalonia, Laurentia, Baltica and Siberia are outlined. a) Early Ordovician. b) Middle to Late Ordovician boundary. c) Early Silurian. d) Late Silurian. Figure from Roberts (2003).

Several bentonite beds have been found in the Ordovician and Silurian, in the Oslo Region, and have been linked to volcanic activity within the Caledonian orogenic belt (Bockelie and Nystuen, 1985). The bentonite beds of Ordovician age have a decreasing thickness eastwards; they are thickest in the Oslo Region and thinnest in western Russia (Bruton et al., 2010). The source for these extensive bentonite beds is thought to be in the Iapetus Ocean (Fig. 4.1), between the Laurentia and the Baltica plates (Huff et al., 2010).

4.1.1 Ordovician-Silurian boundary

Spjeldnæs (1957) stated that the base of the Silurian is younger towards the north, and the most complete succession is found in the south-east in the Oslo Region. He also suggested that the Ordovician-Silurian boundary marks a stop in sedimentation. In the north of the Oslo Region a significant age gap is present, documented by Skjeseth (1963), Worsley et al. (1983) and Owen et al. (1990). Within the Upper Ordovician, the Ashgillian portion is absent where the Mjøsa and Helgøya formations are separated by a karst surface. The Helgøya Formation has also been defined as a member of the Sælabonn Formation inWorsley et al. (1983). Skjeseth (1963) referred the Helgøya Formation to sub-stage 6c, which correspond to the Limovnstangen Member in the Sælabonn Formation.

The upper Ordovician in Ringerike and Hadeland is characterized with the development of a karst surface caused by a drop in sea-level and subaerial exposure (Braithwaite et al., 1995). Braithwaite et al. (1995) also observed an infilling of the karst structures, caused by a small transgression, within an overall regression. In the Oslo District the drop in sea-level is observed by the change of fauna and the development of incised tidal channels (Brenchley and Newall, 1980). The major transgression following the regression is marked with the deposition of the siliciclastic Sælabonn Formation. Thomsen (1982) reported the Sælabonn Formation to be laying conformly on top of the Langøyene Formation. Størmer (1967) observed a siliciclastic input in the upper Ordovician and suggested an epeirogenetic response in southern Scandinavia before the initial build-up of the Caledonian orogenic belt. Brenchley and Newall (1980) suggested that the sea-level variations could also be caused by the development of the ice-cap on the Gondwana continent. Shales, overlying the Ordovician succession, contain graptolites and benthic fauna reflecting distal, quiet water and suggest a rapid transgression in the early Rhuddanian stage caused by the melting of the ice-cap on the Gondwana continent (Brenchley and Newall, 1980).

4.1.2 Global sea-level

The eustatic curve by Johnson et al. (1998) depict eight events (i.e., those beginning with a lowstand and culminating with a highstand) which occurred in the Silurian (Fig. 4.2). In this study Johnson et al. (1998) estimated sea-level lowering and rise by the use of palaeotopographic elements, such as rocky shorelines and coastal valleys. The relative bathymetry of the sea-level curve is indicated by the use of graptolite and conodont zones. The Rhuddanian transgressive event is associated with the Gondwana ice cap (Johnson et al., 1998), which had a glacial maximum in the Hirnantian (Finnegan et al., 2011).
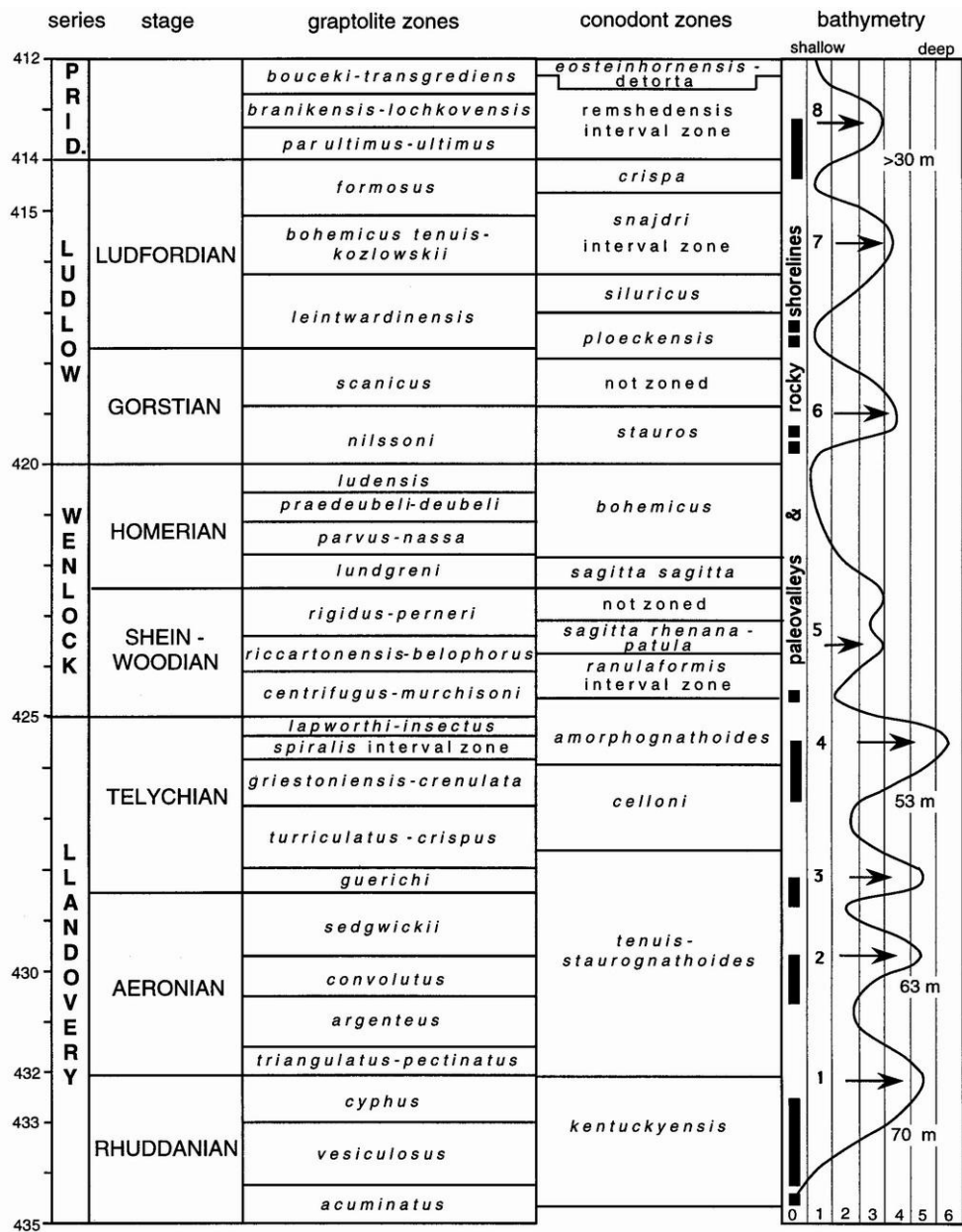
Figure 4.2: Silurian eustatic curve with the burial history of particular palaeovalleys and rocky shorelines marked by black vertical bars under the zero column that indicates land. Relative bathymetry of sea-level curve is indicated by numbers 1 (shallow) to 6 (deep), which represent benthic assemblage zones. Figure and text from Johnson et al. (1998).

The Geology at Ringerike

Silurian

32	Stubdal Formation
33	Sundvollen Formation
34 35 36 37	Steinsfjord Formation
38	Braksøya Formation
39	Bruflat Formation
40 41 42 43	Vik Formation
44	Rytteråker Formation
45	Sælabonn Formation

Middle and Late Ordovician

49	Langøyene Formation
50	Bønsnes Formation
51	Sørbakk Formation
52	Venstøp Formation
53	Solvang Formation
54	Nakkholm/Frognerkil/ Arnestad formations
55	Nakkholm Formation
56	Frognerkil Formation
57	Arnestad Formation
58	Voll Formation
59	Elnes Formation

Figure 4.3: Geological map displaying the distribution of the Middle and Upper Ordovician, and Silurian rocks at Ringerike. Section of geological map Hønefoss 1815 III, M 1:50 000. Modified map from Zwaan and Larsen (2003).

16

4.2 The Latest Ordovician and Silurian succession

In Figure 4.3 a geological map of the Ringerike area is presented, with the occurring formations. An overview of the underlying and overlying formations of the Sælabonn and Solvik formations in the Ringerike, Asker and Oslo districts is presented in Figure 4.4. An overview of the whole Lower Palaeozoic succession in the Oslo Region can be viewed in Figure 4.5, with an estimated age and thickness.

4.2.1 Langøyene Formation

At the time of deposition of the Langøyene Formation (stage 5a and 5b) there was a south-eastward slightly inclined palaeoslope in the Oslo Region (Brenchley et al., 1979). In Larsen and Olaussen (2005), part of Langøyene Formation is interpreted as a possible first clastic wedge from the Caledonian orogeny.

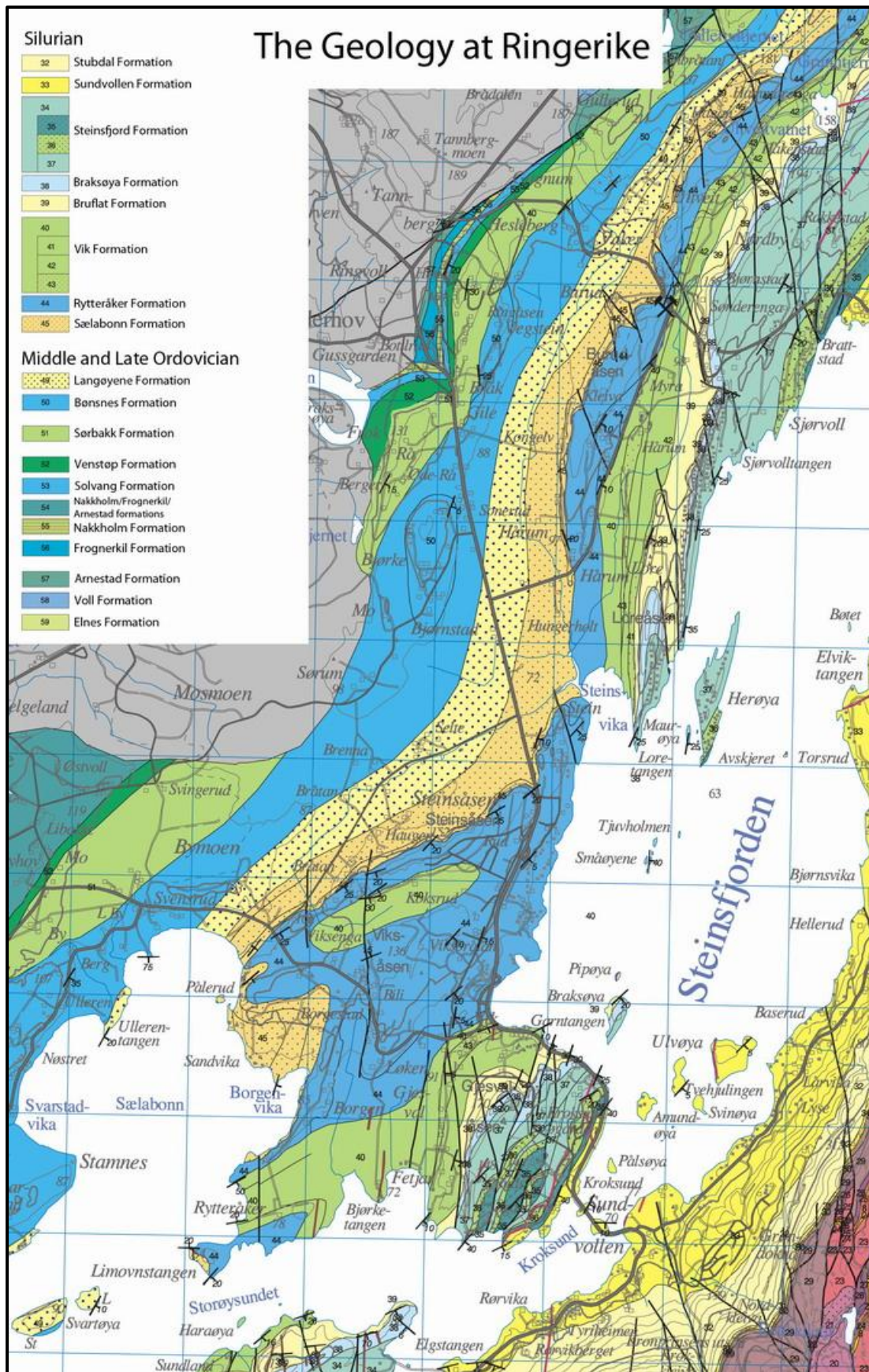The lower part of the Langøyene Formation has an increasing diversity and density in the fauna together with the appearance of nodular limestone, suggesting a moderate regression of this lower unit (Brenchley and Newall, 1980). According to Brenchley et al. (1979) this was a quiet shelf environment where shales and nodular limestone were formed. In between these layers storm beds of silt and fine sand were deposited and transported in from a westerly source. Currents transported the material obliquely across the palaeoslope in a north-westwards direction. In the west (e.g. Langesund, northwest Asker, Ringerike and Hadeland) there was a calcareous facies belt indicating a shallower environment.

Period	Epoch	Age/Stage	Ringerike District	Asker District	Oslo District	Stages
Silurian	Llandovery	438.5 Ma	Rytteråker Fm.	Rytteråker Fm.	Rytteråker Fm.	7 (a, b)
		Aeronian				
		Rhuddanian	Sælabonn Fm.	Solvik Fm.	Solvik Fm.	6 (a, b, c)
		443.8 Ma				
Ordovician	Late	Hirnantian 445.2 Ma	Langøyene Fm.	Langøyene Fm.	Langøyene Fm.	5 (a, b)

Figure 4.4: Stratigraphic illustration of the Langøyene, Sælabonn and Rytteråker formations, based on information from Worsley et al. (1983) and (Owen et al., 1990). The Ordovician-Silurian age gap has not been taken into account. Age from Gradstein et al. (2012).

The upper part of the Langøyene Formation is also interpreted as a regressive succession, where the main regressive event occurred in the uppermost part of the succession (Brenchley and Newall, 1980). There were no major changes in the bathymetry before the later part as the faunal composition had very few variations. Brenchley and Newall (1980) observed the lower part as mud dominated, as the coarse clastic material did not reach the Asker District. The major shallowing in the upper part was interpreted by Brenchley and Newall (1980), based on occurrences of *Holorhynchus* beds and development of channels. They did, however, not report evidence for an emergence of the upper part during the major regression in the Oslo-Asker District.

Brenchley and Newall (1980) suggested that the clastic input in the Langøyene Formation was from a western source ("Telemark land"), which was caused by shallowing or, more likely, tectonic uplift of the source area. The rhythmicity recognized from the Oslo-Asker District in Middle and Upper Ordovician is caused by local control, while the regression of the Langøyene Formation can be seen through the whole of the Oslo Region (Brenchley and Newall, 1980). This indicates that there was a regional regression, most likely caused by the Late Ordovician glaciation (see Chapter 4.1.1).

4.2.2 Sælabonn Formation

The Sælabonn Formation (stages 6a, 6b and 6c) has been studied by Thomsen (e.g. Thomsen, 1982, Thomsen and Baarli, 1982, Thomsen et al., 2006). The Formation is of Rhuddanian and Aeronian age, and is the lowermost formation in the Silurian succession at Ringerike (Thomsen, 1982). The formation has been divided into three members; Store Svartøya Member, Djupvarp Member and Limovnstangen Member (Thomsen, 1982).

The lowermost member, Store Svartøya Member (stage 6a), has been interpreted by Thomsen (1982) as an open marine shelf. The member is characterized by mud, thin sandstone beds and biosparitic "megaripples". The sandstone beds and "megaripples" were, according to Thomsen (1982), deposited during storms. The fauna was dominantly transported, and were observed in the limestone. The sea-level in this member has been interpreted as shallow marine, with an increasing frequency of storm beds upwards in the member (Thomsen, 1982).

The middle member, Djupvarp Member (stage 6b), has been interpreted as an inter-bar and bar complex. The member is composed of shales, biosparitic limestone and calcareous sandstones. It is characterised by thick cross stratified sandstone beds (Thomsen, 1982).

Measurements of the palaeocurrent in the large cross stratified beds and of ripples in thinner sandstone beds show a NE to SW direction (Thomsen, 1982). Storm beds also occur here (Thomsen, 1982). Thomsen (1982) suggested that the Djupvarp Member was affected by a microtidal environment. The sea-level in this member represents a shallow marine environment and was, according to Thomsen (1982), almost dry land. She observed asymmetrical wave ripples with flat crest and wrinkle marks.

The upper member, the Limovnstangen Member (stage 6c), has been interpreted by Thomsen (1982) as an open marine shelf. The member is composed of alternating beds of calcareous siltstone, shales and limestone. The biosparitic limestone increases upwards in the member and is interpreted by Thomsen (1982) as storm beds. The palaeocurrent direction shows a general NW to SE trend (Thomsen, 1982). As in the lower members, Thomsen (1982) observed transported fauna in the limestone beds. The sea-level in this member reflects a regression, where hummocky cross stratification has been observed in the lower part of the member and gravitational cement has been observed in the upper part (Thomsen, 1982). Thomsen (1982) suggested that a transgression must have taken place between the Djupvarp Member and Limovnstangen Member, as the facies are markedly different.

4.2.3 Rytteråker Formation

The Rytteråker Formation (stages 7a and 7b) overlies the Sælabonn/Solvik Formation in all of the nine districts where it is found (Fig. 4.5) (Möller, 1989). According to Möller (1986) the transition between the underlying formation and Rytteråker Formation is gradual in the central and southern districts. However, in the northern districts of Hamar and Ringsaker the border is described as sharp and possible erosional.

The formation was formed in a neritic carbonate environment, with north-south trending arcuate depositional belts migrating eastwards (Möller, 1989). The eastward migration of the belts was cause by continuous transgression lasting to the beginning of the Telychian Stage. This does not correlate with the global regressive-transgressive pattern postulated by Johnson et al. (1985). Möller (1989) suggested that an active orogenic belt was the cause for that. According to Möller (1989) there were two depositional basins, a larger and deeper basin to the west and a smaller, shallower basin to the east which, in periods, were restricted. In the transition between these two basins the depositional belts developed. At Ringerike the lowermost unit is an open platform with a belt of bioclastic shoals and patch reefs which formed landwards (Möller, 1987). This is followed by foreshore deposits of a shoal or barrier.

After the passing of the shoal belt, deposits of biostromes and small bioherms formed seaward. The uppermost part has been interpreted by Möller (1987) as an open marine, sublittoral environment consisting of bioturbated packstone and wackestone with a sharp border to the underlying unit.

The palaeocurrent analysis of the Rytteråker Formation indicates a SSE to NNW direction (Möller, 1987, 1989). However, according to Möller (1989) the data is not sufficient to reconstruct a complete picture throughout the formation. The underlying formation, the Sælabonn/Solvik Formation, appears to be synchronous to the lower Rytteråker Formation according to Möller (1989) and indicates a transport from SSW to NNE (Whitaker, 1973, Thomsen, 1982).

4.2.4 Vik Formation and Ek Formation

The Vik Formation (stage 7c) is thought to represent a deeper depositional environment than the Rytteråker Formation based on fossil fauna (Worsley et al., 1983). The formation also represents an increased influx of clastic sediments. However, the middle member, Garntangen, has a higher content of carbonate which is thought to be caused by a development of shallow marine marl banks. Baarli (1990a) recognized a deepening on the onset of the Vik Formation in the central Oslo District. This was followed by a shallowing with an iterative deepening. The sediments were deposited in water depths close to the preceding Rytteråker Formation but with an increased clastic influx (Baarli, 1990a). The Ek Formation is found in the northern part of the Oslo Region (Fig. 4.5), where shales were formed in deeper water environments than the southern equivalent, Vik Formation (Worsley et al., 1983).

4.2.5 Bruflat Formation

The Bruflat Formation (stages 8a and 8b) was deposited in marine settings, in the late Telychian, and is an environment interpreted to consist of mud and sand-rich submarine fans (Worsley et al., 2011). Several fans were entering the basin as the palaeocurrent measurements of the turbidites show different directions in the districts (e.g. Toten, Ringerike and Modum), with the sources in the west and north (Worsley et al., 2011). In the Ringerike and Modum District the Bruflat Formation is inferred to reflect outer-fan deposits (Worsley et al., 2011). In the same area the upper part of the Bruflat Formation is missing, which was most likely caused by a drop in sea-level during the Ireviken extinction event (Worsley et al., 2011). The event, with the associated sea-level drop, extended for 0.2 Ma around the Llandovery/Wenlock transition (Worsley et al., 2011).

20

4.2.6 Braksøya Formation

The Braksøya Formation (stages 8c and 8d) has been interpreted as a marginal marine carbonate depositional environment, with erosion close to the base of the Wenlock stage. (Worsley et al., 1983). The environment was restricted as the flora and fauna and the occurrence of evaporites in marl succession indicates hypersaline conditions (Worsley et al., 1983). The area seems to be deepening south-eastwards from the Ringerike District to the Modum and Skien districts. The upper part of the formation represents an intra/supratidal depositional environment only observed in the Ringerike District (Worsley et al., 1983).

4.2.7 Steinsfjorden Formation

The Steinsfjorden Formation (stage 9) is represented by supratidal, intratidal and subtidal environment where mixed carbonate and mud were deposited. According to Worsley et al. (1983) the unit has been affected by small-scale transgressive and regressive events, which is reflected in the rhythmic changes in lithology. In all districts where this formation is observed, the upper and lower part reflects a peritidal environment. However the middle parts in all other districts except Ringerike show open subtidal conditions. This formation was likely deposited under arid conditions, since early diagenetic dolomite and celestite occur (Olaussen, 1981). In all districts where this formation is found the upper part is observed to be affected by a large scale transgressiv event, interpreted by the occurrence of favositid bioherms and biostromes (Worsley et al., 1983). During this event there was a short period of normal marine conditions before the Ringerike Group was formed (Worsley et al., 1983).

4.2.8 Ringerike Group

As seen in the previous subchapters the depositional environment changed rapidly, and shifted between siliciclastic wedges (e.g. Sælabonn Formation and Bruflat Formation) and carbonate ramps (e.g. Rytteråker Formation). In the Late Silurian a broad muddy coastal plain environment developed followed by a braided fluvial system (Davies et al., 2005b). These two systems have been named the Sundvollen Formation and the Stubdal Formation, and are comprised in the Ringerike Group (stage 10) at Ringerike (Davies et al., 2005b). The sediments of the Ringerike Group were deposited in the Oslo Region and covered the carbonate background sedimentation (Larsen and Olaussen, 2005). The Ringerike group is a 1250 m thick foreland–basin fill and is divided into two formations (Fig. 4.5), the Sundvollen Formation (490m) and the Stubdal Formation (550m) (Davies et al., 2005b). Halvorsen (2003)

suggested that the Sundvollen Formation developed in a piggy-back basin, where the Stubdal thrust sheet was emplaced on top of the Sundvollen piggy-back basin.
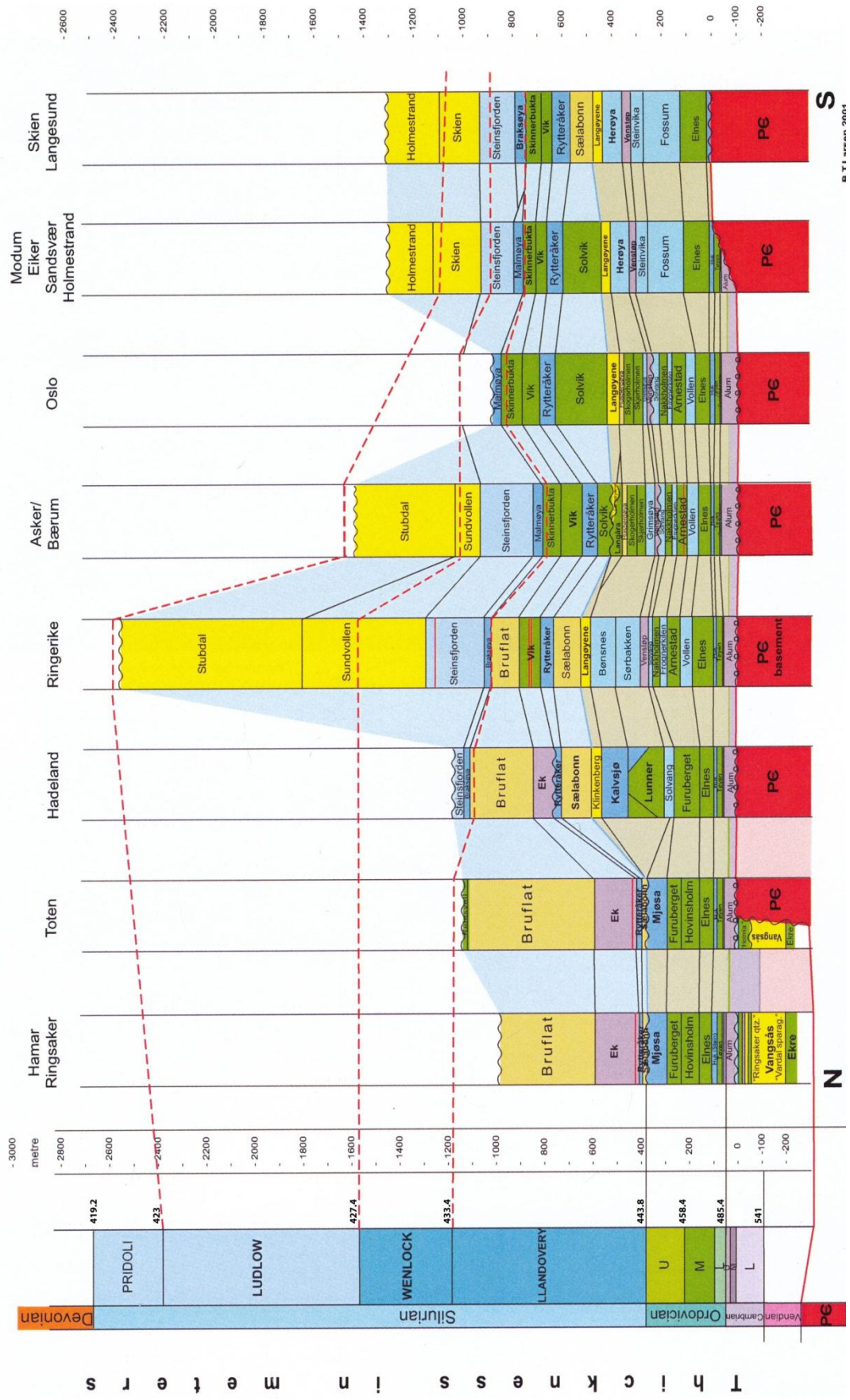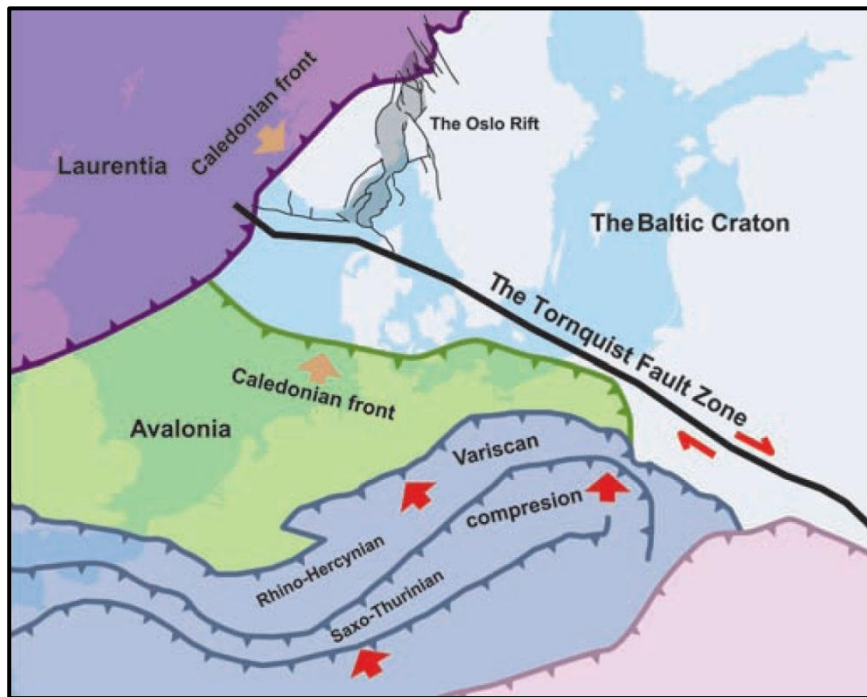
Figure 4.5: The lower Palaeozoic stratigraphy of the Oslo Region. Figure and text from Larsen and Olaussen (2005). Updated ages from Gradstein et al. (2012).

4.3 The Oslo Rift

Figure 4.6: Simplified tectonic overview of Western Europe with the Variscan front in the south, the Tornquist Fault Zone and the Oslo Rift. Also shown are the pre-rift configurations with the Caledonian structures and the boundary of the Baltica Craton. Figure and text from Larsen et al. (2008).

The development of the Oslo Rift has made it possible to study the Lower Palaeozoic succession in the Oslo Region, which otherwise would have been eroded.

The Oslo Rift includes the Oslo Region and Skagerrak, where the Oslo Region stretches from Langesund in the south to the northern part of Mjøsa in the north (Larsen et al., 2007). The total length of the Oslo Rift is 500 km and with a width of 60 km in the Oslo Graben, which is part of the Oslo Rift situated on land (Sundvoll and Larsen, 1994, Larsen et al., 2007). The rift axis has a NNE-SSW trend (Sundvoll and Larsen, 1994).

Between the Lower and Upper Palaeozoic sediments there is a hiatus suggesting an area exposed to erosion, which indicate that the area was a part of a landmass (Sundvoll and Larsen, 1994). There are two main causes for the development of the Oslo Rift. One of the causes was the abnormal high temperature weakening the crust (Larsen et al., 2007). The other was the Sorgenfri-Tornquist zone, where a large transvers fault with a northwest-southeast direction stretched the lithosphere causing a rift and graben to develop (Fig. 4.6) (Larsen et al., 2007). The Oslo Rift was initiated with the development of graben structures in the Late Carboniferous, with the onset of rifting and volcanism 20-30 Ma years later (Larsen et al., 2008). The final termination of the intrusions marks the end of the activity in the Oslo Rift in Early Triassic, 65 Ma after the tectonic and magmatic onset (Larsen et al., 2008).

5 Methods

5.1 Field work

The fieldwork for the different localities was executed in 2011, in a period of four weeks in July and August and two weeks in October and November.
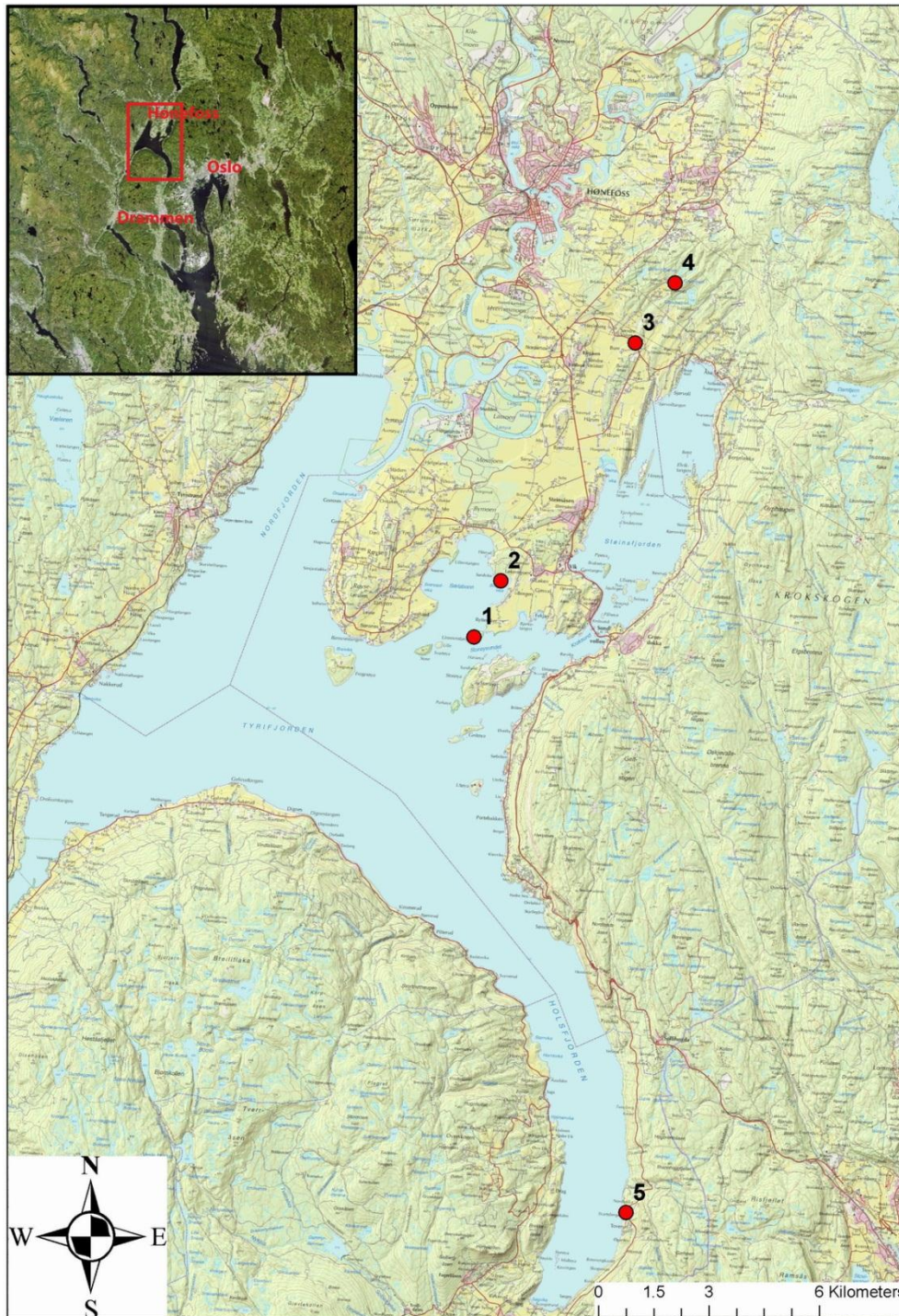

Figure 5.1: Map of the localities in the Ringerike and Modum District. 1: Limovnstangen, 2: Borgen, 3: Åsaveien, 4: Grunntjern, 5: Toverud. Coordinates and description of the localities are found in Appendix B. Map from S.K. (2012).

Five different localities were logged in 2011 by the author (Fig. 5.1), during the summer and part of the autumn. The Borgen and Limovnstangen were the main localities for the study. Several outcrops were logged to get a better understanding of the lateral distribution of the beds. The logging was supervised by Professor emeritus Johan Petter Nystuen (UiO) the first day. The author was followed-up by Professor emeritus Johan Petter Nystuen (UiO), Professor Hans Arne Nakrem (UiO) and Bjørn Tore Larsen (Det norske) during the summer. The outcrops were logged on standard log paper (Appendix I). The outcrops at Limovnstangen, Borgen, Grunntjern and Åsaveien were logged in 1:20 scale. The locality at Toverud was logged in 1:50 scale. The localities in the Ringerike District were of priority. The locality in the Modum District was logged and sampled to get an overview of the lateral variations. All the outcrops at the localities were photographed, to help in the study back at the office. An overview and description of the localities are presented in Appendix B.

Thomsen (1982) and Thomsen et al. (2006) have given different names of the upper member of the Sælabonn Formation. As seen in Table 5.1 the names correlate back to Kiær's old stage numbers. The author will in this thesis use the names from the article by Thomsen (1982) for the localities situated in the Ringerike District. The reason for this is that the names from 1982 are well known in the academic community, and changing them at this stage would cause confusion for the readers. The area where the Toverud locality is situated has been regarded as part of the Oslo-Asker District by Størmer et al. (1953), however, in the paper by Baarli (1988) the Toverud locality (named Sylling locality in that paper) has been included into the Modum District (Fig. 2.1). The use of Modum District for this locality has been continued in this work. The member names used for the Sælabonn Formation within the Modum District follow the terminology from Baarli (1988). A detailed review of the terminology of the Sælabonn Formation and the associated members is presented in Appendix H.

Table 5.1: Member-names from different references used for the Sælabonn Formation in the Ringerike District and Modum District.

	Kiær (1908)	Thomsen (1982)	Thomsen (2006)	Baarli (1988)
Upper member	6c	Limovnstangen	Steinsåsen	Limovnstangen
Middle member	6b	Djupvarp	Djupvarp	Djupvarp
Lower member	6a	Store Svartøya	Store Svartøya	Sylling

5.2 Sampling

During the fieldwork 117 samples were collected, however not all of them were studied. The large collection of samples was due to the lack of permission by Buskerud county municipality to collect samples from one of the main localities, Limovnstangen (Appendix B). Permission was given during the autumn 2011, and samples were then collected. 59 of the samples were used, 25 for thin sections and 34 for acetate-peels. The goal during the sampling was to collect representative samples from all localities, of both carbonates and siliciclastic rocks. All the samples were marked with an arrow to show the way up. Samples from Limovnstangen also show north-south/east-west direction.

5.3 Facies description and facies association

The Folk (1962) classification of carbonate rocks have been used to describe and classify the carbonate rocks at the different localities. A description of Folks classification is seen in Figure 5.2 below, and focuses on the texture of the rock. The carbonate rocks are classified to differentiate between the siliciclastic and carbonate components. The connection between the grain size and the terminology of the siliciclastic component is determined according to the Wentworth (1922) scheme of classification (Table 5.2).
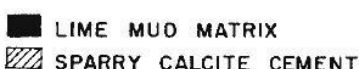

	OVER 2/3 LIME MUD MATRIX				SUBEQUAL SPAR & LIME MUD	OVER 2/3 SPAR CEMENT		
Percent Allochems	0-1 %	1-10 %	10-50%	OVER 50%		SORTING POOR	SORTING GOOD	ROUNDED & ABRADED
Representative Rock Terms	MICRITE & DISMICRITE	FOSSILI-FEROUS MICRITE	SPARSE BIOMICRITE	PACKED BIOMICRITE	POORLY WASHED BIOSPARITE	UNSORTED BIOSPARITE	SORTED BIOSPARITE	ROUNDED BIOSPARITE
1959 Terminology	Micrite & Dismicrite	Fossiliferous Micrite	Biomicrite			Biosparite		
Terrigenous Analogues	Claystone		Sandy Claystone	Clayey or Immature Sandstone		Submature Sandstone	Mature Sandstone	Supermature Sandstone

■ LIME MUD MATRIX
▨ SPARRY CALCITE CEMENT

Figure 5.2: Folks (1962) classification of carbonate rocks. The terminology is used in this thesis to differentiate between the components.

The lithofacies are defined by the structures, texture and lithology. The different facies are determined by observations in the field and by studying pictures from field. The facies represent a depositional event, and can contain more than one sedimentary structure which is associated to the event. Facies associations are collection of different facies, which represent a depositional environment.

Table 5.2: Wentworth's classification of grain size and terminology. Table modified from Wentworth (1922).

Size (mm)	Grade terms
∞ - 256	Boulder gravel
256 – 64	Cobble gravel
64 – 4	Pebble gravel
4 – 2	Granule gravel
2 – 1	Very coarse sand
1 –0,5	Coarse sand
0,5 – 0,25	Medium sand
0,25 - 0,125	Fine sand
0,125 – 0,0625	Very fine sand
0,0625 – 0,0039	Silt
0,0039 - ∞	Clay

5.4 Digitalization of the logs

Adobe Illustrator CS4 was used in digitalizing the logs.

The digitalized logs from fieldwork are found in Appendix A, palaeocurrent measurements are presented in Appendix C. In Figure 5.3 an example log is illustrated. The legend for the logs is found in Appendix A. The main feature is thick sandstone with trough cross-stratification, symmetrical wave ripples and fragments of fossils. Samples are illustrated in the left column where they have been given a PMO-number (number in the Natural History Museum's paleontological collection in Oslo). They are also marked in the log, depending on the kind of sample (red = thin section, blue = acetate peel). Arrows illustrating palaeocurrent measurements are also included, where the real north on the log is directed towards the top. Facies and facies association are presented in the columns to the right.
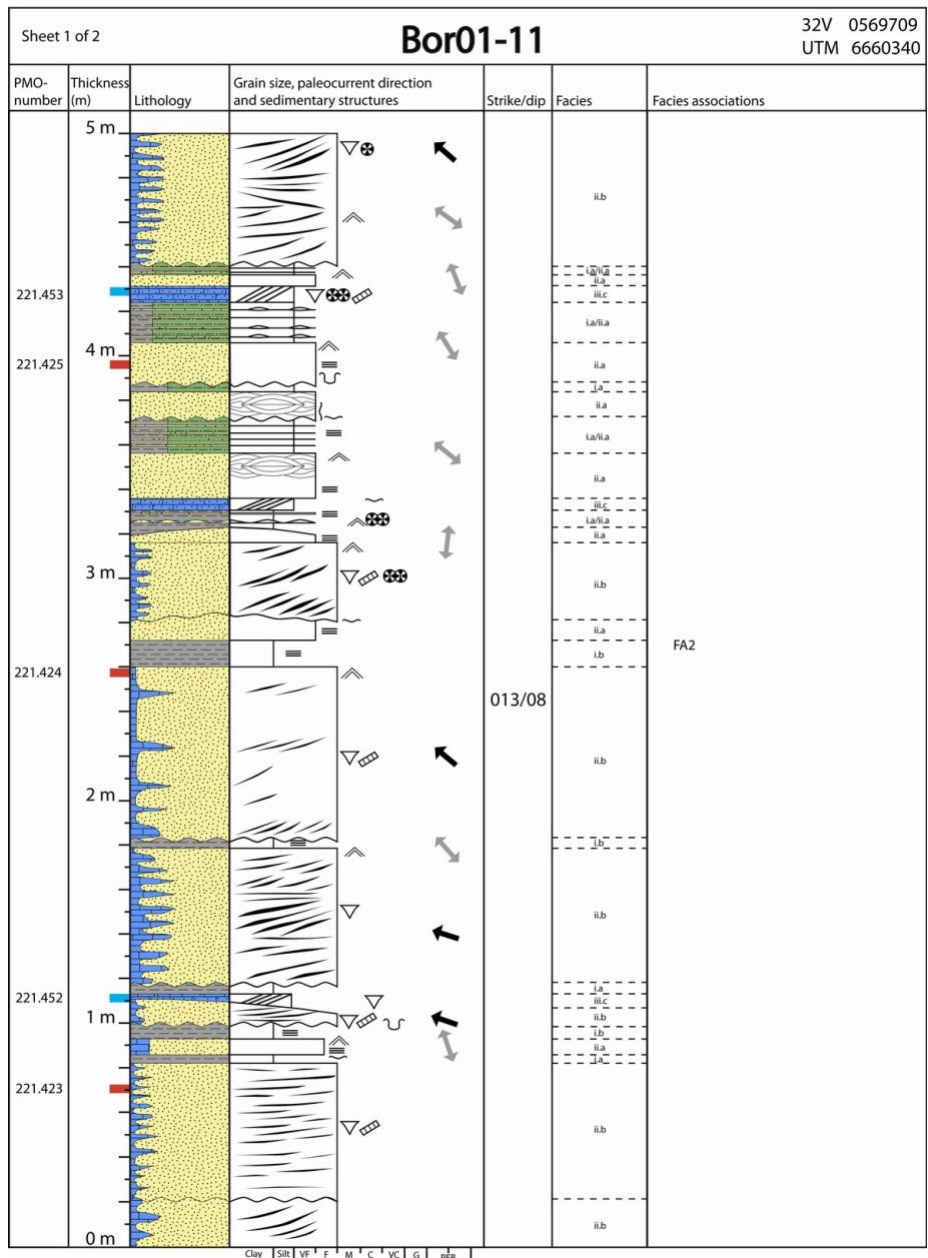
Figure 5.3: Example log from Borgen-locality where the lowermost five meters are illustrated of the Borgen01-11 log. In the right column the different facies are illustrated. Coordinates for the logged outcrop can be viewed in the top right corner. Legend can be viewed in Appendix A.

5.5 Thin sections

25 samples were selected from the five different localities (Fig. 5.1). The samples represent layers of specific interest, but were also picked to get a representative overview of the localities. The samples were cut at the Natural History Museum (Geology) at Tøyen, Oslo. 24 of the samples were sent to the University of Cracow in Poland where they were polished and prepared as standard uncovered petrographic thin sections. The last one was stained in blue epoxy and prepared by Salahalldin Akhavan at the Department of Geoscience, UiO.

The thin sections were cut to a thickness of 30 μm. An overview of the different thin sections is presented in Appendix D, where they have been given a PMO-number and a depth corresponding to the depths in the logs.

5.5.1 Point counting

Qualitative analysis was done before the point counting, to get an overview of the content in the thin sections. The main components are 1) quartz, 2) calcite cement, 3) mica, 4) K-feldspar, 5) plagioclase, 6) fossil fragments, 7) pyrite, 8) limonite and 9) opaque minerals. In each thin section 400 points were counted. The author split the quartz in two separate groups, one for single crystalline quartz and one for polycrystalline/undulating quartz. As the thin sections were not coloured and the grains have a small size, difficulty separating feldspar from quartz is a source of error. The abundance of feldspar is most likely much higher than the results show. A complete overview of the content in the thin sections is presented in Appendix D. The Quartz/Feldspar ratio can be viewed in Appendix E.

5.5.2 Description

The grain description of the quartz was done in 20 of the samples. In each sample ten grains were randomly picked. The grain size was then classified using the Wentworth (1922) scale for grain size. The roundness and sphericity of the grains were classified according to the Pettijohn (1975) scale. The results are presented in Figure 6.18.

5.6 Acetate peels

34 acetate peels were made by the author at the Natural History Museum (Geology) in Oslo. The samples were first cut, and polished with Silicon Carbide paper down to 1000 grit. The carbonate rocks were then put in an acid bath, with an HCl concentration of 5% for 4 seconds, before they were cleaned in hot water. The rocks were left to cool before immersing the polished surface with acetone and applying an acetate sheet. After a few minutes the acetate sheet was taken off, and put in a slide-frame for study under the microscope.

The acetate peels can only be used to identify the carbonate component in the samples, so the other components not consisting of carbonate are classified as "unidentified grains" during description and point counting. Most of the "unidentified grains" are most likely composed of quartz.

An overview of the acetate-peels is presented in Appendix F, where they have been given a PMO-number and a depth, which is linked to the logs in Appendix A.

5.6.1 Description

Each of the samples was described and notes were taken regarding texture, sorting and state of the fossil fragments. Part of the idea by using acetate peels was to get a larger view of the content, sorting and grading in the carbonate rock. Several of the samples had to be split in two, to fit under the microscope.

5.6.2 Point counting

Qualitative analysis was done before the counting, to get an overview of the content of the acetate-peels. The main components in the samples are 1) "unidentified grains", 2) calcite matrix 3) brachiopods, 4) bryozoans, 5) trilobites, 6) crinoids, 7) undetermined bioclasts, 8) intraclasts, 9) micrite, 10) gastropods and 11) corals.

Because of the varying size of the fragments in the carbonate samples double counting may occur. This is especially applicable for brachiopod and bryozoan fragments. In each acetate peel 300 points were counted. A complete overview of the content in the acetate peels are presented in Appendix F.

6 Results

6.1 Facies and facies association

6.1.1 Facies description

In this chapter facies have been defined based on the criteria for facies in Chapter 5.3. An overview of the facies is presented in Table 6.1. Each locality is identified in the map (Fig. 5.1). The facies description is solely based on observations in the field and pictures, and not on the laboratory data (e.g. detailed description of the fossil content).

Table 6.1: An overview of the facies observed at the studied sections.

Facies nr.	Description	Physical structures	Figure
I	**Mudstone**		
Ia	Structureless mudstone	No laminae	6.9B
Ib	Parallel-laminated mudstone	Developed with weak laminae	6.1
II	**Sandstone**		
IIa	Laminated and structureless sandstone	Parallel lamination, hummocky cross-stratification, and structureless beds. Ripples on top of bed and development of soft sediment deformation	6.1, 6.2, 6.9B
IIb	Trough cross-bedded sandstone	Sets with trough cross-bedded sandstone, fossil fragments at the base on the stoss and lee side of sets	6.5
IIc	Folded laminated sandstone	Folded laminated sandstone with a higher content of fossil fragments at the base of the unit	6.6
IId	Granule-rich sandstone	Poorly sorted granule sandstone in very fine sandstone	6.7
III	**Limestone**		
IIIa	Nodular limestone	Beds of nodular limestone	6.8
IIIb	Biosparitic limestone	Parallel-laminated and structureless beds of biosparite	6.9, 6.5B
IIIc	Cross-bedded biosparitic limestone	Cross-bedded biosparite beds with fossil fragments in a carbonate matrix	6.10

Facies I: Mudstone

Ia   Structureless mudstone

Description: This facies has clay to silt grain size, with a varying amount of the different fractions. It is characterized by no internal structures (Fig. 6.9B). Horizontal bioturbation is observed at some levels. Fossils which have been abraded are present at certain levels in the facies. The thickness varies from c. 1 cm to c. 1.4 m. Facies Ia is present at the Limovnstangen, Borgen, Åsaveien, Grunntjern and Toverud localities.

Interpretation: During fair weather conditions mud is deposited as it falls out of suspension (Collinson et al., 2006). The massive mudstone is formed by continuous deposition of clay and silt and/or later destruction of sedimentary laminae by biogenic activity.

Ib Parallel-laminated mudstone

Figure 6.1: Facies Ib; parallel-laminated mudstone and Facies IIa; parallel-laminated sandstone (Borgen).

Description: This facies is dominated by sediments of clay to silt grain size, with a varying amount of the different fractions. It is observed with weak parallel lamination (Fig. 6.1). The thickness varies from c. 4 cm to c. 13 cm. The facies is present at the Limovnstangen and Borgen localities.

Interpretation: During fair weather conditions mudstone is deposited as it falls out of suspension (Collinson et al., 2006). The weak laminated mudstone is caused by a decrease in biogenic activity.

Facies II: Sandstone

IIa Laminated and structureless sandstone

Description: The facies consists of very fine to fine sand which is generally homogenous, and is partly calcite cemented. Bioclastic material is present in the bed, with the highest concentration of fossil fragments at the base. Facies IIa is observed with parallel lamination (Fig. 6.1),
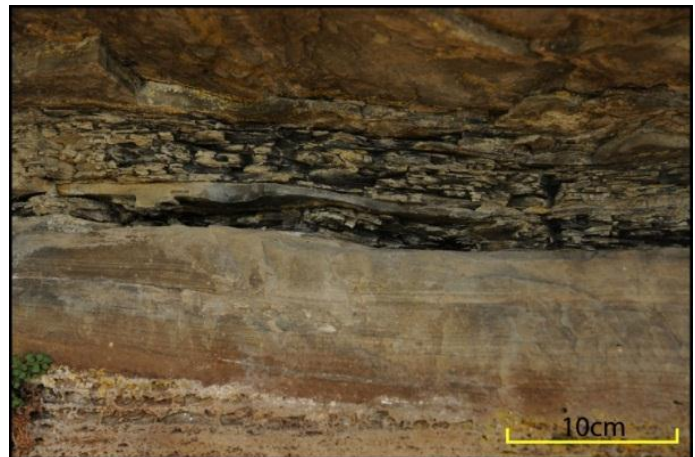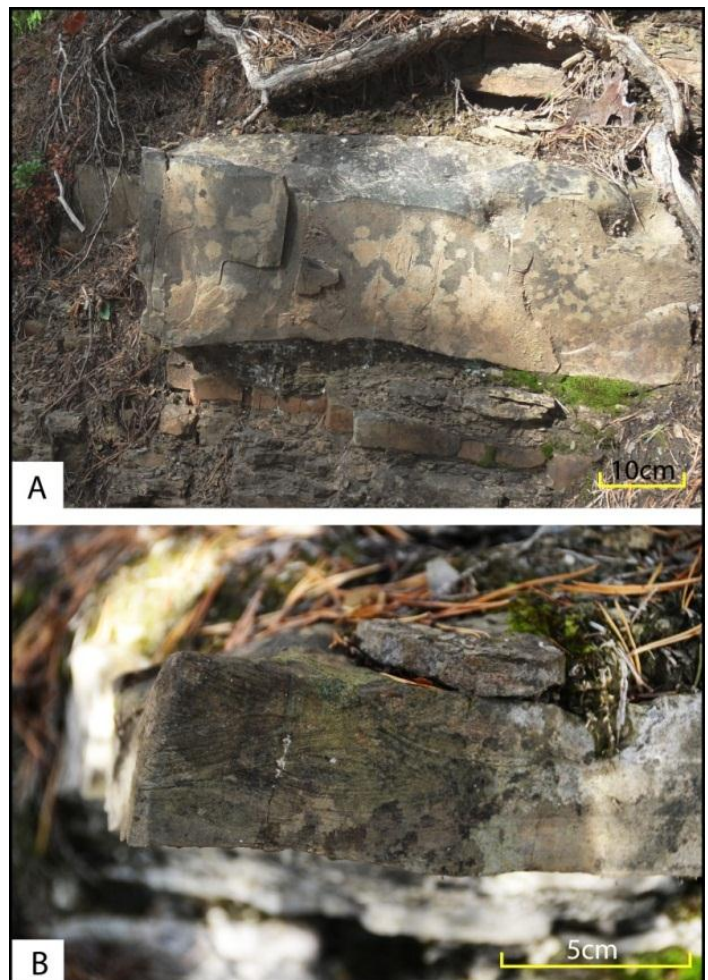

Figure 6.2: A) Facies IIb; massive sandstone, B) Facies IIb; hummocky cross-stratified sandstone (Limovnstangen).

hummocky cross-stratification (Fig. 6.2B) and as structureless sandstone (Fig. 6.2A). The base is observed as both erosive and non-erosive with gutter casts. This facies can contain parallel lamination, hummocky cross-stratification and structureless sandstone together in the same bed, but also separated in single beds. Soft sediment deformation is seen at the base and at the top of beds (e.g. loaded ripples, load casts and ball-and-pillow structures). Ripples with rounded crests are seen at the top. Asymmetric ripples are observed. Water escape structures are also recorded in some beds of this facies. Vertical bioturbation is present and also horizontal bioturbation is seen at the top and at the base of the beds. Beds of Facies IIa are laterally continuous for several meters where they have wavy tops. Isolated lenticular beds also occur (Fig. 6.9B). The facies range in thickness from c. 1 cm to c. 40 cm. Facies IIa is present at the Limovnstangen, Borgen, Åsaveien, Grunntjern and Toverud localities.
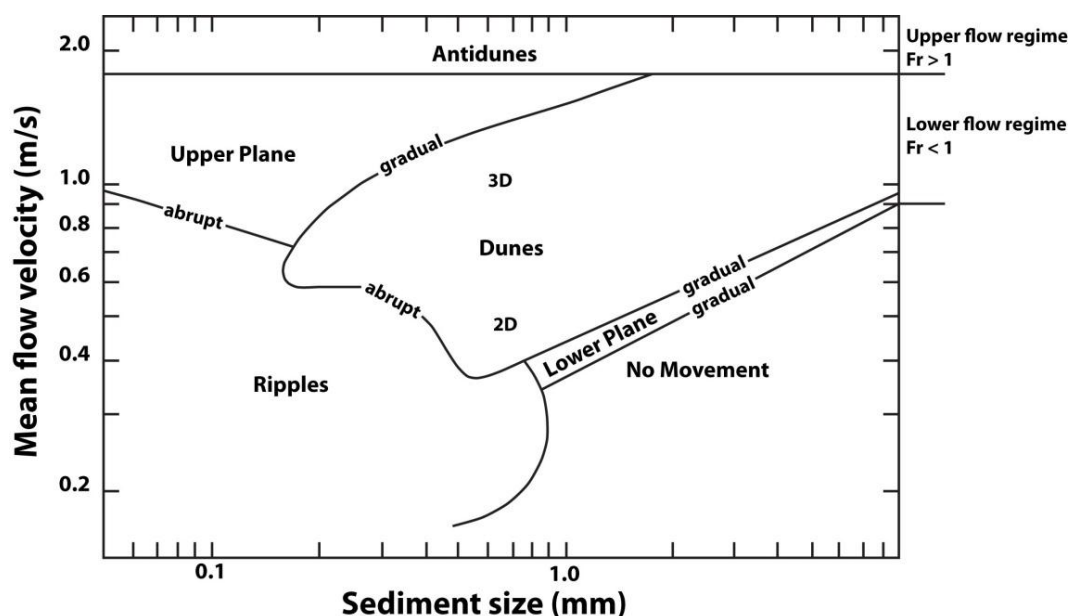

Figure 6.3: Diagram of the formation of bedforms, the relationship between the mean flow velocity and sediment size. Figure modified from Southard and Boguchwal (1990).

Interpretation: The sharp contact to the underlying beds is caused by either erosion of geostrophic currents or wave oscillatory flow (Myrow and Southard, 1996). Parallel lamination represents deposition during powerful wave oscillations that are followed by weaker ones (Myrow and Southard, 1996). Hummocky cross-stratification is created by unidirectional flows, most likely from geostrophic currents and wave oscillations (Myrow and Southard, 1996, Dumas and Arnott, 2006). Hummocky cross-stratification falls within the domain of ripples in the flow-regime diagram (Fig. 6.3). Gutter cast is an erosional structure

created by a stage of erosion followed by a stage of deposition as the energy decreases during storms (Myrow, 1992b). The symmetrical ripples have been created in the waning stages of the storm by the wave generated oscillatory flow. Post-depositional loading structures are formed due to porosity differences between the mudstone and the sandstone, likely indicating a rapid deposition of the sandstone beds (Collinson et al., 2006). The beds which appear structureless were either deposited too rapidly for any structures to form, or the structures have been destroyed during reworking by organisms (cf. Collinson et al., 2006). The former is more likely as intense bioturbation is lacking. The silt to fine sand composition of the sandstone beds (Fig. 6.18) is in accordance with the occurrence of hummocky cross-stratification (Dott and Bourgeois, 1982, Li and King, 2007). Together these sedimentary structures are characteristic for storm deposits (Dott and Bourgeois, 1982, Myrow, 1992a, 1992b, Dumas and Arnott, 2006). Storm deposits show a change in deposition (e.g. sedimentary structures and grain size) upward in the bed and can be split into several levels, and are termed tempestites (Myrow and Southard, 1996). An idealized storm sequence has been named Dott-Bourgeois sequence (Dott and Bourgeois, 1982) (Fig. 6.4).
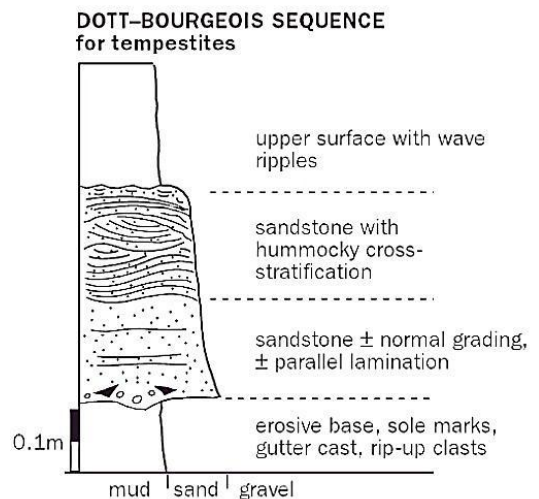

Figure 6.4: Idealized storm sequence; Dott-Bourgeois sequence. Figure from Stow (2005).

IIb Trough cross-bedded sandstone

Description: The facies consists of fine-grained sandstone in bed sets. The sandstone is homogeneous and partly calcite cemented. Facies IIb is made up of bed sets characterized by trough cross-bedding (Fig. 6.5A). At the lee side of each set fragments of corals, bryozoans and brachiopods occur, sometimes draped in a silt carbonate matrix forming a lag layer (Facies IIIb) (Fig. 6.5B). This is also observed on the stoss side; however, in a lesser degree. The beds of this facies have erosive bases. The fragments are in the size order of c. 0.5 cm to c. 10 cm, where the majority is smaller than 2cm. At some of the outcrops symmetrical sinuous ripples are observed superimposed on the stoss side. Strata of this facies extend laterally for several meters and show little variation in thickness. Beds of the facies range in thickness from c. 10 cm to c. 1.75 m. The majority of the beds are thicker than 1m. Facies IIb is present at the Borgen and Åsaveien localities.

Interpretation: The trough cross-bedded sandstone develops by migration of unidirectional three-dimensional dunes (Ashley, 1990) which are deposited in the upper part of the lower flow regime (Fig. 6.3). The lag deposit is formed by erosion of the beds and the reactivation surface between the sets. The process of sorting has been mentioned in Kreisa (1981), where the eroded beds have been winnowed; sorting the material. The palaeocurrent orientation of the foreset varies because of the sinuous pattern of the crestlines in the trough cross-bedded sets.
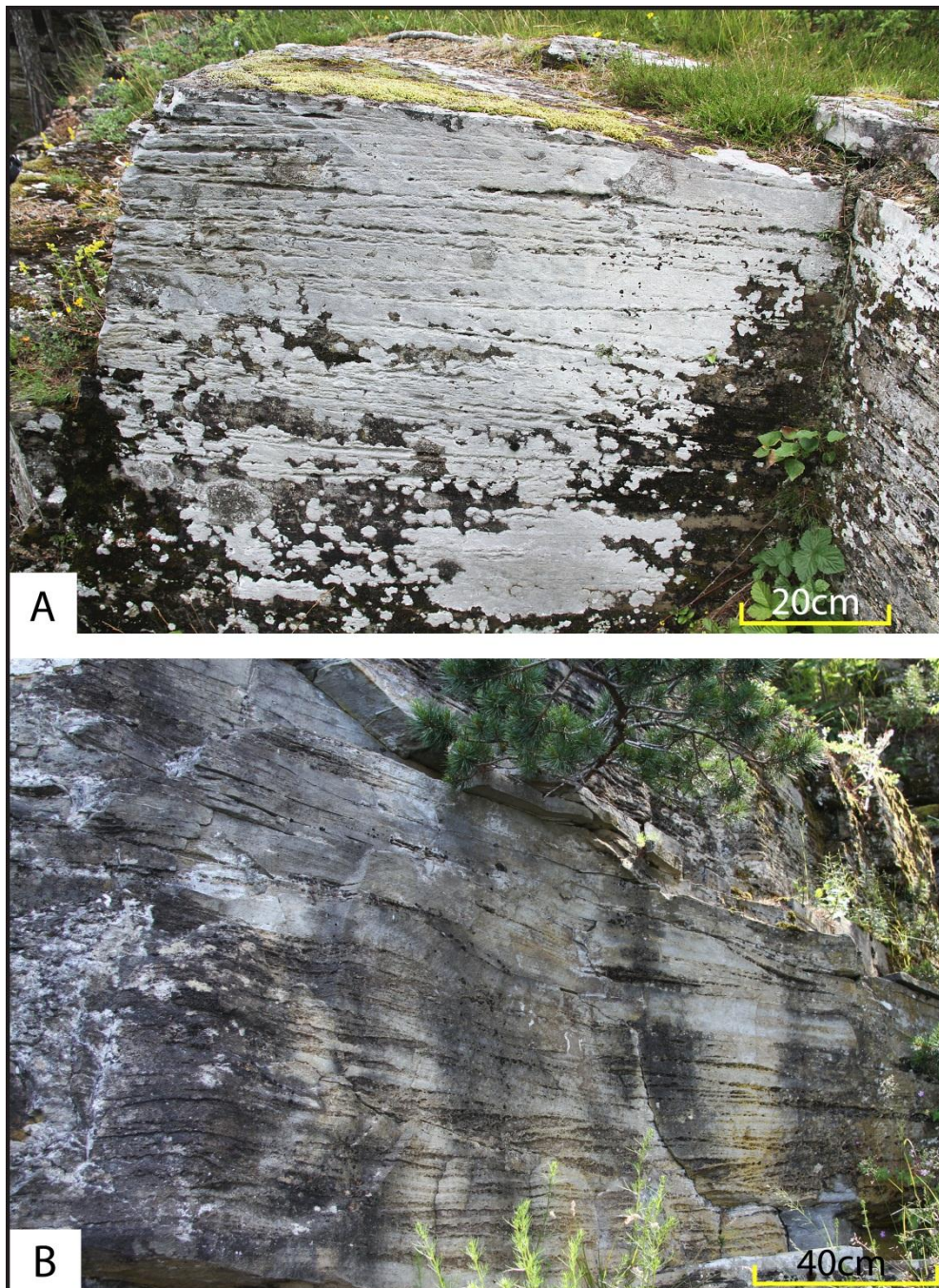

Figure 6.5: A) Facies IIb; Trough cross-bedded sandstone (Borgen). B) Facies IIb; Trough cross-bedding (Borgen).

IIc Folded laminated sandstone

Description: Facies IIc consists of very fine-grained sandstone with fossil fragments, with an upward decrease in fossil fragments in the depositional units. The lower part of the laminated sandstone unit has horizons with higher bioclastic concentration. The upper part, which is mainly dominated by siliciclastic material, has an internal folded lamination (Fig. 6.6B). The base of the layer is observed as abrupt and slightly erosive (Fig. 6.6A). The bioclastic content consists of fossil fragments; corals, brachiopods, gastropods and bryozoans. This facies occurs in a c. 83 cm thick unit. The lateral extent is difficult to determine. The facies is only present at the Åsaveien locality.

Interpretation: This bed is a slump-folded unit which is recognized by the undisturbed underlying and overlying units, as generally described by Collinson et al. (2006). Slumping units usually occur in interbedded units, with a high proportion of fine-grained sediments. Unconsolidated sediments resting on a slope might become unstable due to high pore-fluid pressure in a particular layer (Collinson et al., 2006). The layers resting on top will then become unstable and move down slope due to gravity.
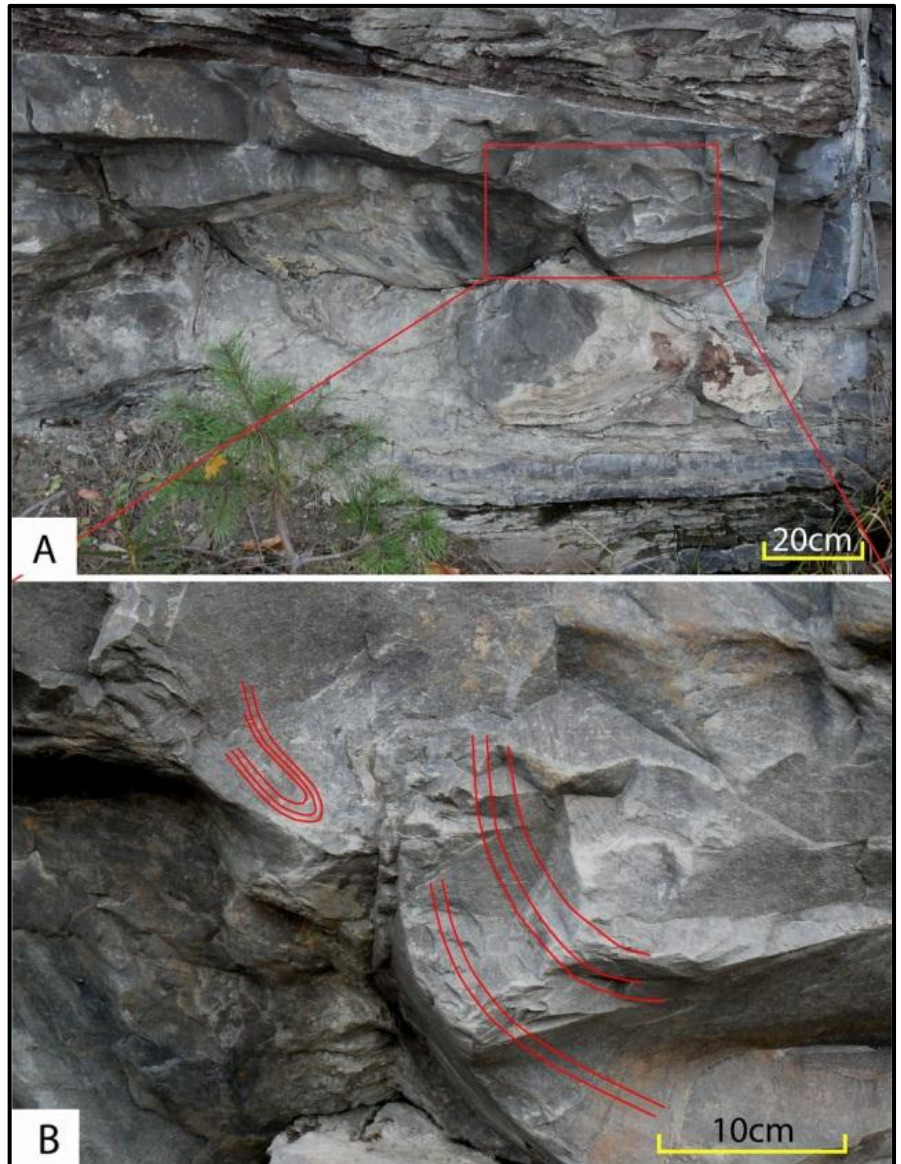

Figure 6.6: A) Facies IId; folded laminated sandstone (Åsaveien). B) Facies IId; close up of the folded laminated sandstone (Åsaveien).

37

IId Granule-rich sandstone

Description: The facies comprises beds characterized by abundant poorly sorted grains of quartz granules. The beds contain about 50% granule grains that are rounded and embedded in a matrix dominated by very fine sand (Fig. 6.7). The base of Facies IId beds is erosive where the sandstone fills runnels in the underlying Ordovician strata beneath the Sælabonn Formation. Presence of pyrite is observed where the granule-rich sandstone is bounded to the underlying massive limestone. The thickness of the Facies IId beds is c. 5 cm. Facies IId is only present at the Toverud locality.

Interpretation: The granule quartz grains are deposited during erosion of the underlying sediments and have later been in-filled by very fine sandstone. The quartz grains are rounded which suggest a high degree of reworking.

Figure 6.7: Facies IId; granule-rich sandstone (Toverud).

Facies III: Limestone

IIIa Nodular limestone

Description: This facies is characterized by carbonate nodules which form layers (Fig. 6.8A). The nodules are sub-rounded (Fig. 6.8B). Depositional units of this facies range in thickness from c.10 cm to c. 20 cm. The facies is only present at the Toverud locality.

Interpretation: According to Möller and Kvingan (1988) the formation of nodular limestone in shales is connected to the palaeogeographic setting. Clays containing carbonate sediments are deposited below the fairweather wave base. Formation of nodular limestone will occur during diagenesis of the sediments.
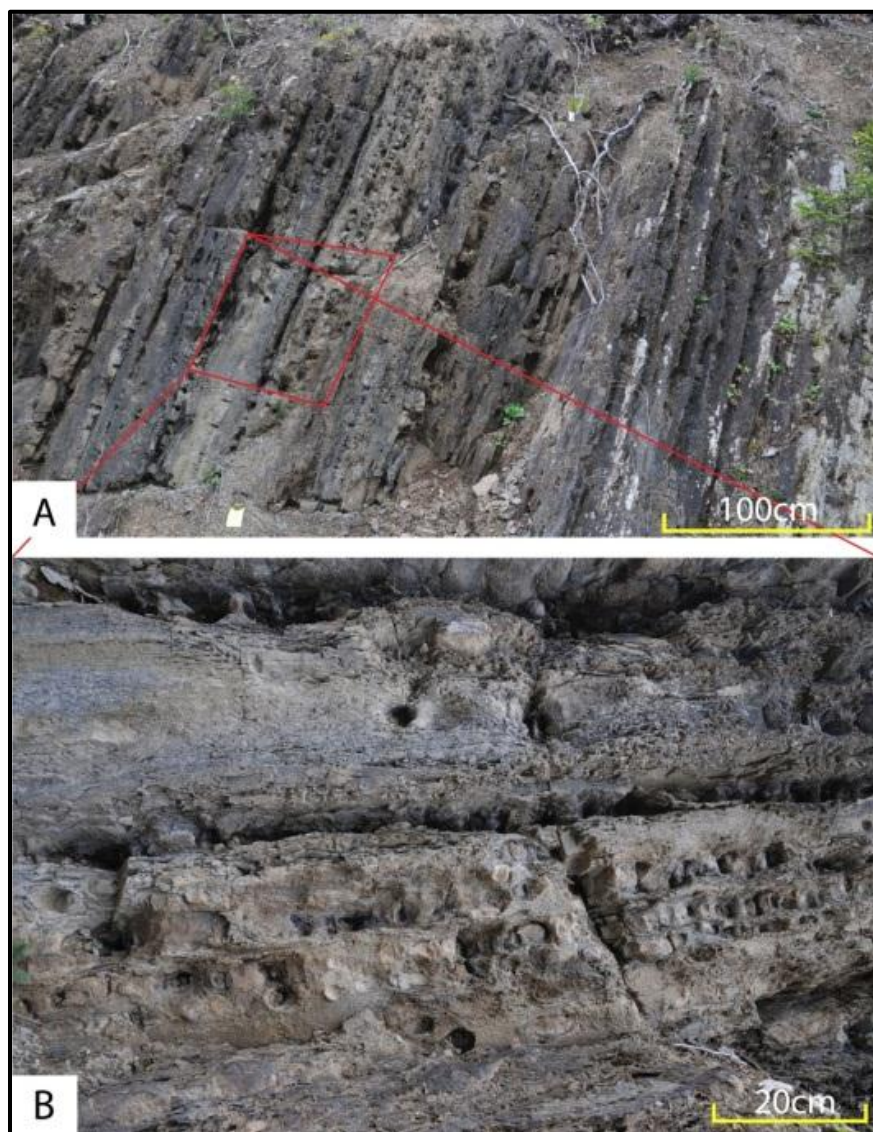

Figure 6.8: A) Facies IIIa; nodular limestone (Toverud). B) Facies IIIa; close up picture of nodular limestone facies rotated 90° (Toverud).

IIIb Biosparitic limestone

Description: The grain size has a homogenous distribution in beds of this facies. The matrix has silt to very fine grain size. The beds are composed of a calcareous matrix which has fragments and whole fossils in it. A varying degree (small amounts) of siliciclastic material is present. Clasts composed of siliciclastic material also occur (Fig. 6.9A). Parallel-laminated and structureless beds are abundant in the facies. The parallel lamination is observed with thin laminae (<=1 mm) of siliciclastic material marking the lamination. Beds of Facies IIIb are present with either non-erosive or erosive bases. Bed thickness of this facies ranges from c. 1 cm to c. 20 cm. Thin beds or laminae of this facies also occur as lag deposit on trough cross-bedded sets at Borgen and Åsaveien (Fig. 6.5B). Depositional units of the facies are laterally extensive through the outcrop forming isolated bodies of lenticular geometry (Fig. 6.9B). This facies is observed at the Limovnstangen, Borgen, Åsaveien, Grunntjern and Toverud localities.

Interpretation: The beds are termed as bioclastic or coquina beds and are defined as biosparitic beds by Folk (1962). As the sandstone beds (Facies IIa), the biosparitic limestone beds also display parallel lamination and formation of gutter casts at the base. This suggests that the same type of process has been responsible for the deposition of these beds. However, the lack of structures such as hummocky cross-stratification is explained by the coarse grain size of the material present. The shell fragments make it harder to
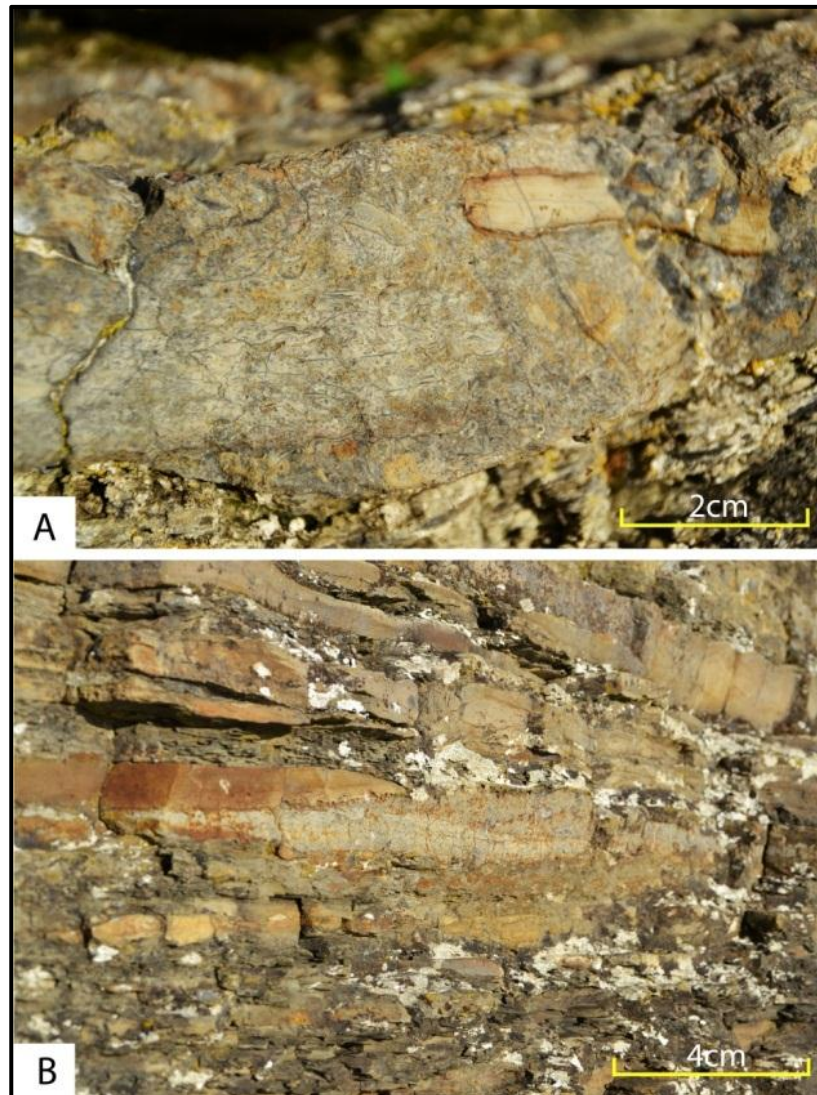

Figure 6.9: A) Facies IIIb; Massive biosparite bed with siliciclastic intraclasts. B) Facies IIIb; Isolated lenticular biosparite bed.

40

form structures. The clasts observed are intraformational as storms have eroded and winnowed adjacent and underlying beds.

IIIc Cross-bedded biosparitic limestone

Description: Grain size has a homogenous distribution in the facies, where the matrix has a silt grain size. The beds are composed of a calcite matrix and have fragments as well as whole fossils in them. The facies is characterized by cross-bedding. A varying amount of siliciclastic material is present in the facies, where it marks the cross-bedding (Fig. 6.10A). The base of the facies is sharp and is both erosive and non-erosive. The geometry of the beds is laterally extensive, with wavy tops forming small dunes (Fig. 6.10B). The crestlines of the dunes seem to be straight but are difficult to observe. The bed thickness of this facies ranges from c. 6 cm to c. 18 cm. Facies IIIc is recorded at the Limovnstangen and Borgen localities.

Interpretation: The cross-bedded biosparitic limestone are two-dimensional dunes that are deposited in the lower flow regime (Fig. 6.3) (Southard and Boguchwal, 1990). They have previously been referred to as mega ripples by Thomsen (1982). These dunes migrate and erode new material from lower beds.
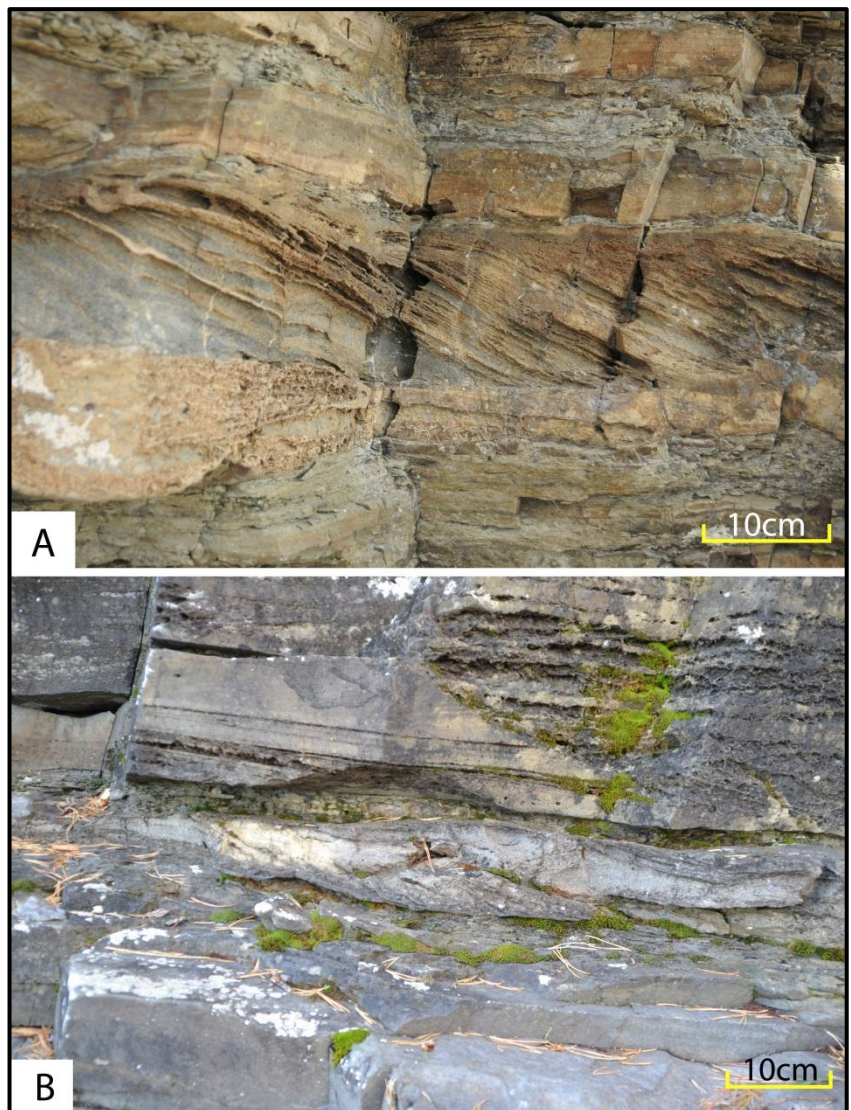

Figure 6.10: A) Facies IIIc; Cross-bedded biosparitic limestone (Limovnstangen). B) Facies IIIc; Cross-bedded biosparitic limestone (Borgen).

6.1.2 Facies associations

Based on the defined facies in Table 6.1, five facies associations and sub-facies associations are defined. The two logs from the Borgen locality and the three logs from the Limovnstangen locality have been merged to make one log for each locality, which illustrate the general development at the locality.

Table 6.2: An overview of the facies association at the studied sections, based on facies presented in table 6.1. Detailed logs of the outcrops are presented in Appendix A.

Facies association	Sub-facies associations	Facies nr.	Logs	Figure
FA1	FA1a	Ia, Ib, IIa, IIIb	Lim01-11, Lim02-11, Lim03-11, Tov-11, Grunn-11	6.11
	FA1b	Ia, IIa, IIIb	Lim01-11, Lim02-11, Lim03-11, Tov-11	6.11
	FA1c	Ia, IIa, IIIb, IIIc	Lim01-11, Lim02-11, Lim03-11, Tov-11	6.11
FA2		Ia, Ib, IIa, IIb, IIc, IIIc	Bor01-11, Bor02-11, Åsa-11	6.12, 6.13
FA3		IId	Tov-11	6.7

FA1

Description

This facies association has been divided into three sub-facies associations based on the dominating lithology in the sections. These sub-facies associations are present at the Limovnstangen, Toverud and Grunntjern localities (Appendix B). It should be noted that the division of the sub-facies associations are more detailed at Limovnstangen than at Toverud, due to scale. Facies IIIb are observed following Facies IIa, as couplet beds. This occurs for the most parts in sub-facies association FA1c.

FA1a

This sub-facies association is characterized by the dominance of mudstone (Facies Ia and Facies Ib), which is interbedded by beds of sandstone (Facies IIa) and biosparitic limestone (Facies IIIb) (Fig. 6.11). The sandstone and biosparitic limestone beds are further spaced from each other with mudstone in between in this sub-facies association. The thickness of the beds varies between the thinnest and thickest occurrences of the respective facies (Chapter 6.1.1). Several levels of this facies association are observed at the different outcrops, except

42

Grunntjern (log Grunn-11) where only one level is recognized. The thickest unit is observed at Toverud where it ranges from 23.5 m to 52.3 m. Sub-facies association FA1a is both underlying and overlying the sub-facies association FA1b or FA1c. The sub-facies association is recognized at the Limovnstangen, Toverud and Grunntjern localities.
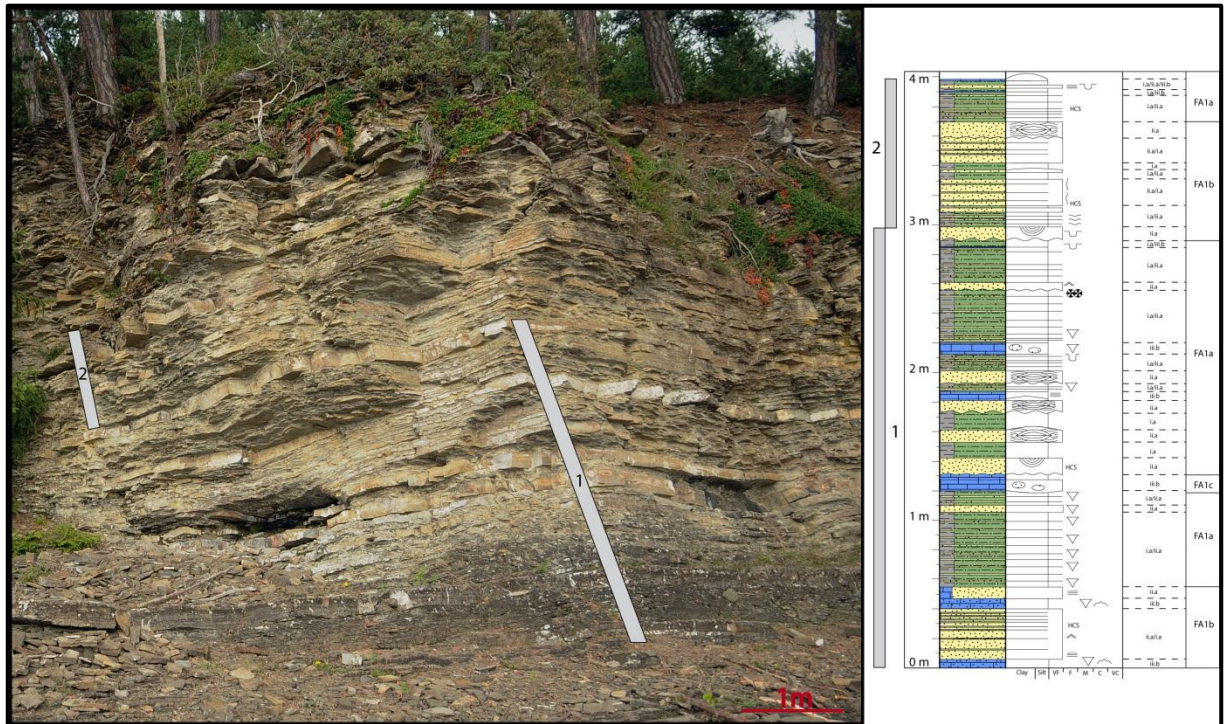

Figure 6.11: Example of the succession in facies association FA1 at the Limovnstangen locality (log Lim01-11).

FA1b

This sub-facies association is characterized by the dominance of sandstone of Facies IIa, which is interbedded in mudstone of Facies Ia, together with biosparitic limestone of Facies IIIb (Fig. 6.11). The dominance of the sandstone beds in this sub-facies association is both related to spacing and thickness of the beds. Several levels of this facies association are observed. It has a decreasing occurrence towards the top of the Sælabonn Formation. The thickest unit is seen at Toverud (log Tov-11) where it ranges from 52.3 m to 64.5 m. Facies association FA1b is succeeding and succeeded by either FA1a or FA1c at all localities. The sub-facies association is recognized at the Limovnstangen and Toverud localities.

FA1c

This sub-facies association is characterised by the dominance of biosparitic limestone of Facies IIIb and cross-bedded biosparitic limestone of Facies IIIc (Fig. 6.11). The limestone is, together with the sandstone (Facies IIa), interbedded in mudstone (Facies Ia). The dominance

of the limestone beds in this sub-facies association is both related to spacing and thickness of the beds. The thickest unit is recognized at Toverud (log Tov-11) where it ranges from 5.9 m to 7.5 m. Sub-facies association FA1c is succeeding and is succeeded by either FA1a or FA1b at all localities. The sub-facies association is recognized at the Limovnstangen and Toverud localities.

Interpretation

The sub-facies associations display the same type of depositional environment, but the energy and material available varies between these sub-facies associations. Dattilo et al. (2008) discussed two possible causes for the formation of couplet beds; (i) storm-winnowing proximality and (ii) episodic starvation. The former model is favoured for the Sælabonn Formation. This occurrence is explained by currents from storms which acted on the sea-bottom concentrating shells from the underlying substrata, and deposited them as layers (cf. Kreisa, 1981, Drummond and Sheets, 2001). The bioclastic layers were later covered by the siliciclastic sediments as they were transported out to the area of deposition, forming an upward fining storm sequence. The Markov chain analysis (Table 6.3) showed that this occurred in 30% of the cases, suggesting that there are fluctuations in the energy present. These bioclastic deposits are autochthonous while the siliciclastic sediments are allochthonous, transported in from a siliciclastic source, interpreted in accordance with the principles by Kreisa (1981).

Units of the sub-facies association **FA1a** have been deposited into areas where the energy has been lower, with less frequency or availability of material. According to Thorne et al. (1991) tempestites get thinner and more uniform with increasing water depth, as the length of the waves are connected to the depth of the orbitals.

Units of the sub-facies association **FA1b** have been deposited in areas where the energy has been high as siliciclastic material has been transported out and deposited on to the shelf.

Units of the sub-facies association **FA1c** have been deposited in areas where the energy has been high enough to sort out the bioclastic material from the adjacent areas. Beds where only a bioclastic layer is present, not as couplets, suggests more proximal conditions as the siliciclastic component has been transported further basinward (Dattilo et al., 2008). According to Pérez-López and Pérez-Valera (2012) low energy and short distance for sediments transport or high energy with no lateral transport would cause the wave winnowing bioclastic deposits.

44

In summary, the FA1a represents periods with lowest energy, and FA1b represents periods with higher energy. FA1c represents periods of a more proximal position where bioclastic layers were deposited and siliciclastic sediments were transported further basinward. These sediments are deposited in the offshore-transition area on the shelf (Fig. 3.4).

FA2

Description

This facies association is recognized at the Borgen and Åsaveien localities (Appendix B), and is characterized by trough cross-bedded sandstone (Facies IIb), where the sets are draped with biosparitic limestone (Facies IIIb).
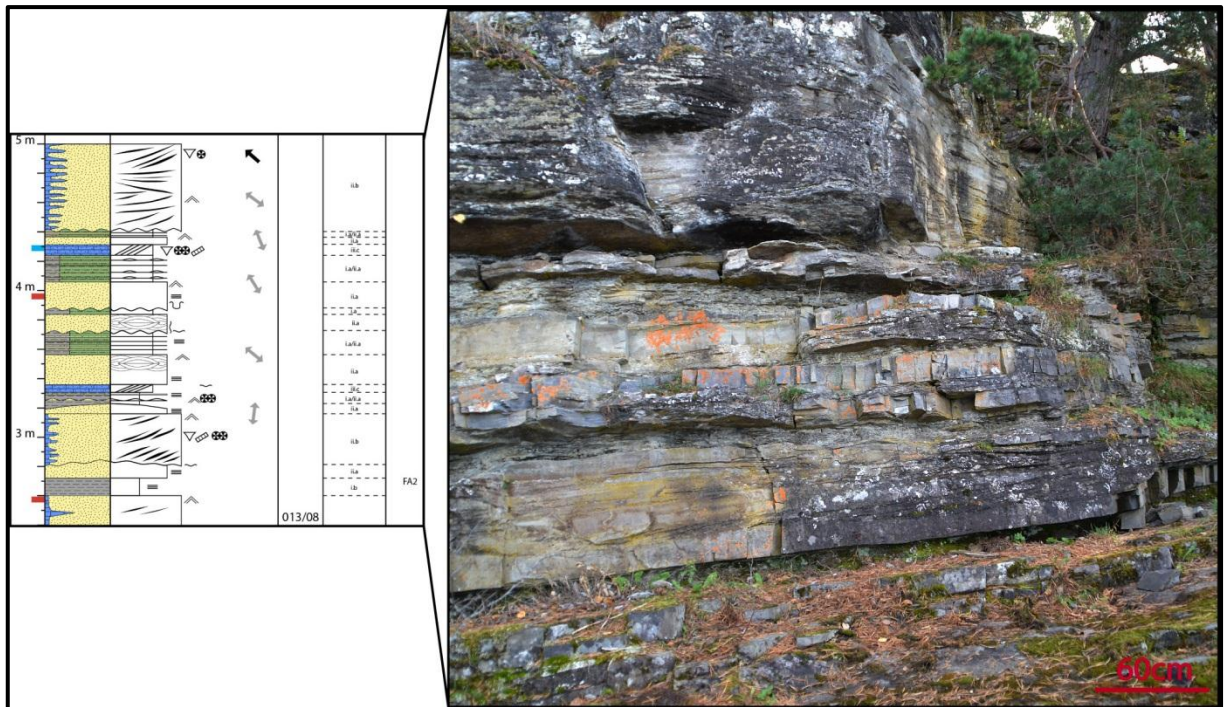

Figure 6.12: The two levels where Facies IIIc is succeeding Facies Ia and is followed by Facies IIa at Borgen (log Bor01-11).

The thickness of the facies association at Borgen is 9.2 m. Thick cosets of trough cross-bedded sandstone (Facies IIb) are succeeded by mudstone of Facies Ia and Facies Ib, or cross-bedded biosparitic limestone of Facies IIIc. The mudstone is interbedded with sandstone beds of Facies IIa. Facies IIIc beds are often succeeding beds of Facies IIb, except in two levels (3.30 m and 4.25 m) where it is succeeding Facies Ia and succeeded by Facies IIa (Fig. 6.12). A repeating pattern of trough cross-bedded sandstone (Facies IIb) followed by mudstone (Facies Ia) or cross-bedded biosparitic limestone (Facies IIIc) is recorded (Fig 6.13). The thickness of the depositional unit of this facies association at Åsaveien is 9.3 m. The cross-bedded biosparitic limestone (Facies IIIc) is not observed, and the siliciclastic component is

more dominant. The trough cross-bedded sandstone is succeeded by mudstone of Facies Ia or sandstone of Facies IIa. This is recognized as a repeating pattern. A unit (0.58m – 1.40m) of folded laminated sandstone (Facies IId) is observed succeeding mudstone (Facies Ia) which is interbedded by sandstone (Facies IIa).
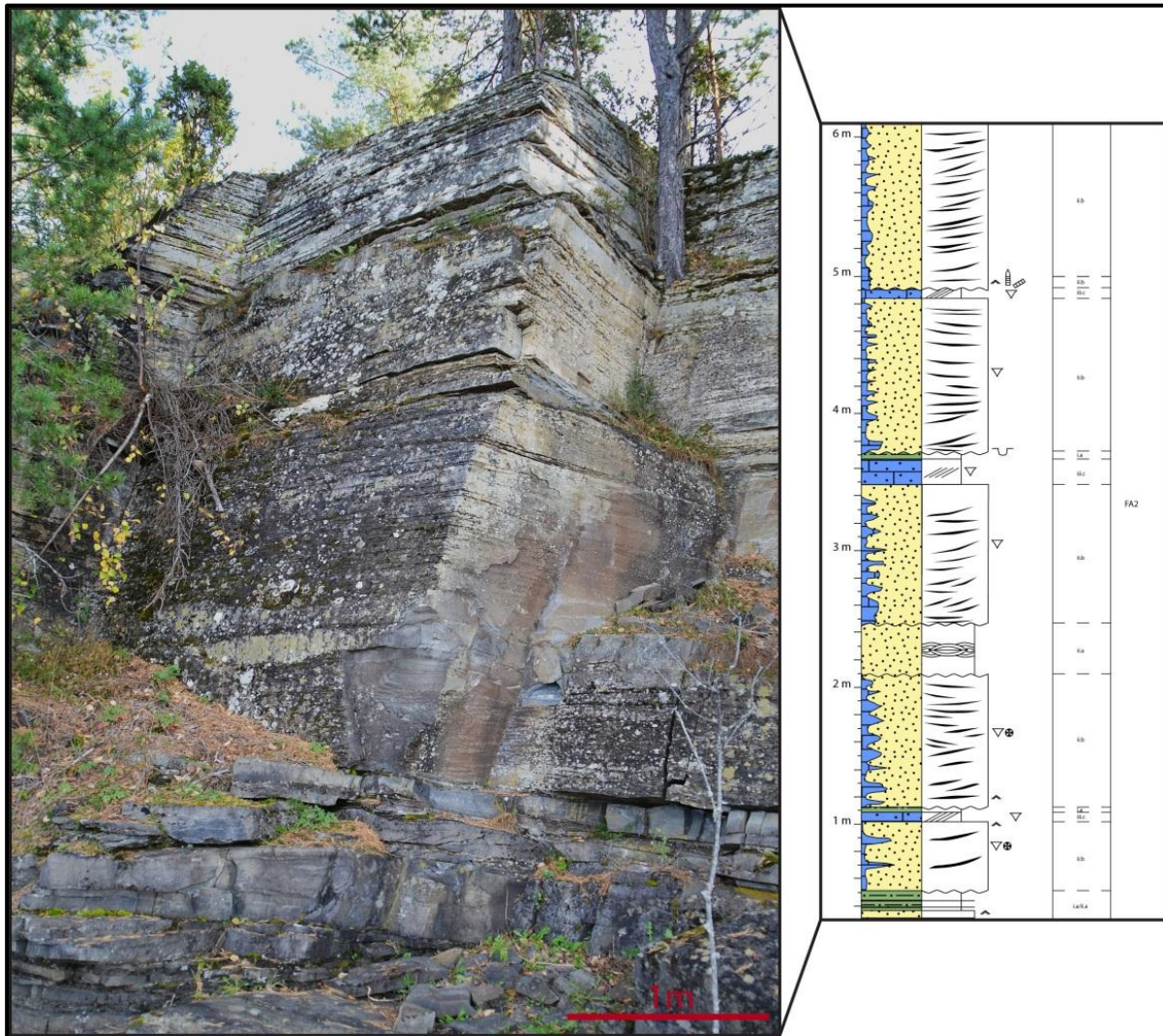

Figure 6.13: A repeating pattern of Facies IIb beds succeeded by Facies IIIc at Borgen (log Bor02-11).

Interpretation

This facies association represents siliciclastic shoals with the presence of migrating three-dimensional dunes. They are probably not sand ridges, as they do not show the same composition as the sand ridges in the paper by Gaynor and Swift (1988). However, this need further study. The cyclicity observed is due to the allocyclic conditions where an increase in sea-level traps the siliciclastic sediments further shoreward. The abrupt change in both lithology and energy (sandy 3D-dunes to biosparitic 2D-dunes) suggests an increase in water-level as the bioclastic component starts to dominate forming storm modified dunes. The

continued increase in sea-level is indicated by deposition of fair-weather deposits such as mudstone (Facies Ia or Ib) interbedded by tempestites of sand (Facies IIa). The biosparitic lag deposit in the 3D-dunes suggests a continuous presence of bioclastic material which starts to dominate as the siliciclastic component is shut off. The low abundance of bioclastic material at the Åsaveien locality could be caused by the intra-shoal position, as the bioclastic 2D-dunes did not migrate that far. Penland et al. (1989) observed that the offshore sand shoals could extend for several kilometres in both length and width. Factors controlling the cyclicity could be eustatic sea-level rise, which could be related to Milankovitch cycles, or regional sea-level rise caused by tectonic movement. The overall trend in the Djupvarp Member, at Borgen and Åsaveien, suggests a transgression, as the shoal migrates. The channel observed at Borgen was caused by alongshore and onshore winds which set up down welling that created rip currents which cut through the dunes. This is an interpretation which is in accordance with the principles by Kreisa (1981). The slumping at Åsaveien is caused by a disturbance of sediments on the dunes, causing a collapse of adjacent sediments.

In summary this facies association represents storm dominated shoals where three-dimensional dunes were present, which occasionally were drowned by increased sea-level as the sediment supply was not able to keep-up with the rising sea-level.

FA3:

Description

The facies association FA3 is characterized by a c. 5 cm thick layer of granule quartz grains in very fine sandstone (Facies IId) which is present at the base Sælabonn Formation/top Langøyene Formation. This facies association is a special case only containing one facies, but it might be present as a thicker unit elsewhere composed of several facies. Facies association FA3 is only recognized at Toverud.

Interpretation

The granule quartz grains have been eroded from the underlying Ordovician strata, where the flow of water, which has created the karst surface, has not been strong enough to transport the quartz grains any further. The very fine sandstone has later been in-filled by a transgression causing the formation of this lag layer. The erosional boundary depicts a ravinement surface created during a transgression (Yang, 2007).

6.2 Petrographic and sedimentological descriptions of the studied localities

6.2.1 Limovnstangen

Sedimentological description

Figure 6.14: Limovnstangen locality.

At the Limovnstangen locality (Fig. 6.14) 32 meters were logged, and the Limovnstangen Member is recognized. This locality was logged at three outcrops (logs Lim01-11, Lim02-11 and Lim03-11) to get a better coverage of the locality. The outcrops belong to facies association FA1, which has an internal variation in the occurrence of the sub-facies associations FA1a, FA1b and FA1c (Fig. 6.11 and Fig. 6.15). The base of the Limovnstangen Member is not observed at this locality. The top is observed at 31 meters where the Rytteråker Formation is the overlying unit (Fig. 6.15). The member has an upward decrease in limestone beds with a minimum at 19 meters, with an upward increase from 20 meters. The sandstone beds generally decrease in frequency upward, with maximum and minimum peaks one to two meters apart (Fig. 6.15). Sub-facies association FA1a is the dominant component, whereas sub-facies association FA1b and FA1c are recognized as pulses. Units of these sub-facies associations are on the average thinner than FA1a units.

Table 6.3: Results of Markov chain analysis of the facies occurring at the Limovnstangen locality. The relationships between the facies are presented in % and (#).

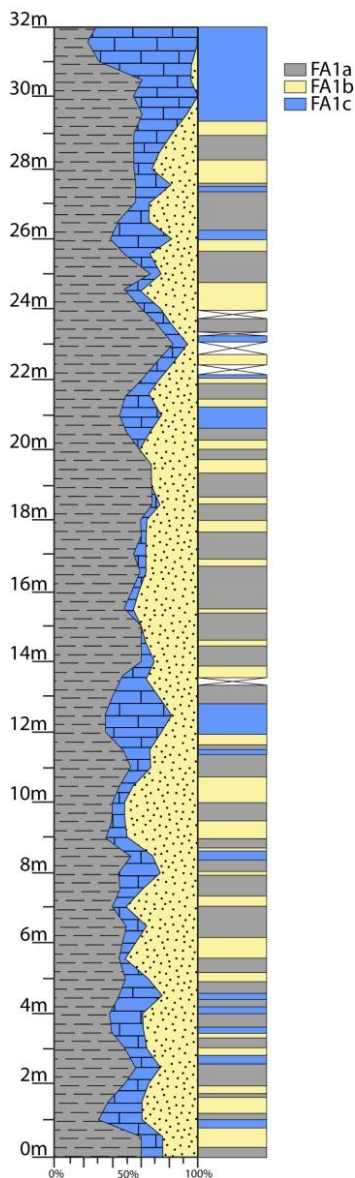|		Overlying facies				
		IIa	Ia	IIIb	Ib	IIIc
Underlying facies	IIa	0,4587 (2)	92,89 (405)	6,422 (28)	0,2294 (1)	0 (0)
	Ia	77,41 (394)	0,1965 (1)	21,41 (109)	0 (0)	0,9823 (5)
	IIIb	29,93 (0)	70,07 (0)	0 (0)	0 (0)	0 (0)
	Ib	0 (0)	0 (0)	100 (1)	0 (0)	0 (0)
	IIIc	0 (0)	100 (4)	0 (0)	0 (0)	0 (0)

Limovnstangen

Figure 6.15: Lithological log of the Limovnstangen section, with the occurring sub-facies associations in the section.

A Markov chain analysis was tested out to see if there was a statistically significant pattern between the occurrences of the different facies at the locality (Table 6.3). The results show that there is a 30% and a 70% chance of Facies IIIb being succeeded by Facies IIa or Facies Ia, respectively. There is a 93% and a 6% chance of Facies IIa being succeeded by either Facies Ia or Facies IIIb, respectively, and Facies Ia has a 77% chance of being succeeded by Facies IIa and a 21% chance of being succeeded by Facies IIIb, respectively. As there are too few occurrences of the other facies, their percentages are insignificant to the statistic.

Mineral content and texture

Seven thin sections were prepared from Limovnstangen, all from the Limovnstangen Member. The main components in the samples are quartz and calcite, where quartz ranges from 15.0% - 55.0% and calcite from 32.0% − 80.5%. Undulating and polycrystalline quartz account for 1.3% - 8.0% of the total quartz content in the samples. The feldspars account for 2.8% − 10.8% of the content in the samples. Mica (0.3% − 1.8%), fossil fragments (0.3% − 1.8%) and opaque minerals (0.3% − 1.0%) are present in four of the samples and are close to insignificant. Small amounts of pyrite and limonite are also observed in the samples, where the former can be seen in one sample (0.5%)
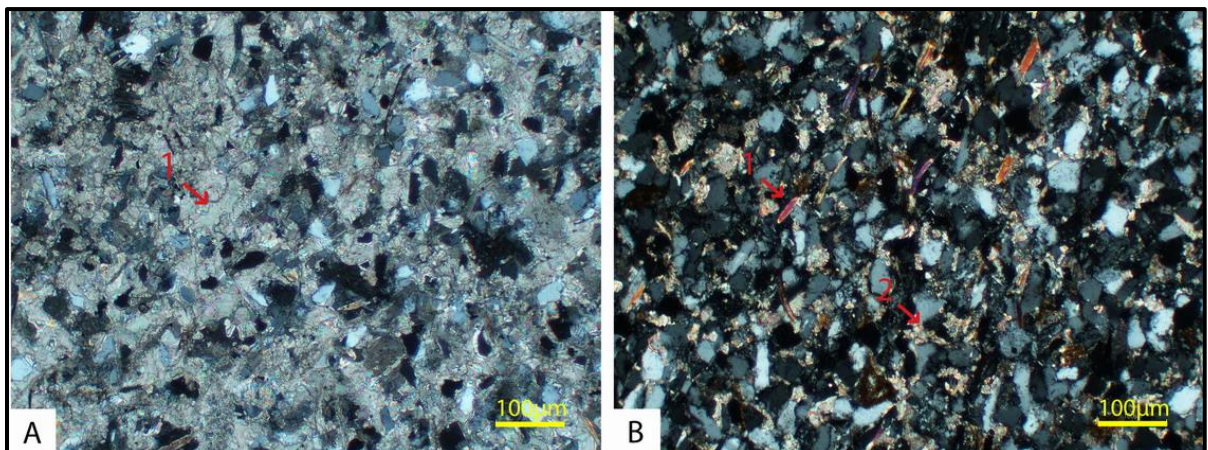

Figure 6.16: A: 1) Calcite cement. B: 1) Mica. 2) Patchy calcite cement.

49

and the latter in two samples (0.3% and 0.8%). A full overview of the content in the samples is presented in Appendix D.

The rocks are calcite cemented, where the pore space is filled with calcite enclosing the detrital grains in the samples (e.g. fossil fragments, quartz, K-feldspar, mica, plagioclase). The calcite cement in the samples occurs as patchy between grains of various types (Fig.
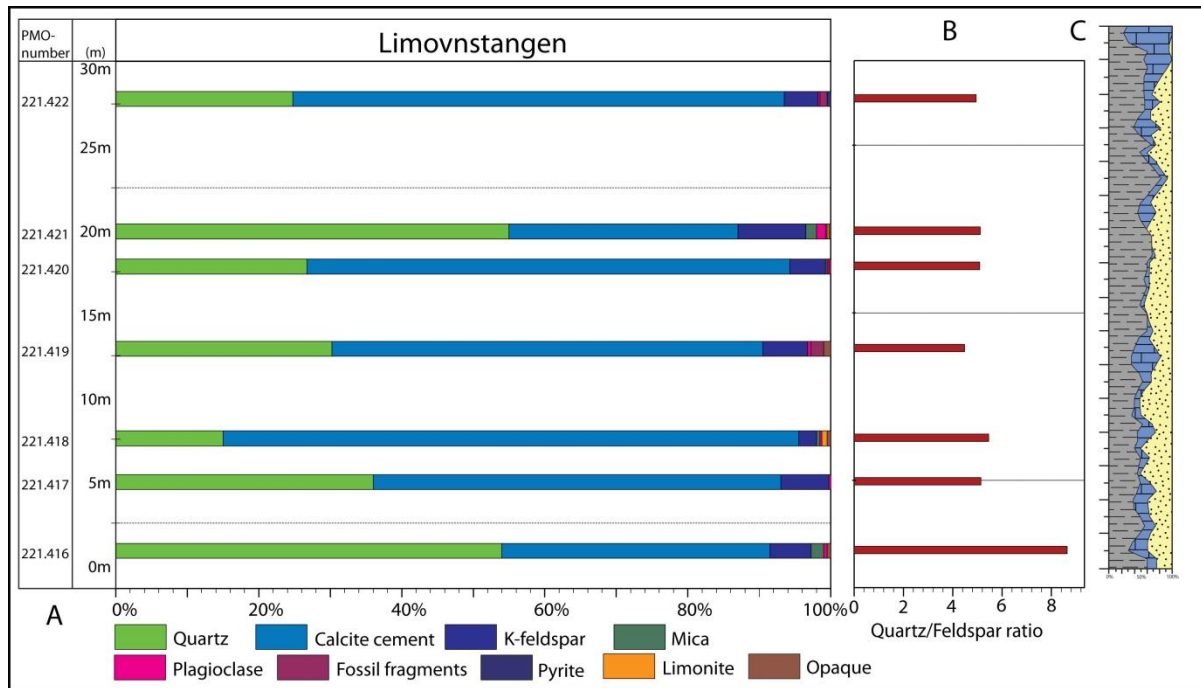

Figure 6.17: A) Mineral content from point counting of thin sections. B) Feldspar/Quartz ratio. C) Simplified log.

6.16). The samples (Fig. 6.17) have an upward increase in the calcite content from sample 221.416 to 221.418, and an upward decrease from sample 221.419 to 221.421 with a following upward increase to sample 221.422. The variation in the calcite content is related to the decrease and increase in the quartz content (Fig. 6.17). The quartz/feldspar ratio varies from 4 to 5, except for the lowermost sample (221.416) which shows a value of 9. In some of the samples the quartz and feldspar grains show corrosion.

The grain size in the measured samples at Limovnstangen shows silt as the average grain size at this locality (Fig. 6.18). All samples (221.416, 221.417, 221.419, 221.421 and 221.422) were collected from Facies IIa, which represent the coarsest material at the locality. The grains show an average roundness from very angular to sub-angular. It should be noted that the grain size in the logs is exaggerated by one fraction from the measured grain size in the samples.
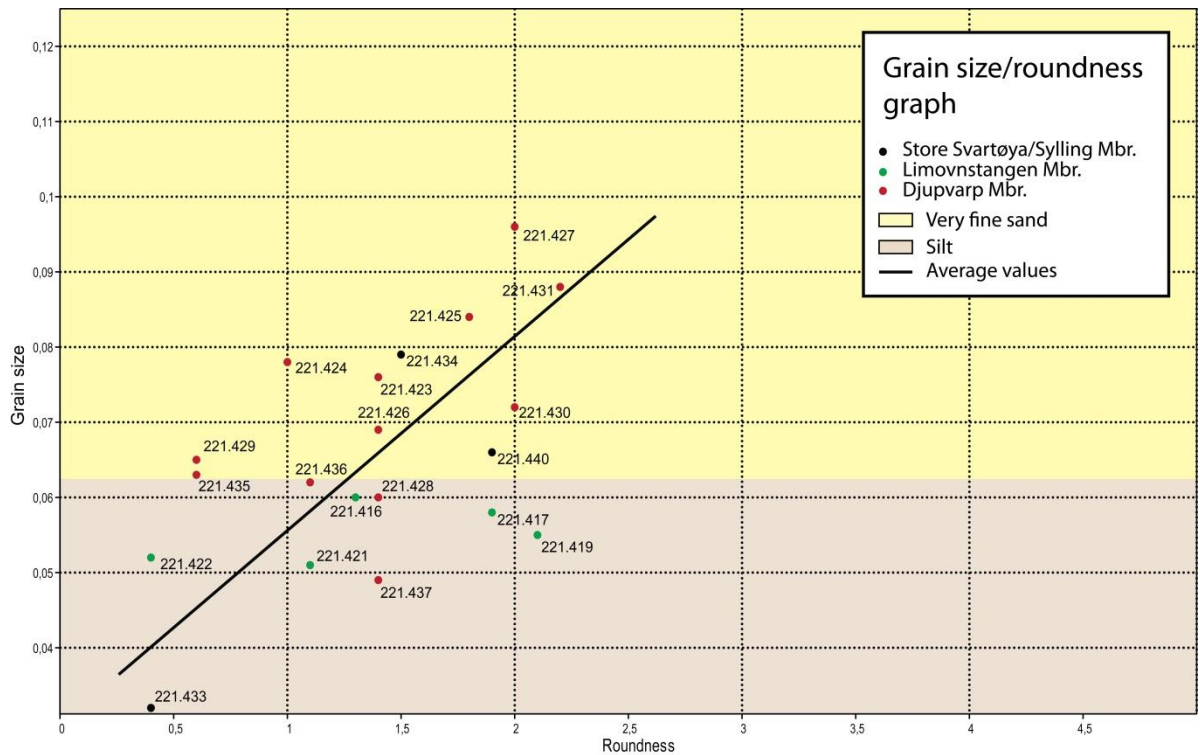
50

Figure 6.18: Grain size/roundness graph illustrate the relationship between the grain-size and the roundness of the grains in the different samples. Each sample shows an average of the different grains in the sample.

Palaeocurrent

A detailed overview of the palaeocurrent measurements are presented in Appendix C, with the depth and the measured orientation corresponding to each of the logs. The rose diagrams in figure 6.19 to 6.22 are based on all measurements from the locality.
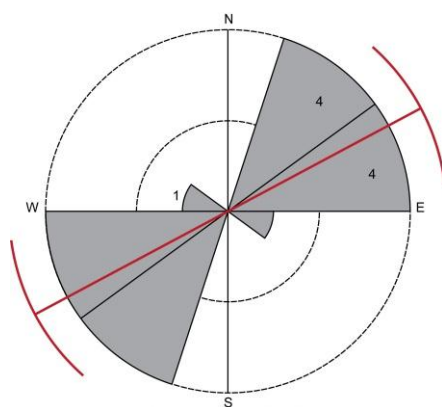

Figure 6.19: Palaeocurrent measurements of gutter casts. Mean orientation: 62-242. # = measurements.
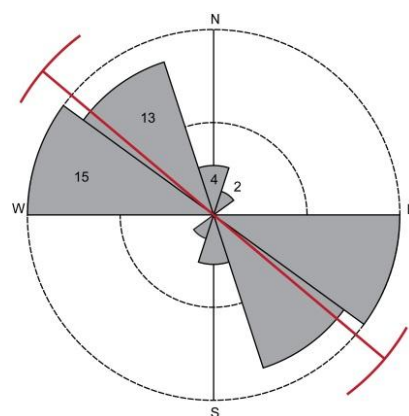

Figure 6.20: Palaeocurrent measurements of symmetric ripples. Mean orientation: 130-310. # = measurements.
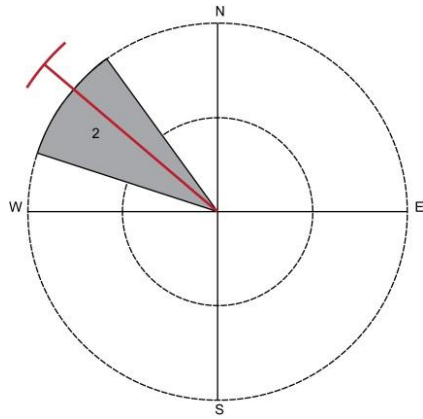
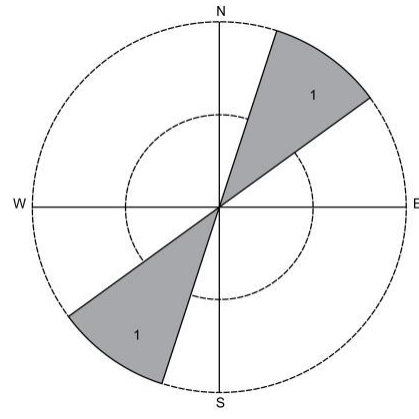Figure 6.21: Palaeocurrent measurements of asymmetric ripples. Mean orientation: 310. # = measurements.

Figure 6.22: Palaeocurrent measurements of cross-bedded biosparitic limestone. # = measurements.

6.2.2 Borgen

Sedimentological description

Figure 6.23: Borgen locality. Photo by H. A. Nakrem.

At the Borgen locality (Fig. 6.23), previously referred to as Djupvarp in Worsley et al. (1982), a 9.2 meters thick section of the Sælabonn Formation, the Djupvarp Member, is studied (Fig. 6.24). The locality was logged at two outcrops (logs Bor01-11 and Bor02-11) to observe the lateral variation. The outcrops belong to facies association FA2 where eight upward fining units are identified (0 m – 1 m, 1 m – 1.18 m, 1.18 m – 1.82 m, 1.82 m – 2.8 m, 2.8 m – 4.4 m, 4.4 m – 5.6 m, 5.6 m – 6.7 m and 6.7 m – 8.18 m).

The trough cross-bedded sandstone (Facies IIb) has an erosive base lying on top of mudstone (Facies Ia or Ib), sandstone (Facies IIa) or trough cross-bedded sandstone (Facies IIb). The overlying unit is either mudstone (Facies Ia or Ib) or biosparitic limestone (Facies IIIb). At one level (5.5 m) the sandstone of Facies IIa is succeeding the trough cross-bedded sandstone (Facies IIb). The fifth upward fining unit (2.8 m – 4.4 m) has an increased frequency of Facies IIa, where it is succeeded by Facies Ia at all levels (Fig. 6.24). The increased frequency seems to be local, as laterally the beds get thinner before they disappear.
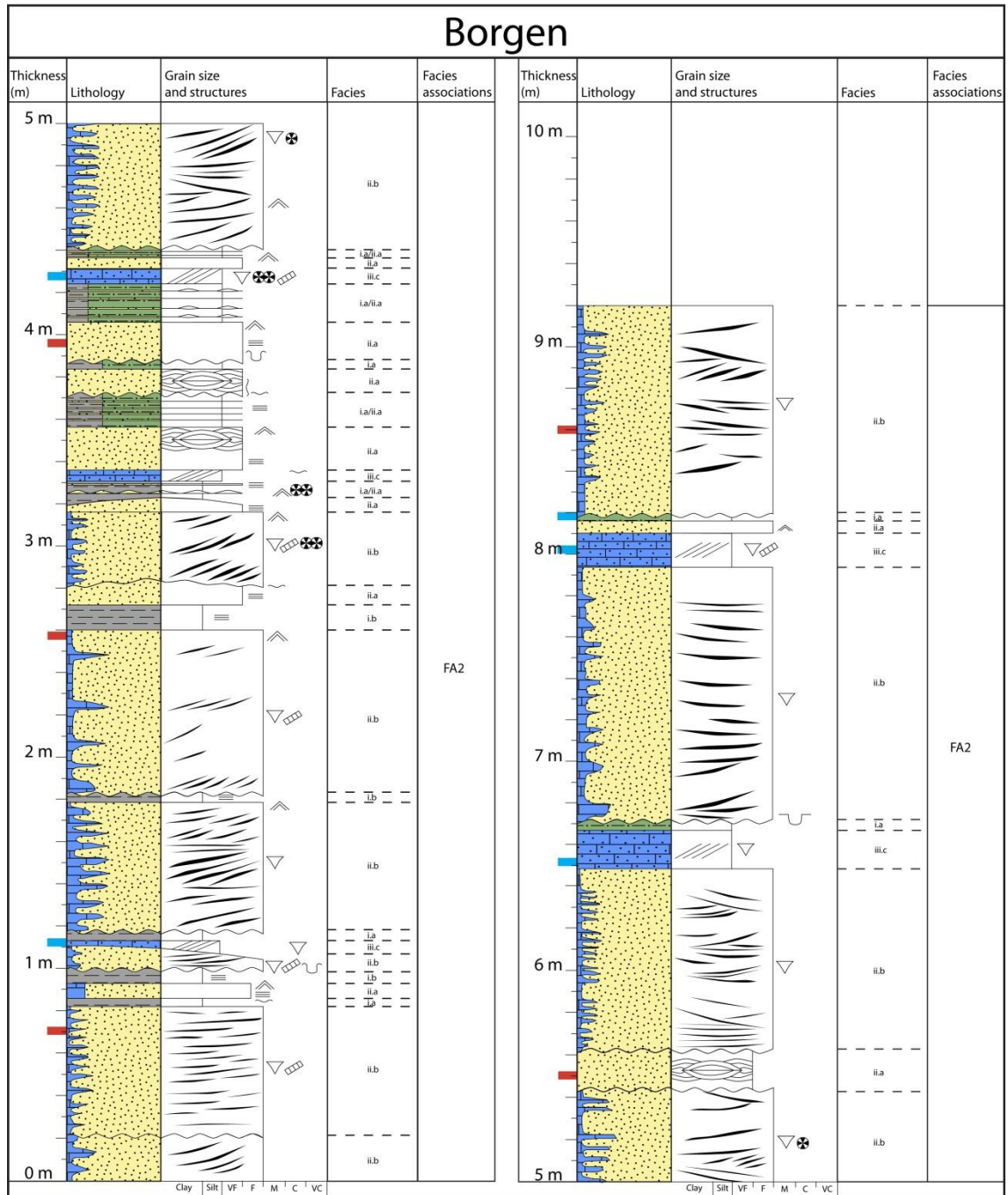

Figure 6.24: General log of the Borgen section. The blue markers are acetate peels, the red markers are thin sections. Legend is presented in Appendix A.

Mineral content and texture

Five thin sections were prepared from Borgen, all from the Djupvarp Member (Fig. 6.25).
Two samples were collected from Facies IIa (221.425 and 221.427) and three samples from
Facies IIb (221.423, 221.424 and 221.426). The main component in the samples are quartz,
where the quartz content ranges from 54.4% − 71.8%. The calcite content ranges from 18.0%
− 32.2%. Undulating and polycrystalline quartz accounts for 2.5% − 6.8% of the total quartz
content in the samples. The feldspars account for 6.0% − 10.8% of the content in the samples.
Mica (0.5%), pyrite (0.3%), opaque minerals (1.2% − 2.5%) and limonite (0.5% − 4.0%) can
also be observed in some of the samples, but are close to insignificant. The largest
concentrations of fossil fragments occur in sample 221.423 with 5.1%, whereas in the other
samples the fossil content is 0% or close to 0%. A full overview of the content in the samples
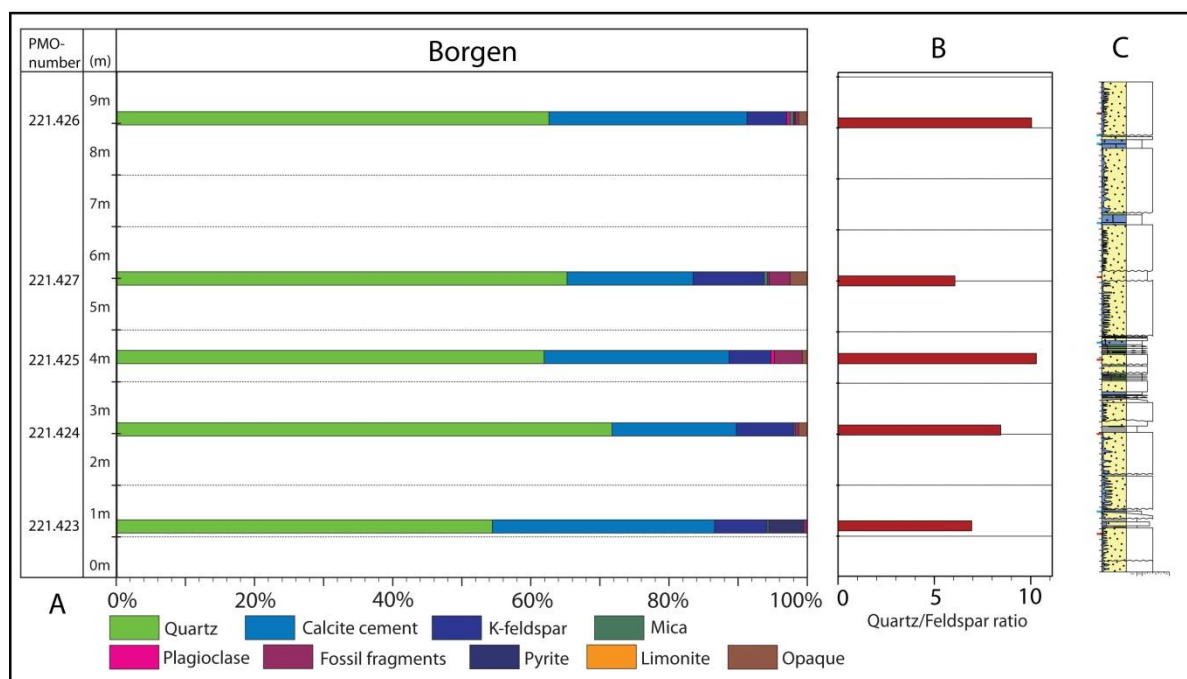is presented in Appendix D.

Figure 6.25: A) Mineral content from point counting of thin sections. B) Feldspar/Quartz ratio. C) Simplified log.

All of the samples are grain supported, where the calcite cement occur in patches (Fig. 6.26).
An indication of compaction is observed as there is a presence of fractured mica, and
corroded quartz and feldspar grains (Fig. 6.27). The quartz/feldspar ratio has two upward
increasing intervals. The values of the first interval (221.423 to 221.425) go from 7 to 10. In
the second interval (221.427 to 221.426) the values go from 6 to 10 (Fig. 6.25).
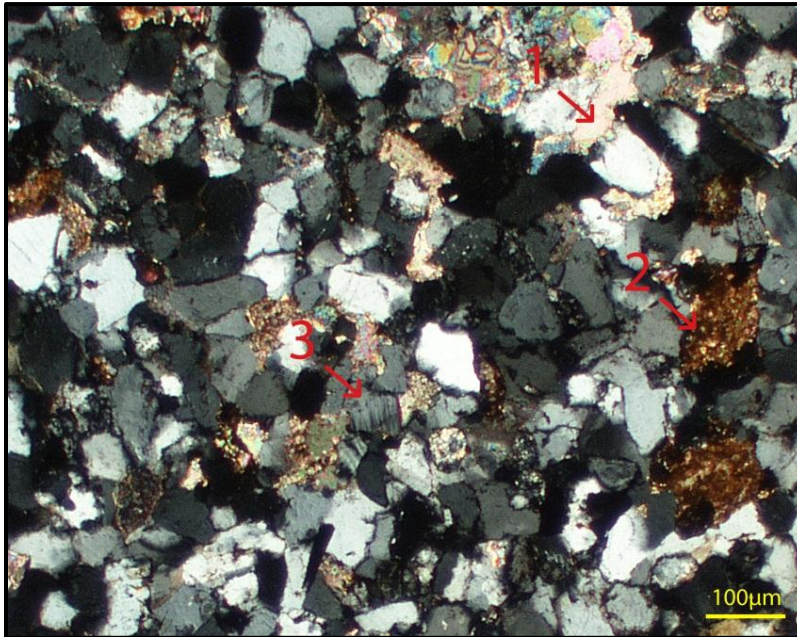
54

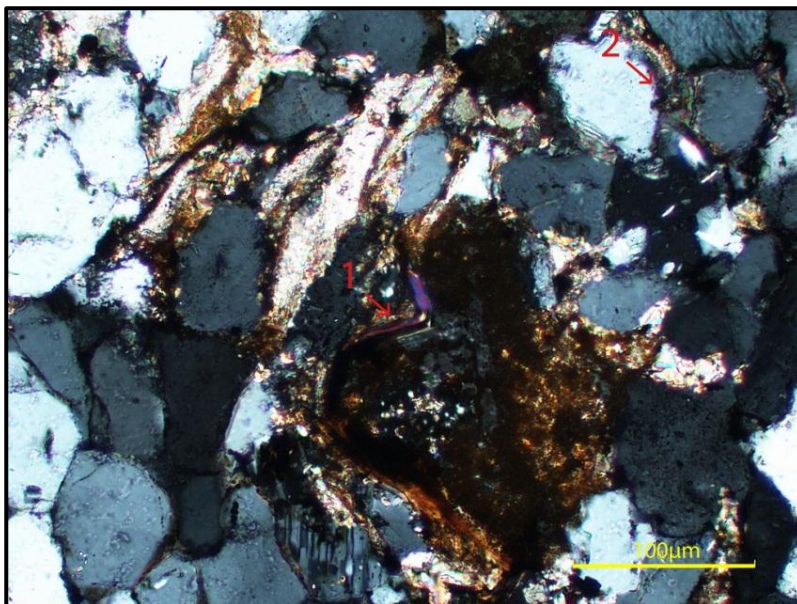Figure 6.26: 1) Patches of calcite cement. 2) Limonite. 3) Microcline.

Figure 6.27: 1) Fractured mica. 2) Corroded quartz.

The grain size in the measured samples at Borgen show very fine sand as the average grain size (221.423, 221.424, 221.425, 221.426 and 221.427) (Fig. 6.18). The grains show an average roundness from angular to sub-angular. It should be noted that the grain size in the logs is exaggerated by one fraction from the measured grain size in the samples.

Palaeocurrent

A detailed overview of the palaeocurrent measurements are presented in Appendix C, with the depth and the measured orientation corresponding to each of the logs. The rose diagrams in figure 6.28 to 6.30 are based on all measurements from the locality.
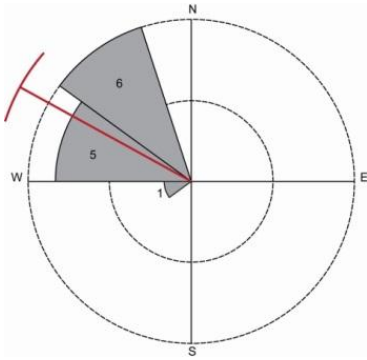
Figure 6.28: Palaeocurrent measurements of trough cross-bedding and cephalopods. Mean orientation: 118. # = measurements.
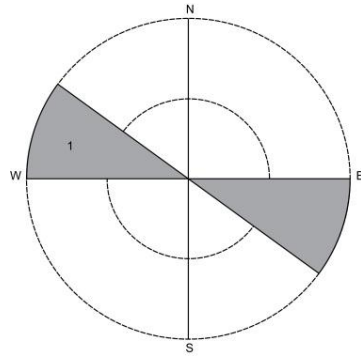
Figure 6.29: Palaeocurrent measurements of gutter cast. Orientation: 112-292. # = measurements.
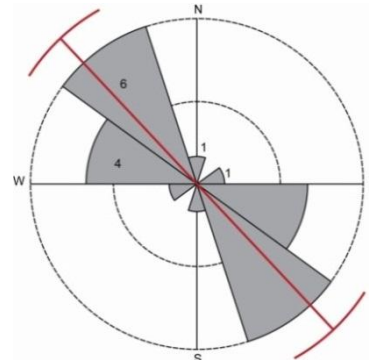
Figure 6.30: Palaeocurrent measurements of symmetric ripples. Mean orientation: 137-317. # = measurements.

6.2.3 Åsaveien

Sedimentological description

Figure 6.31: Åsaveien locality.

At the Åsaveien locality (Fig. 6.31), previously been referred to as Veltikøll by Whitaker (1977), an interval of 9.3 meters of the Sælabonn Formation, the Djupvarp Member (log Åsa-11), is studied (Fig. 6.32). The outcrop belongs to facies association FA2, where one unit is upward coarsening (0 m – 1.4 m) and four upward fining units are seen (1.4 m – 2.08 m, 2.08 m – 3.98 m, 3.98 m – 4.43 m and 4.43 m – 7.6 m).

The upward coarsening unit is composed of mudstone (Facies Ia) interbedded by sandstone (Facies IIa) and is succeeded by a bed of folded laminated sandstone (Facies IIc). The upward fining units are composed of trough cross-bedded sandstone which is succeeded by mudstone (Facies Ia), beds of sandstone (Facies IIa) or trough cross-bedded sandstone (Facies IIb). The

trough cross-bedded sandstone (Facies IIb) is either overlying itself, mudstone (Facies Ia) or the sandstone beds (Facies IIa), with an erosive base. The upward fining units are recognized as a repeating pattern in this section. The sandstone beds (Facies IIa) are seen to occur with higher frequency than at Borgen, with thin layers of mudstone (Facies Ia) separating them.
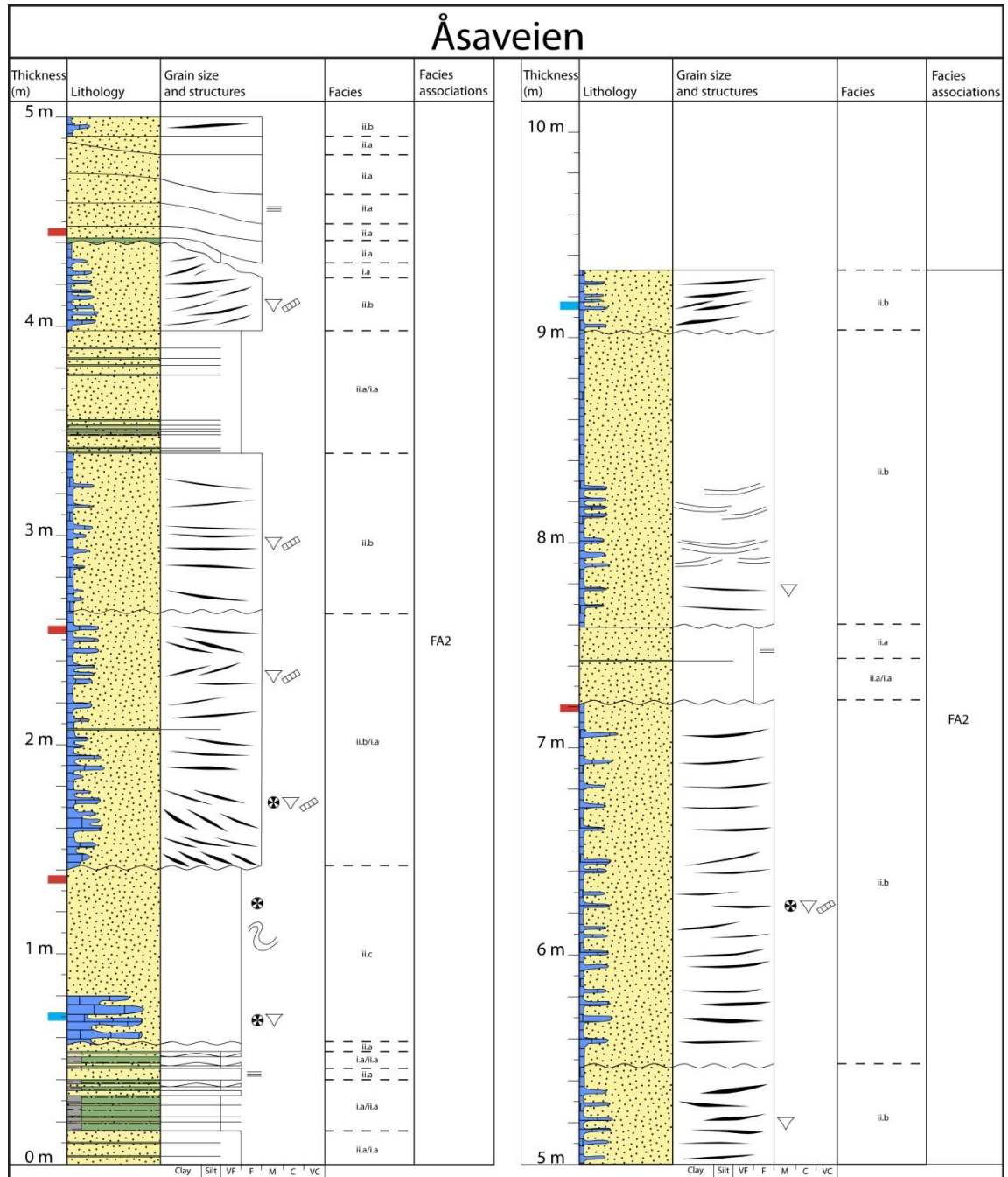

Figure 6.32: General log of the Åsaveien section. The blue markers are acetate peels, the red markers are thin sections. Legend is presented Appendix A.

Mineral content and texture

Four thin sections were prepared from Åsaveien, all from the Djupvarp Member (Fig. 6.33). One sample was selected from Facies IIc (221.428), one sample from Facies IIa (221.430)

and two samples from Facies IIb (221.429 and 221.431). The main components in the samples are quartz and calcite, where the quartz content ranges from 37.3% - 69.8% and the calcite content from 2.0% - 49.0%. Undulating and polycrystalline quartz accounts for 2.0% - 6.5% of the total quartz content in the samples. The feldspars account for 5.3% - 16.5% of the content in the samples. Mica (0.3% - 1.3%), fossil fragments (0.3% - 2.8%), pyrite (0.3%) and limonite (2.5% – 3.3%) can also be observed in some of the samples. Opaque minerals (2.3% - 8.8%) are also present in four of the samples. A full overview of the content in the samples is presented in Appendix D.

The samples from this locality are grain supported, where calcite cement fills the pore spaces in patches. The quartz and feldspar grains are corroded. The quartz/feldspar ratio ranges from 4 to 7, where the section is divided into two upward decreasing units. The decrease in each unit is small but noticeable, as the first unit decreases from c. 5 to c. 4 (221.428 to 221.429) and the second unit has a value of 7 (221.430 to 221.431).
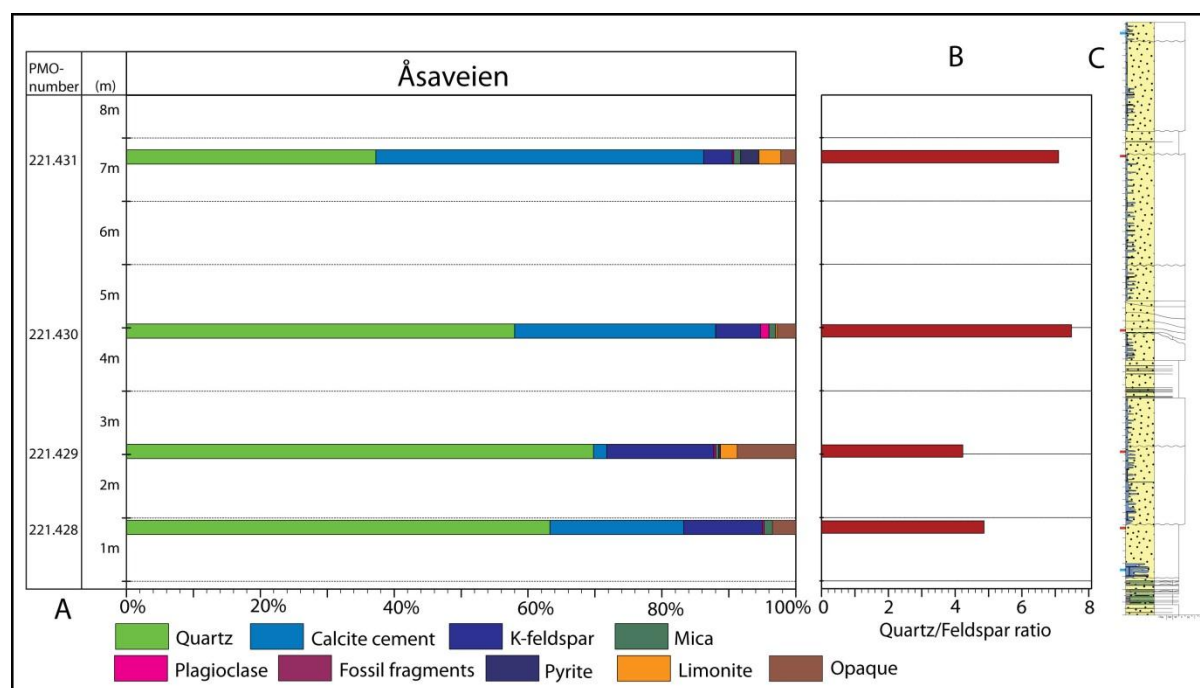
Figure 6.33: A) Mineral content from point counting of thin sections. B) Feldspar/Quartz ratio. C) Simplified log.

The grain size in the measured samples at Åsaveien shows very fine sand as the average grain size at this locality (221.428, 221.429, 221.430 and 221.431) (Fig. 6.18). The grains show an average roundness from angular to sub-angular. It should be noted that the grain size in the logs is exaggerated by one fraction from the measured grain size in the samples.

Palaeocurrent

A detailed overview of the palaeocurrent measurements are presented in Appendix C, with the depth and the measured orientation corresponding to each of the logs. The rose diagram in Figure 6.34 is based on all measurements from the locality.
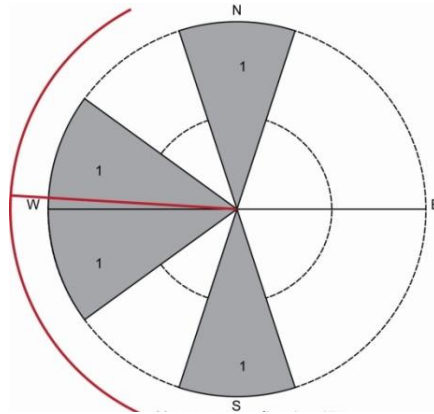
Figure 6.34: Palaeocurrent measurements of cross-stratification. Mean orientation: 274. # = measurements.

6.2.4 Grunntjern

Sedimentological description

Figure 6.35: Grunntjern locality. Photo by H. A. Nakrem.

At the Grunntjern locality (Fig. 6.35) 80cm of the Sælabonn Formation, the Store Svartøya Member (log Grunn-11), is observed lying on top of the Langøyene Formation, a massive limestone (Fig. 6.36). Sub-facies associations FA1a is recognized at this locality. The mudstone with the interbedded sandstone is lying on top of a massive limestone, where the

limestone has a wavy top. From the section, four levels of sandstone beds of Facies IIa are prominent, where the sections are made up by one or more beds.
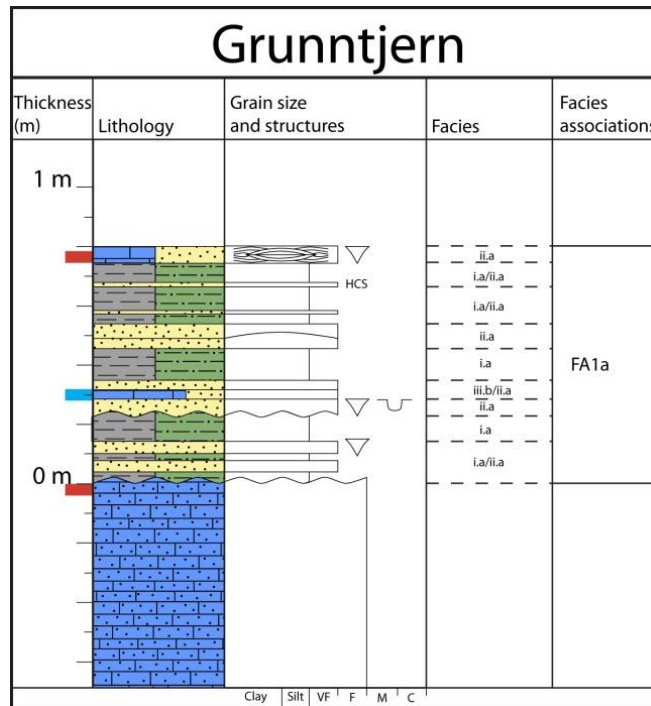
Figure 6.36: The Grunntjern section. Blue markers are acetate peels, red markers are thin sections.

Mineral content and texture

Two thin sections were prepared from Grunntjern, one from the uppermost Langøyene Formation (221.439) and the second from the lowermost part of the Store Svartøya Member (221.440) (Fig. 6.37). Both of the samples have calcite as the main component. The sample from Store Svartøya Member contains 83.5% calcite. It also contains quartz (8.0%), K-feldspar (0.3%), fossil fragments (5.5%), limonite (1.8%) and opaque minerals (1.0%). The sample from the Langøyene Formation is composed of 91.5% calcite, but also contains 2.3% quartz and 6.3% fossil fragments. The fossil fragments differ from what is known in the Sælabonn Formation (Chapter 6.3), as ooids, algae fragments and oncoids are present (Chapter 6.3). The samples are grain supported, but do however contain a large amount of calcite cement.

The grain size in the analysed sample from Grunntjern shows very fine sand as the average grain size at this locality (221.440) (Fig. 6.18). The grains show sub-angular roundness.
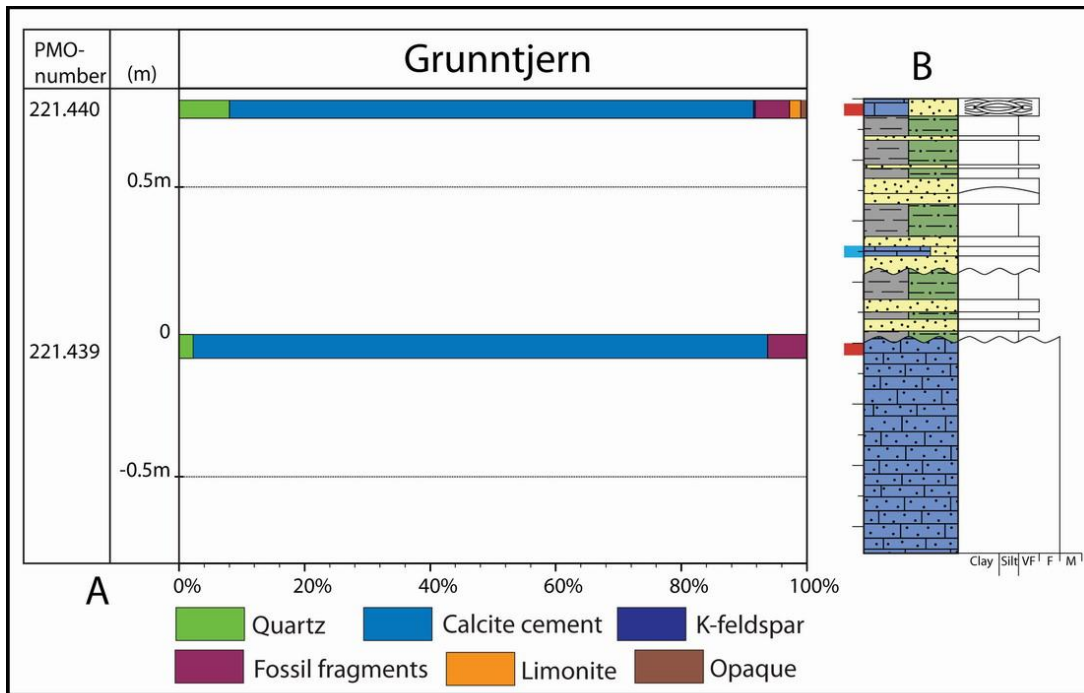
Figure 6.37: A) Mineral content from point counting of thin sections. B) Simplified log.

6.2.5 Toverud

Sedimentological description

Figure 6.38: Toverud locality. Photo by H. A. Nakrem.

At the Toverud locality (Fig. 6.38) the Sælabonn Formation makes up a section of 100 meters (Fig. 6.39). The underlying Langøyene Formation and the overlying Rytteråker Formation are also exposed at the locality, a road section. The Sælabonn Formation (log Tov-11) has been divided into three members at the Toverud locality by Baarli (1988); Sylling Member, Djupvarp Member and Limovnstangen Member. Sub-facies associations FA1a, FA1b and

61

FA1c are present at this locality as well as the facies association FA3 at the base of the Sælabonn Formation.

The outcrop is dominated by sub-facies association FA1a but has a higher frequency of sub-facies association FA1b from 52 meters to 80 meters. Sub-facies association FA1c is present at one level close to the base (6 m) and at the top (Fig. 6.39).

Mineral content and texture

Seven thin sections were prepared from Toverud (Fig. 6.40). Six samples were selected from Facies IIa (221.433, 221.434, 221.435, 221.436, 221.437 and 221.438) and one sample was selected from Facies IId (221.432). The samples from the Sælabonn Formation have quartz and calcite as the main components. The quartz content ranges from 5.8% – 70.1% while the calcite content ranges from 6.5% – 84.5% in the samples. Undulating and polycrystalline quartz accounts for 0.3% – 4.5% of the total quartz content. The samples also contain feldspar (1.3% - 10.1), mica (0.3% - 0.5%), fossil fragments (0.2% – 4.0%), pyrite (0.3% – 1.0%), limonite (0.5% - 8.8%) and opaque minerals (0.3% - 5.3%). The sample from the lowermost part of the Sælabonn Formation (Facies IId) has calcite as the main component (52.5%), but it also contains quartz (29.3%) where 5.8% is undulating and polycrystalline quartz. Feldspar (3.1%), fossil fragments (0.3%), pyrite (14.8%) and opaque minerals (0.3%) are also present.

The rocks show a grain-supported configuration, where the pore space is filled patches of calcite cement. The samples have an upward increase in the quartz content
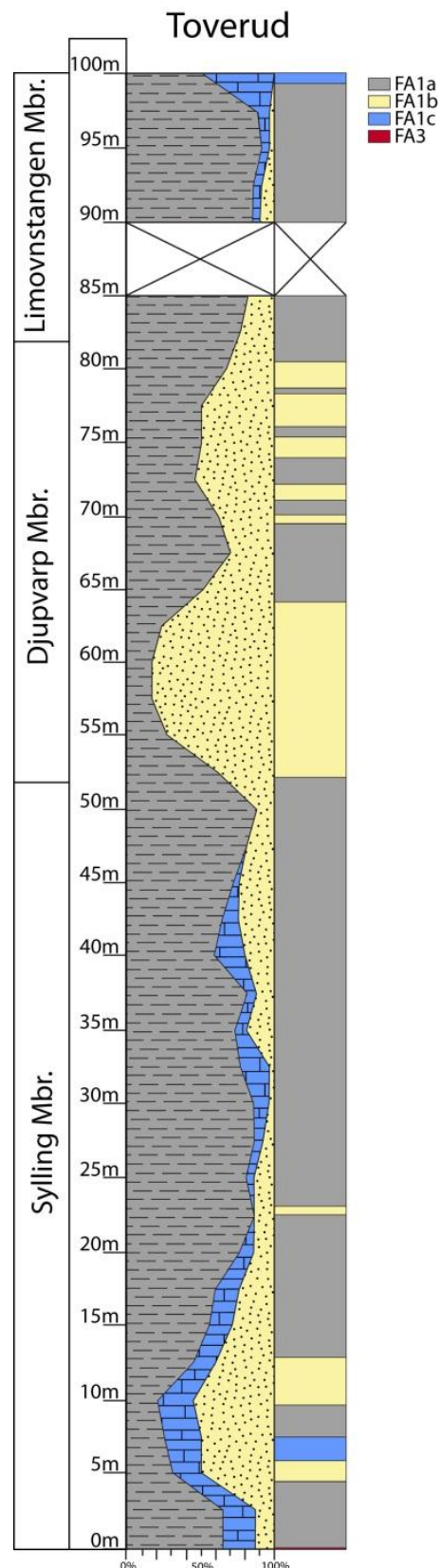

Figure 6.39: Lithological log of the Toverud section, with the occurring sub-facies associations and facies associations in the section.

from samples 221.432 to 221.436, followed by an upward decrease from sample 221.436 to 221.438 (Fig. 6.40). As the quartz content decreases or increases the amount of calcite increases or decreases, respectively. It should also be noted that the occurrence of fossil fragments is highest in the uppermost sample. There is an increase in the amount of the K-feldspar in sample 221.434, 221.435 and 221.436. The quartz and feldspar grains have also here been corroded. The quartz/feldspar ratio shows an upward decrease (10 - 6), followed by an increase (7 – 9) and ending with a decrease in the uppermost sample (5) (Fig. 6.40).
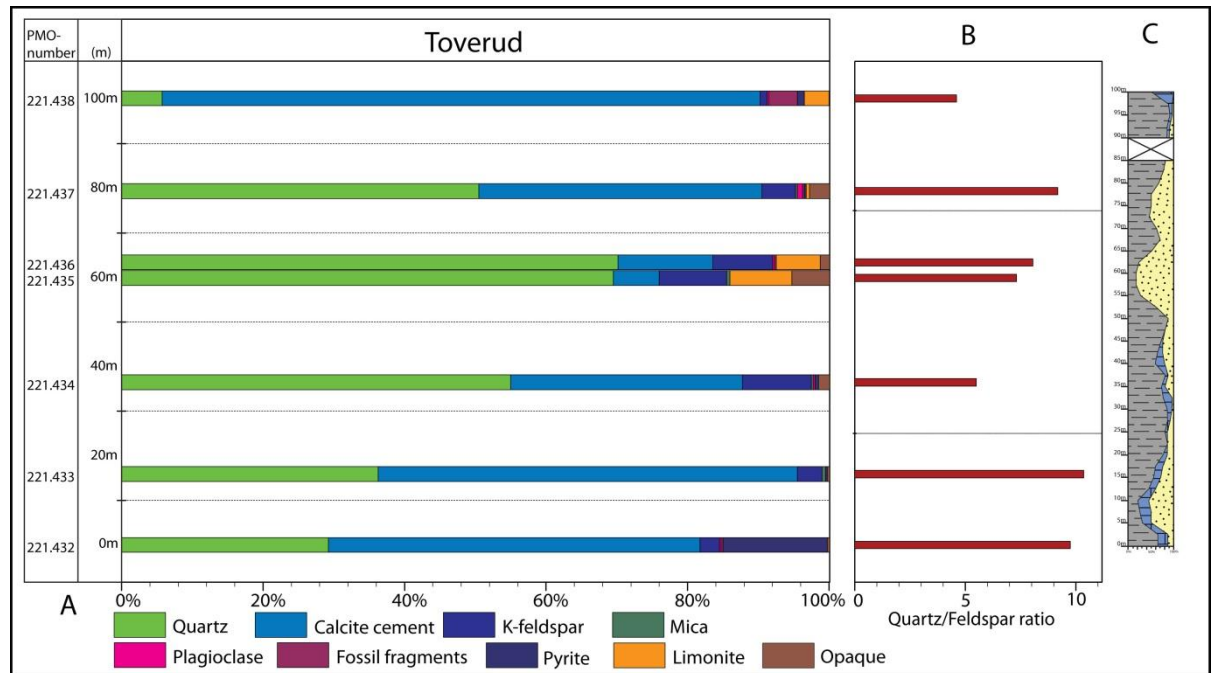
Figure 6.40: A) Mineral content from point counting of thin sections. B) Feldspar/Quartz ratio. C) Simplified log.

The grain size in the measured samples at Toverud shows silt to very fine sand as the average grain size (221.433, 221.434, 221.435, 221.436, 221.437) (Fig. 6.18). All three members of the Sælabonn Formation are present at this locality, where the beds with the coarsest sand (very fine sand) occur at the top of the Sylling Member (221.434) and in the Djupvarp Member (221.435 and 221.436). The samples from the lower part of Sylling Member (221.433) and the upper part of the Djupvarp Member (221.437) have a silt grain size. The grains show an average
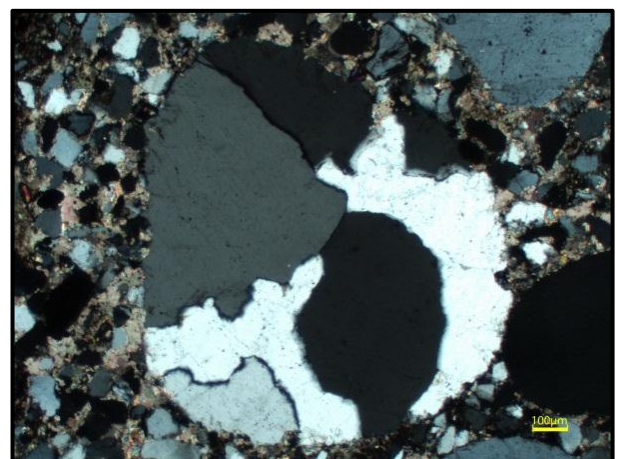
Figure 6.41: Facies association FA3. Well-rounded, polycrystalline granular quartz grain.

63

roundness from very angular to angular. In the sample collected immediately above the Ordovician-Silurian boundary (221.432) well-rounded, granule quartz grains are present (Facies IId) (Fig. 6.41).

Palaeocurrent

A detailed overview of the palaeocurrent measurements are presented in Appendix C, with the depth and the measured orientation corresponding to each of the logs. The rose diagrams in Figure 6.42 and 6.43 are based on all measurements from the locality.
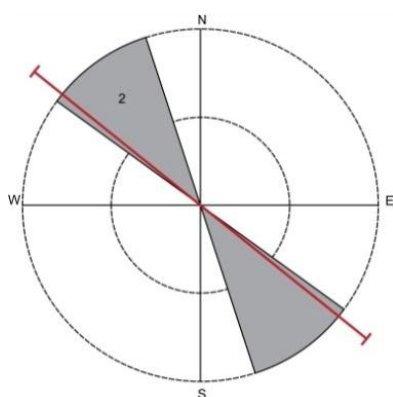
Figure 6.42: Palaeocurrent measurements of symmetric ripples in the Limovnstangen and Djupvarp Member. Mean orientation: 129-309. # = measurements.
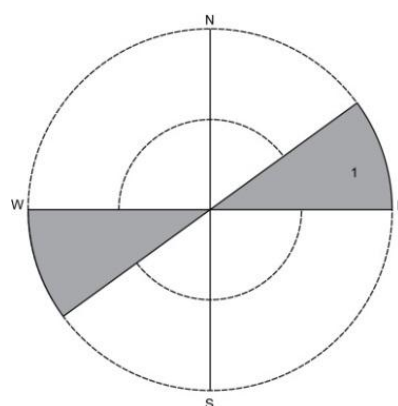
Figure 6.43: Palaeocurrent measurements of gutter cast in the Djupvarp Member. Orientation: 55-235. # = measurements.

6.3 Fossil content

The biosparitic limestone beds in the Sælabonn Formation are composed of fossil fragments embedded in a matrix of siltstone or/and calcite. Samples were collected at the different localities, and acetate peels were prepared and point-counted (Chapter 5.6). Several different groups of organisms are observed and variations in species content will be in focus. A detailed overview of the percentage of the samples is presented in Appendix E.

6.3.1 Limovnstangen

Eleven samples were collected from the Limovnstangen locality. The calcite matrix (27.9% - 75.9%) is the largest component in the samples, with "unidentified grains" (0.6% - 51.4%) as the second largest contributor (Fig. 6.44). The samples belong to Facies IIIb (Chapter 6.1.1). The majority of the fossil fragments are brachiopods (1.2% - 12.8%), bryozoans (3.5% – 15.7%), crinoids (0.5% – 6.2%) and trilobites (0.9% – 5.3%). Intraclasts are also observed in five of the samples (Fig. 6.45). A detailed overview of the sample content is found in Appendix F. At the locality the sampled beds show three levels with an upward increase of "unidentified material" (1.15m – 3.6m, 6.4m – 10.2m and 12.5m – 20.4m). The uppermost

Figure 6.44: A) Overview of content from point counting of acetate peels. B) Simplified lithostratigraphical log from the Limovnstangen section.

(221.451) shows a dominance of the calcite matrix, which is the sample closest to the Sælabonn Formation - Rytteråker Formation (transitional) boundary.

The fossil material of the samples shows a tendency of grading as the largest fossil fragments are located at the bottom of the bed. The elongated brachiopod shells are deposited parallel with the bedding of the layers. The brachiopods do not show any preferred
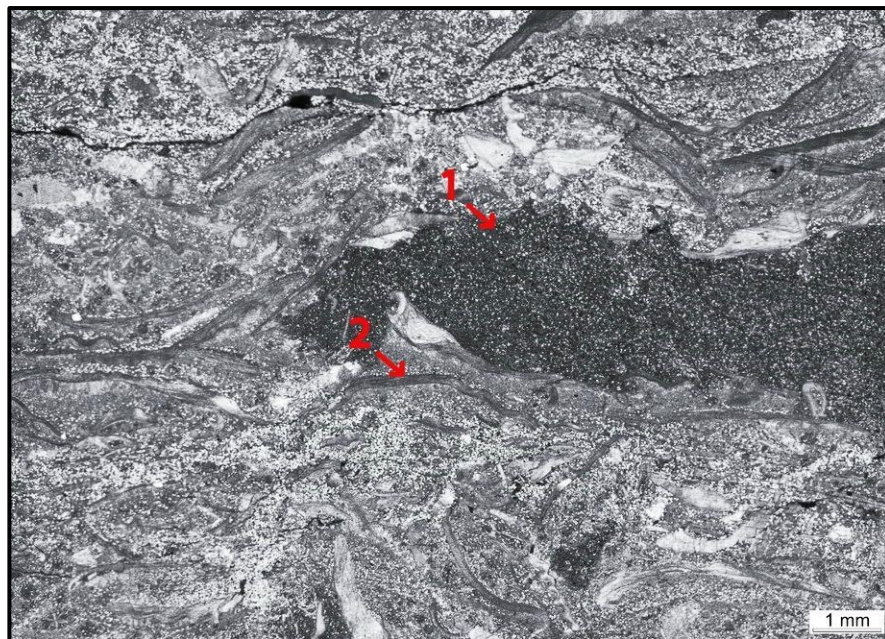
Figure 6.45: Sample 221.449; 1) Intraclast. 2) Brachiopod shell.

orientation regarding the concave or convex side up, however, the majority of the largest brachiopods are oriented with the convex side up. Reworking and transport of the fossils fragments are noticeable as only parts of brachiopod shells and trilobites are present. Sub-rounded bryozoans with chambers filled by micrite and "unidentified grains" are also an indicator for this (Fig. 6.46).
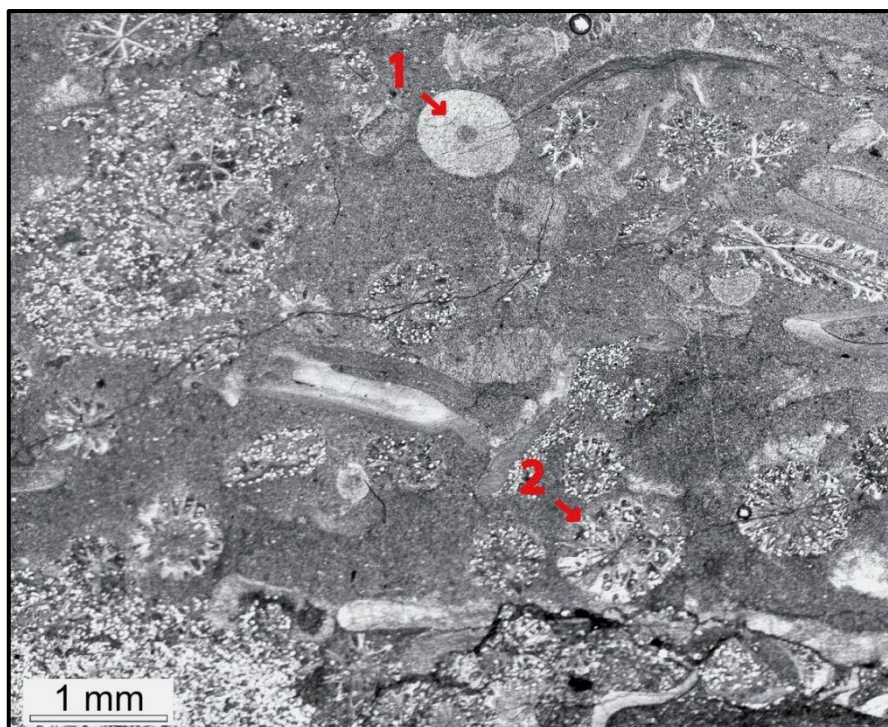
Figure 6.46: Sample 221.448; 1) Crinoid. 2) Bryozoan.

6.3.2 Borgen
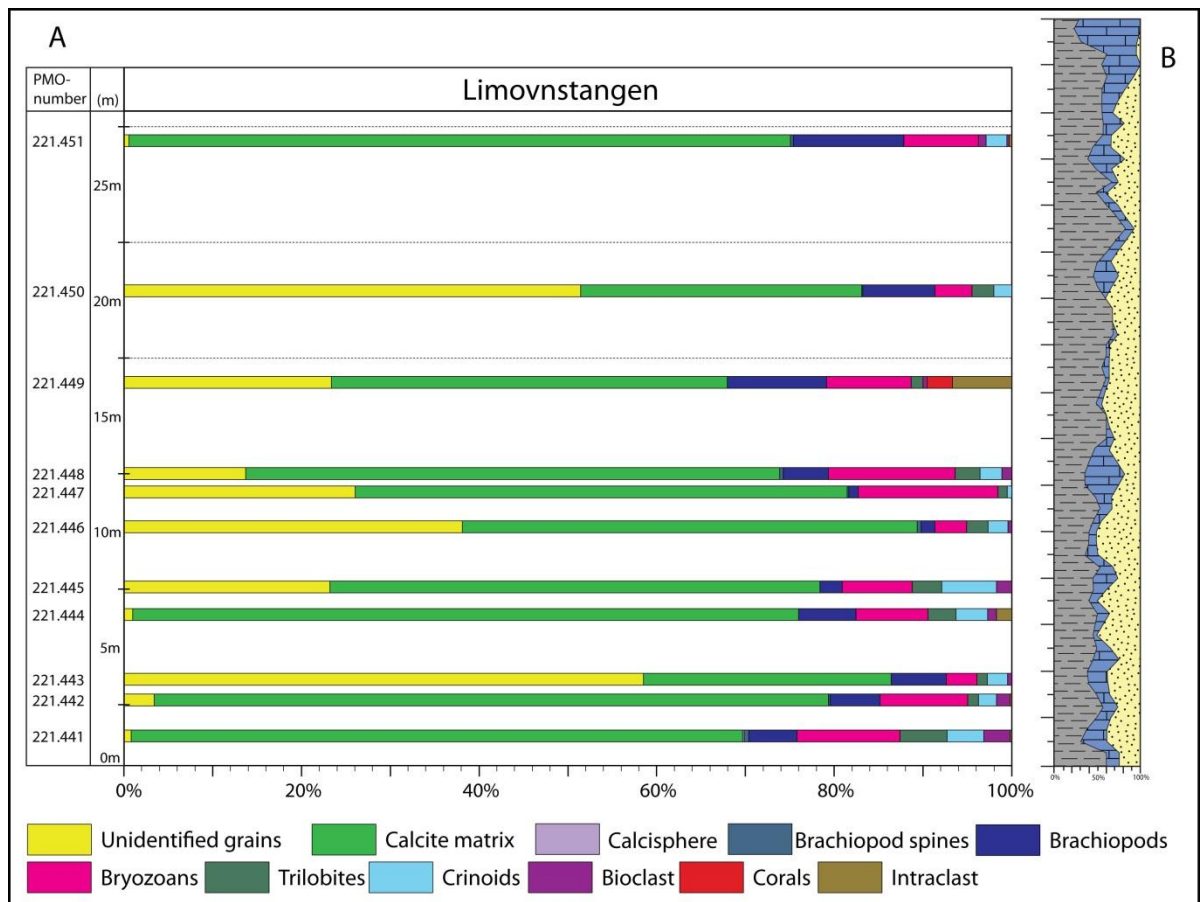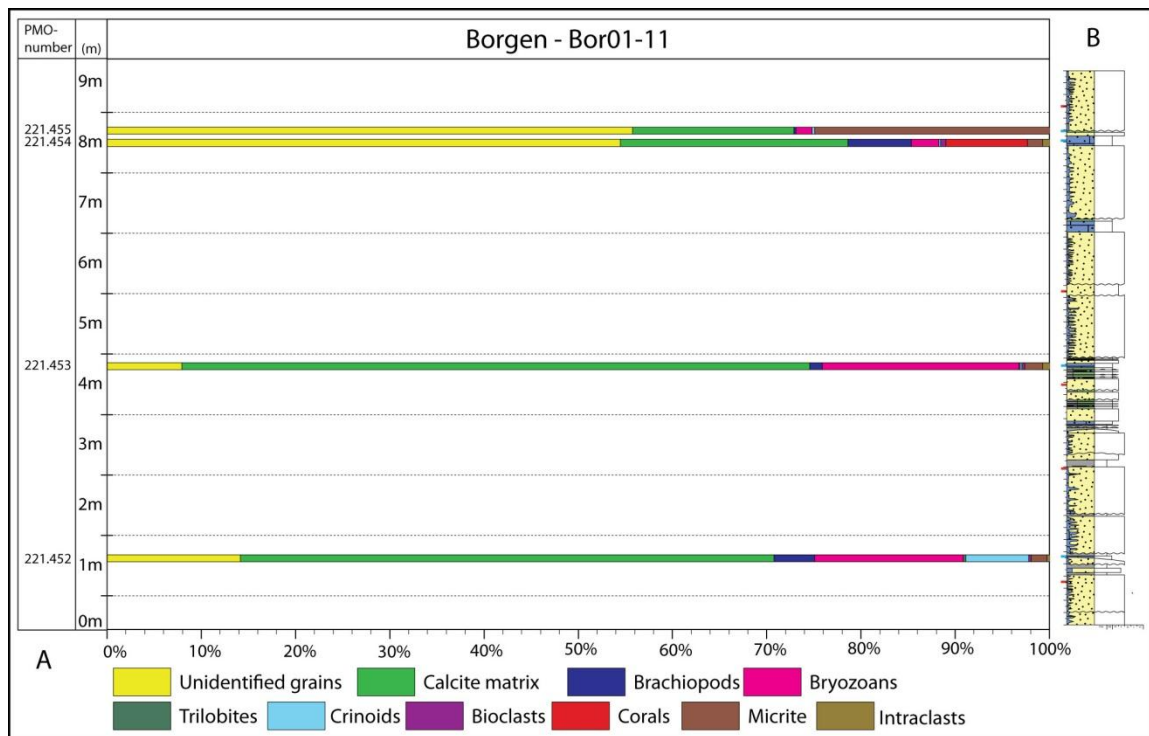

Figure 6.47: A) Overview of content from point counting of acetate peels. B) Simplified log from the Borgen section (general log).

Figure 6.48: A) Overview of the content from point counting of the acetate peels. B) Simplified log from the Borgen section (Log Bor02-11).

Six samples were collected from the Borgen locality. Four of them were collected from log Bor01-11 (Fig. 6.47) and two from log Bor02-11 (Fig. 6.48). Sample 221.453 and sample 221.456 correspond to the same biosparitic limestone layer, where the lateral distance between the samples are 23.6 meters. The results from the point counting of the acetate peels show an upward increase of "unidentified grains" (7.9% - 55.7%). The calcite matrix ranges from 17.1 to 66.6. Fragments of brachiopods (0.2% – 6.5%), bryozoans (1.7% – 20.9%) and crinoids (0.1% – 13.8%) are present in all samples. Some samples also contain micrite (0.4% – 24.9%). Sample 221.455 was collected from Facies IIb (Chapter 6.1.1) which has a higher sand content. The other samples were collected from Facies IIIc (Chapter 6.1.1).

The samples from Facies IIIc show that with the increasing "unidentified grains" the occurrence of brachiopods also increases, while the amount of carbonate matrix and bryozoans decreases. The difference between 221.453 and 221.456, which correspond to the same layer, is the amount of fossil fragments, with a higher amount in sample 221.456. In both sections the "unidentified grains" and the calcite matrix are the dominant components. The samples have a homogenous distribution with the calcite matrix as the largest component (Fig. 6.49). In the samples where "unidentified grains" are the largest component the sorting is more defined, and there is an upward increase in the amount and size of the fossil fragments (Fig. 6.50). In all samples the elongated fragments (e.g. bryozoans and brachiopods) are oriented close to parallel with the bedding (Fig. 6.49).
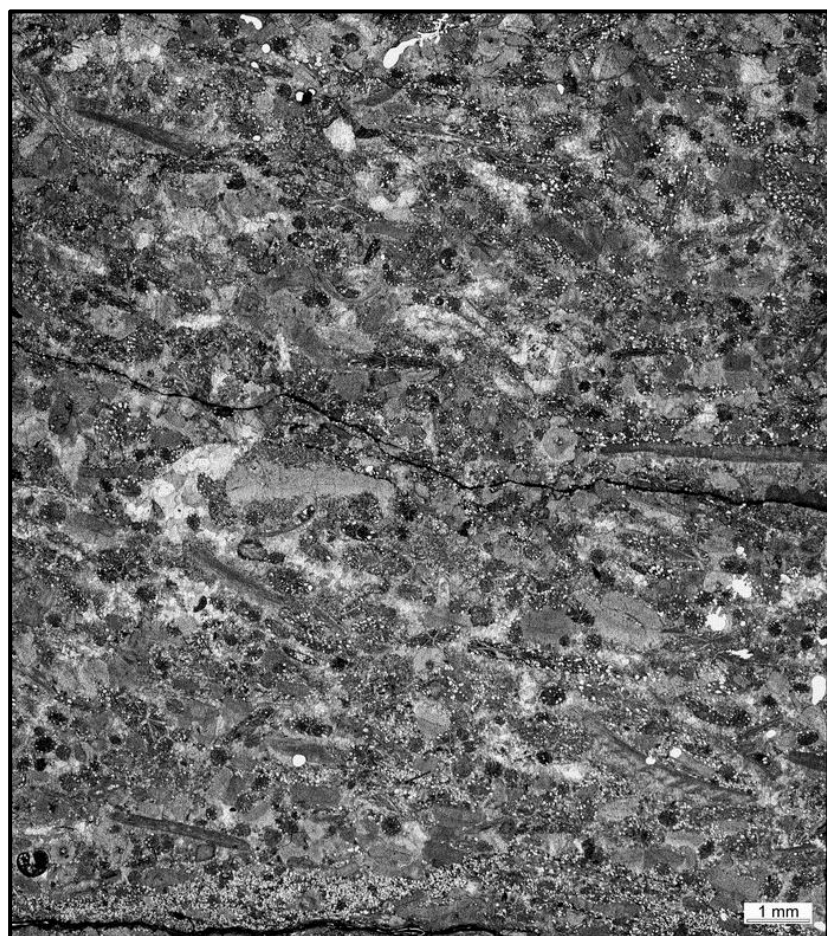
Figure 6.49: Sample 221.456; acetate peel with dominance of calcite matrix with a homogeneous distribution of fossil fragments.
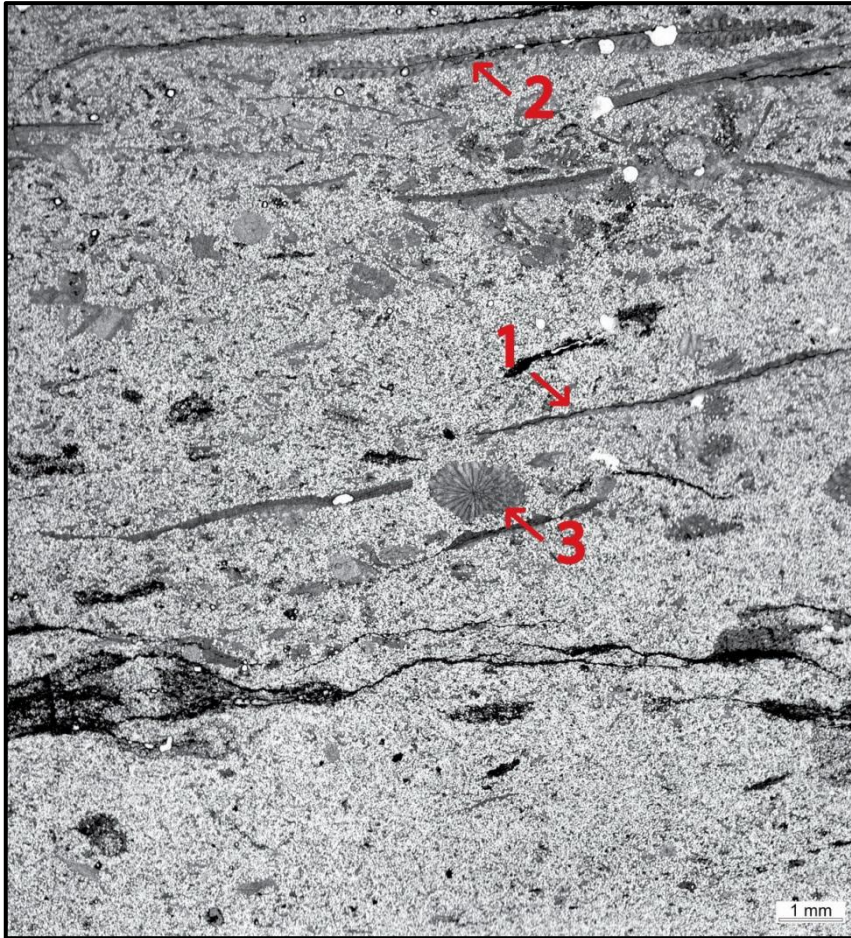
Figure 6.50: Sample 221.454; acetate peel with dominance of "unidentified grains". 1) Brachiopod, 2) Longitudinal section of bryozoan, 3) Cross section of bryozoan.

6.3.3 Åsaveien

Two samples were collected from the Åsaveien locality (Fig. 6.51), from the beds with the highest concentration of carbonate material. Sample 221.458 was collected from Facies IId and sample 221.459 was collected from Facies IIc. A detailed overview of the sample content is found in Appendix F.

The main components in the samples are "unidentified grains" (50.3% − 68.7%) and calcite matrix (18.7% - 37.8%). In sample 221.459 fragments of brachiopods (4.4%), bryozoans (4.4%) and crinoids (1.7%) have the highest abundance, while in sample 221.458 brachiopods (3.0%), bryozoans (2.7%) and gastropods (4.0%) have the highest abundance. Sample 221.458 is well sorted, with the largest fossil fragments concentrated at the base. Sample 221.459 is poorly sorted, where the fragments are randomly oriented in the bed. The size of the fossil fragments is variable where the majority is 1 mm or less. The gastropods (Fig. 6.52), bryozoans (Fig. 6.52), brachiopods and corals are the largest fossil fragments in the samples.
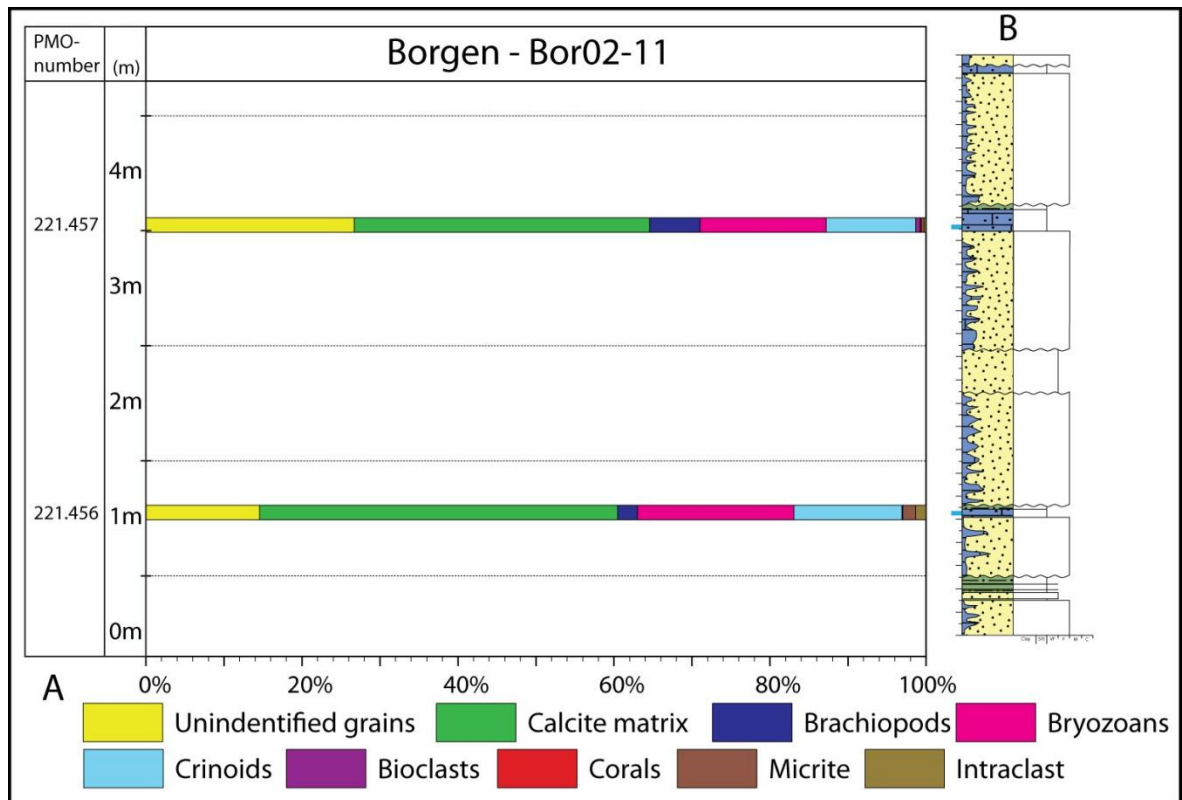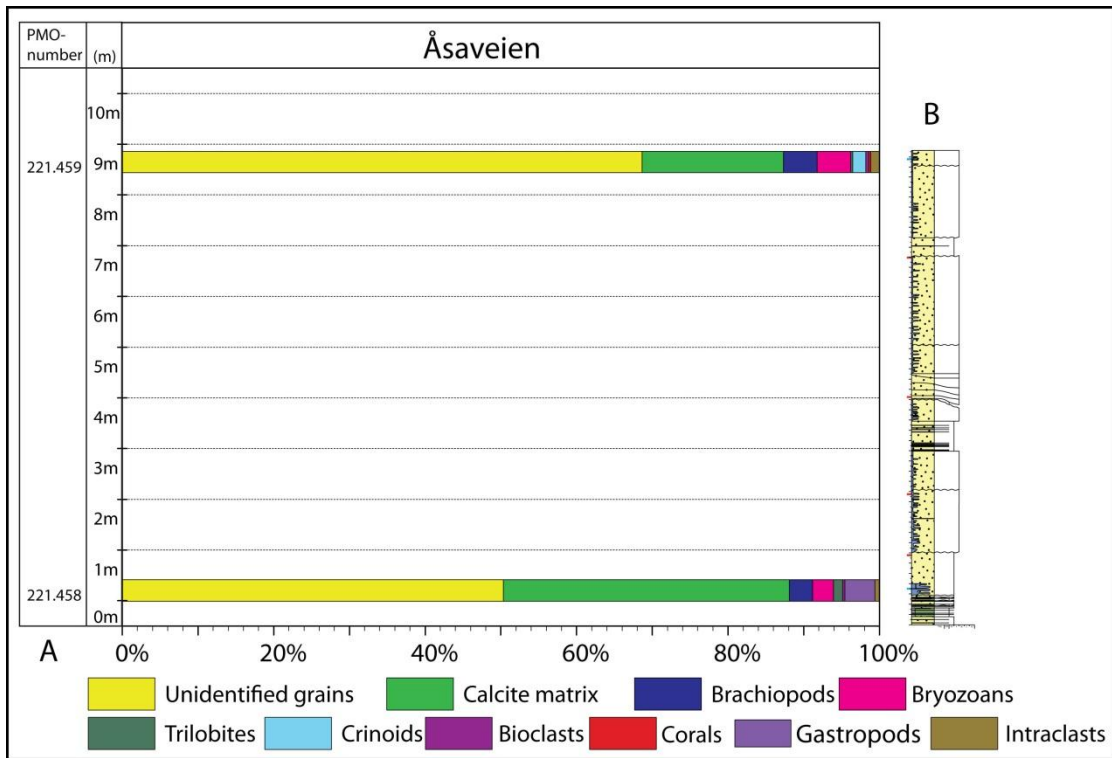
Figure 6.51: A) Overview of the content from point counting of the acetate peels. B) Simplified log from the Åsaveien section.
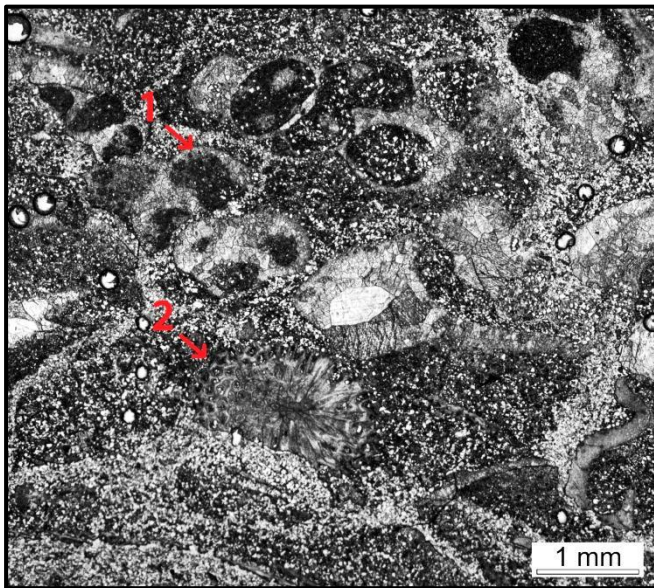
Figure 6.52: Sample 221.458; 1) Gastropod, 2) Bryozoan.

6.3.4 Grunntjern

One sample was collected at the Grunntjern locality (Fig. 6.53) from the bed with the highest content of carbonate material. The sample belongs to Facies IIIb. A detailed overview of the sample content is found in Appendix F.
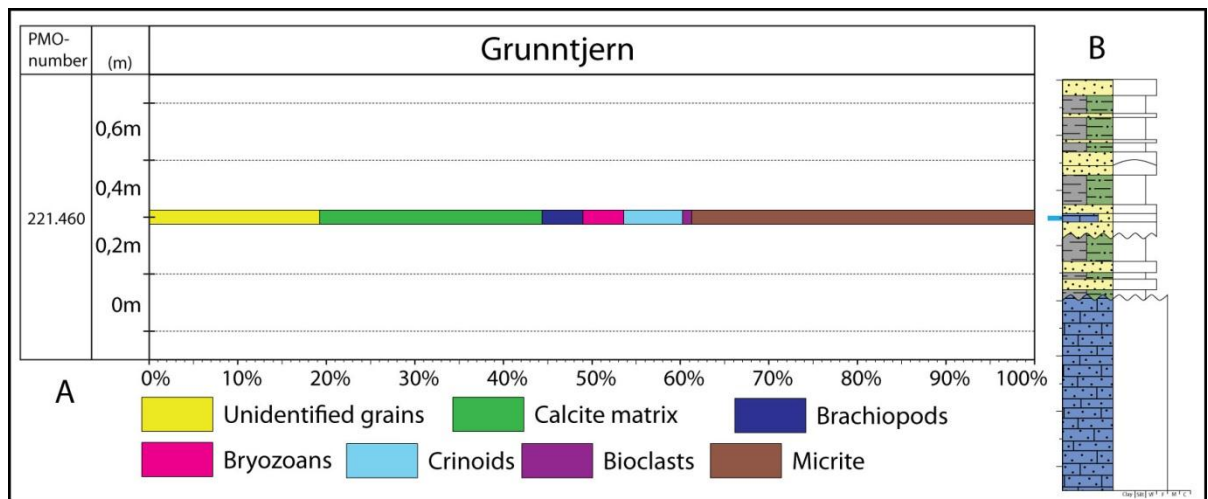
Figure 6.53: A) Overview of the content from point counting of the acetate peels. B) Simplified log from the Grunntjern section.

The main components of this layer are "unidentified grains" (19.2%), calcite matrix (25.1%) and micrite (38.7%), but fossil fragments of crinoids (6.7%), bryozoans (4.6%) and brachiopods (4.6%) are also observed in the acetate peel. The majority of the fragments are less than 1 mm and the grading of the bed shows an upward decrease in number of fragments in the bed (Fig. 6.54).
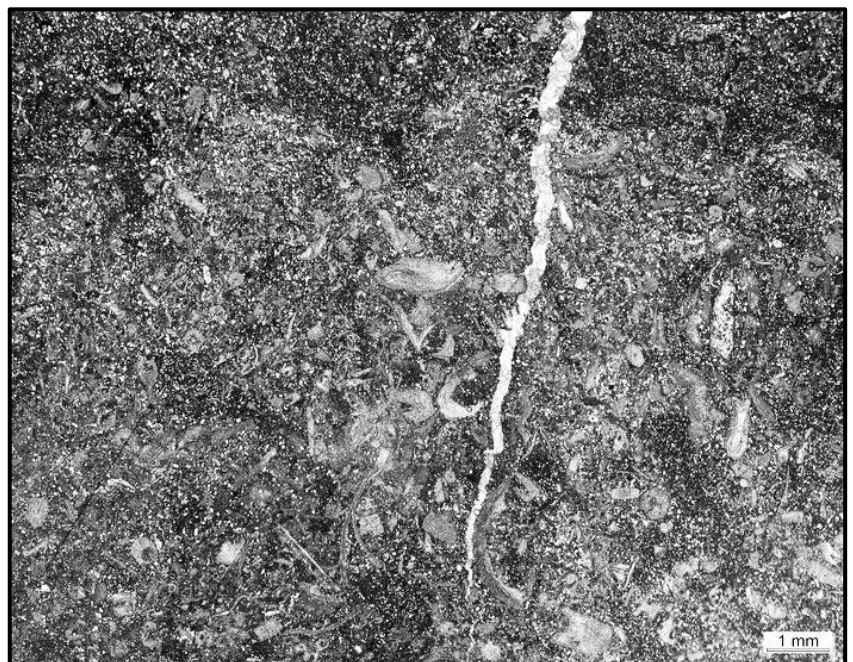
Figure 6.54: Sample 221.460, with decreasing concentration of fossil fragments towards the top of the bed.

6.3.5 Toverud

Thirteen samples were collected from the Toverud locality (Fig. 6.55). All collected samples belong to Facies IIIb. Note that not all samples are presented in Figure 6.55, as some of them are too closely spaced to have any illustrative purposes. All samples and detailed results from point counting are presented in Appendix F.
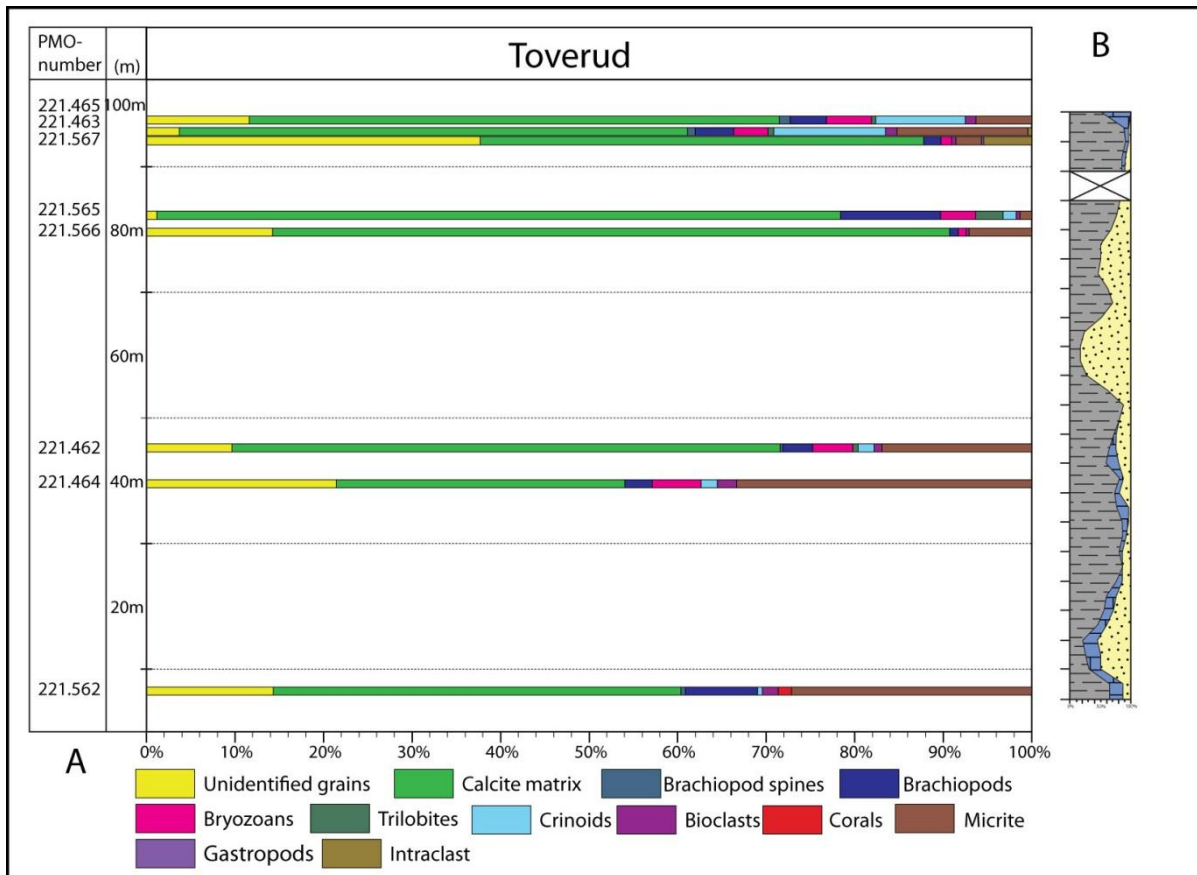
Figure 6.55: A) Overview of the content from point counting of the acetate peels. B) Simplified lithostratigraphical log from the Toverud section.

The main component in the samples is the calcite matrix (32.6% - 77.2%). The two other major components are "unidentified grains" (1.2% - 37.7%) and micrite (1.3% - 33.3%). Sorting of fragments do occur in these beds, where the fossil fragments are highest in concentration near the base of the bed, with a decreasing size of the fragments upwards in the bed (Fig. 6.56). The "unidentified grains" component is mixed with the calcite matrix in many of the beds. In beds where there is a low amount of this component the sorting of the fossil fragments is less prominent and the calcite matrix is dominant (Fig. 6.57). Fragments of corals are only present in the three lowermost samples, while there is a high abundance of crinoids in the two uppermost samples, compared to the other samples. Brachiopods are present in all the samples. The bryozoans present in the samples indicate reworking as they are filled with quartz grains and micrite, and are sub-rounded. The brachiopod and coral fragments have been reworked as well, as they are rounded and fragmented. The average size is less than 1mm for the fossil fragments in the samples. The largest fragments, brachiopods and corals, have a size of more than 2 mm. The majority of the largest brachiopods are

72

oriented with the convex side up, while the smaller ones do not show any preferred orientation.
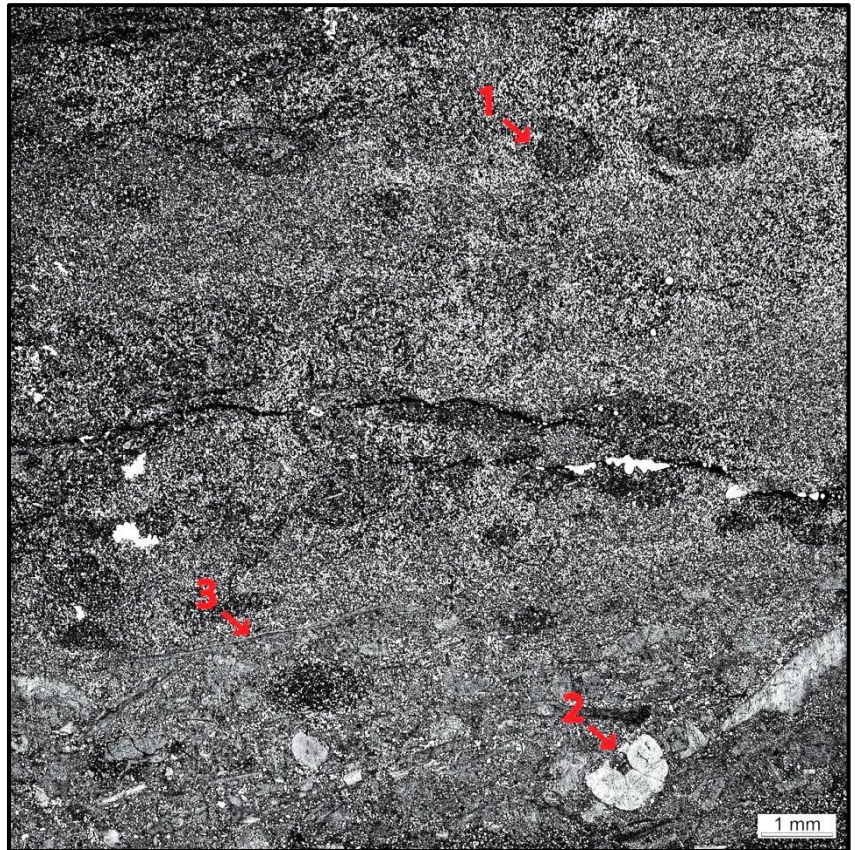
Figure 6.56: Sample 221.464; The bed has a relatively high amount of siliciclastic material, and a sorting is prominent. 1) Bioturbation. 2) Crinoid. 3) Brachiopod.
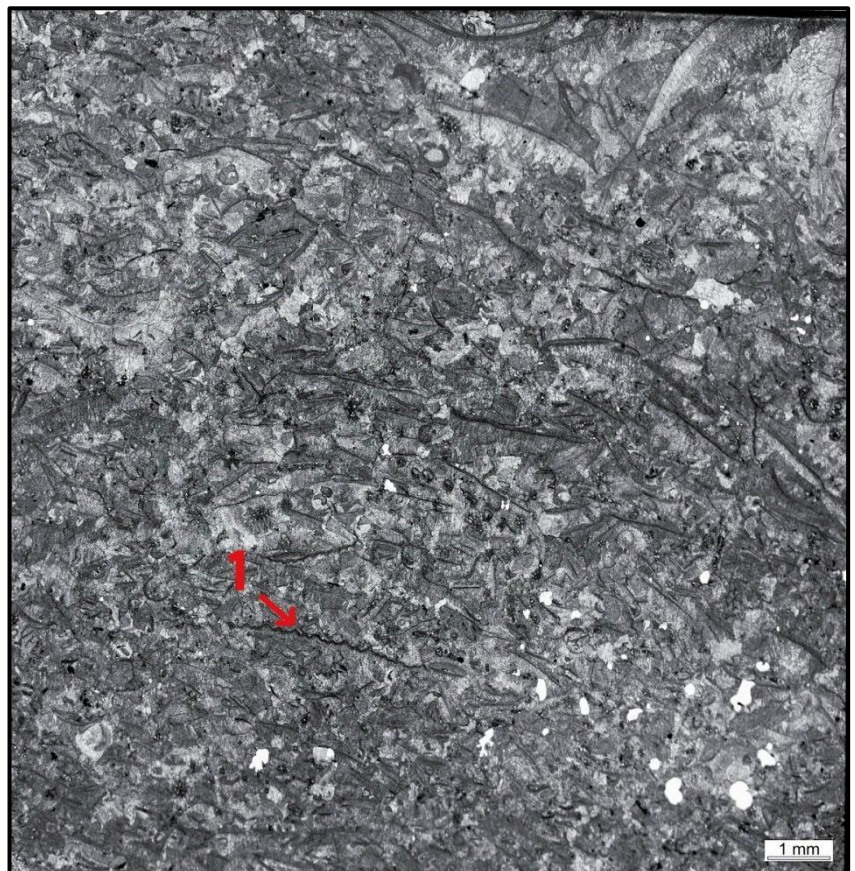
Figure 6.57: Sample 221.565; The carbonate matrix is dominant in the sample where the fossil fragments show very little sorting. 1) Brachiopod.

6.4 Ichnology

Trace fossils are important in the understanding of the depositional environment, but the classification and name setting might be difficult as the exposure and quality of the trace fossils are not always of satisfactory quality. Therefore, their occurrence and shape will be in focus and not their names, as it is difficult to be 100% certain of their names based on the observations done in the field. Most of the observations were done in the Limovnstangen Member at the Limovnstangen locality (Chapter 6.2.1). Pictures of the trace fossils are presented on plates in Appendix G.

Palaeophycus

Plate: 1A-C, 2B-D, 3C, 4C-D, 5A-D, 6B-C, 7A, 7D and 8A-B.

These samples are composed of elongated weakly curved burial tracks (Plate 1A) which are located on top and base of the very fine sandstone beds. The burial tubes which are filled with sand show a sinuous geometry in the sand bed (e.g. Plate 1A and 2B). However, they do not penetrate very deep into the sand, and are observed at the top and base of the beds where the tubes also bifurcate (e.g. Plate 1B and 7A). They are 5 mm to 1 cm in diameter and are filled with sand from the sandstone beds, which indicates that the organism thrived in the sand. This type of trace fossil shows a variable abundance where the smallest specimens have the highest abundance. From the BI-index by MacEachern and Bann (2008), the beds range from 1 to 4 in value. Based on the appearance and behaviour of the trace fossils in these samples, they are classified as *Palaeophycus* (Benton and Gray, 1981).

Chondrites

Plate: 3A, 4B, 6D-E and 7B-C.

These samples are composed of branching structures where each of the branches bifurcates regularly. They have a variable size where the smallest branches are 0.5 mm wide (Plate 6D) and the largest are 3 mm wide (Plate 6E) and are observed at the top and at the base of sandstone beds. The branches are easily visible as they are filled with mud, which indicates that the producing organisms have burrowed through the mudstone before reaching the sandstone. The samples occur with one or several individual branches. The largest specimens occur alone. From the BI-index (MacEachern and Bann, 2008) these beds range from 1 to 2 in value. Based on the behaviour and appearance, these are classified as the *Chondrites* (Benton and Gray, 1981).

Escape structure

Plate: 2A and 6A.

These samples are composed of vertical shafts where animals have moved through the sandstone beds. This is illustrated in Plate 2A and 6A, where there is a disruption of the laminae in the bed. The shafts are c. 5 mm across in the cross section of the beds. The whole shaft is not visible in the cross-sections, which makes it difficult to determine the exact width and geometry of the shafts. The BI-value of these beds is 1, as the laminae are still distinctive and only a few traces are visible (MacEachern and Bann, 2008).

Vertical burrows

Plate: 4A and 6B.

Vertical burrows occur in some beds. Shafts are filled with the sediments from the burrowed sediments. The shafts are seen at the base and at the top of the bed, and are 5 mm to 9 mm in diameter. The bed in Plate 6B has a value of 2 in the BI-index, while the bed in Plate 4A is more abundant, and has a value of 3 in the BI-index (MacEachern and Bann, 2008).

Horizontal burrows

Plate: 3B and 3D.

These trace fossils occur as horizontal burrows at the base (Plate 3B) and at the top (Plate 3D) of beds. They are observed as straight burrows with an infill of mud. The traces have a diameter of 2 mm to 4 mm. The beds have a value of 2 in the BI-index (MacEachern and Bann, 2008).

7 Discussion

The discussion is based on field observations, the logged sections (Appendix A), palaeocurrent measurements (Appendix C) and visual interpretations of thin sections (Appendix D), acetate peels (Appendix F) and trace fossils (Appendix G). The logs cover only vertical sections, and therefore present lateral constraints for the depositional strike and the lateral extent of the formation in an otherwise 3D-depositional system. To get an understanding of the lateral extent of the area, information from published sources needs to be taken into account.

7.1 Structural outline

7.1.1 Palaeocurrent and palaeodepth indicators

Palaeocurrent measurements are useful for the understanding of transport of material in the system. Both the asymmetric and symmetric ripples can be formed by oscillatory motion (Evans, 1941). Palaeocurrent measurements of the symmetrical ripples display a stable trend for the Djupvarp Member and Limovnstangen Member at Limovnstangen (Fig. 6.20), Borgen (Fig. 6.30) and Toverud (Fig. 6.42). At all localities they have a NW-SE biomodal palaeoflow direction. The measurements of the symmetrical ripples from Toverud are few and are therefore not statistically valid. They do, however, give an indication of the orientation of the palaeocurrent of the wave ripples. The asymmetrical ripples from Limovnstangen show a NW unimodal palaeoflow direction (Fig. 6.21). As the palaeoflow of the wave ripples are directed close to perpendicular on the shoreline (Duke, 1990), the palaeoshoreline must have had a NE-SW orientation during the time of deposition of these two members. The trough cross-bedded sandstone (Facies IIb) and cephalopods of the Djupvarp Member at Borgen (Fig. 6.28) and Åsaveien (Fig. 6.34) indicate an average transport in a W-NW direction, slightly oblique on the palaeoshoreline. The bipolar direction of the cross-bedded limestone (Fig. 6.22) (Facies IIIc) has been suggested by Broadhurst (1968) to be formed as a result of tidal influence. They display a transport direction to the NE and SW, parallel to the shoreline. There are, however, no other visible indications for tidal influence in the Limovnstangen Member, indicating a different process. A possible cause could be that the two-dimensional dunes were strongly sinuous, which would display distorted directions. The measurements from both the through cross-bedded sandstone (Facies IIb) and the cross-bedded biosparitic limestone (Facies IIIc) are few, and might not be statistically valid.

The gutter casts measured in the Limovnstangen Member at Limovnstangen show a mean SW-NE orientation (Fig. 6.19). The gutter cast in the Djupvarp Member at Borgen (Fig. 6.29) and Toverud (Fig. 6.43) show W-NW to E-SE and W-SW to E-NE direction. The gutter casts at Limovnstangen and Toverud show a shore-parallel orientation which suggests a set-up of currents which were created by unidirectional geostrophic flows (cf. Myrow, 1992b, Myrow and Southard, 1996). The Djupvarp Member at Borgen illustrates a shore-oblique direction of the gutter cast which were formed under unidirectional, shore-oblique geostrophic flow in accordance with formation of gutter casts as interpreted by Myrow and Southard (1996). Gutter casts oriented perpendicular to the shoreline has been formed by oscillatory flows generated by waves during storms (Plint, 1996). This suggests a dominance of geostrophic flow during deposition of the upper two members. The dominance of either of these two forces might be controlled by storm intensity and duration, wave height and water depth (Varban and Plint, 2008). It's important to note that there are few measurements from the Toverud and Borgen locality and that the palaeodepth indicators may not be statistically valid.

7.1.2 Palaeogeographic setting

The palaeocurrent direction illustrates a shore line which was directed from SW to NE. The gutter casts indicate a more proximal position for the Ringerike District than the Modum District, which suggests a palaeoslope inclined towards the present southeast, which is also confirmed by the work done by Thomsen (1982) and Baarli (1985). The amount of coarser material is decreasing from the northwest to the southeast, which is observed in the Djupvarp Member at the Toverud and the Borgen localities. The presence of tempestites in the Solvik Formation (Baarli, 1985), suggests that the deepest part of the Oslo Region was not positioned under maximum storm wave base. A transect from the Solvik Formation in the central Oslo District (Baarli, 1985), Sælabonn Formation at Hadeland (Braithwaite et al., 1995) and Helgøya Formation in the Mjøsa districts (Skjeseth, 1963, Worsley et al., 1983) displays the same trend. This indicates a source area for the siliciclastic material to the present west or northwest, rather than the east. The tectonic transport of the Caledonian orogeny displays a general NW to SE transport, where local differences occur in the Oslo Region (Bruton et al., 2010, Hjelseth, 2010). This suggests that during the formation of the Sælabonn Formation the palaeoshoreline was oriented close to parallel with the evolving Caledonian orogeny.

The Solvik, Sælabonn and Helgøya formations represent the first siliciclastic units of the Silurian succession in the Oslo Region and were formed on a shallow shelf. The second and

third units are represented by the Bruflat Formation and the Ringerike Group. In between these pulses carbonate rich units are present, represented by the Rytteråker Formation as the first unit and the Braksøya and Steinsfjorden formations as the second units at Ringerike. The Sælabonn Formation is succeeding the Langøyene Formation where these two formations are bound by an erosional surface, which coincides with the Ordovician-Silurian boundary (Worsley et al., 1983, Braithwaite et al., 1995). The shifts in facies patterns, high siliciclastic input and carbonate dominance, suggest interactions between tectonic events.

7.2 Petrography

The fine grain size (Fig. 6.18) indicates a transport through suspension load and not as bedload. Work performed by Krumbein (1941) suggests that smaller grains are less rounded than larger grains, transported over the same distance. The size and roundness of the grains in the Sælabonn Formation suggest the same (Fig. 6.18). It should be noted that the initial distance from source to deposition is difficult to calculate for the Sælabonn Formation.

The mineral content of the thin sections shows a high amount of quartz and calcite. As mentioned in Chapter 5.5 the total feldspar content of the samples might be underestimated, and the real abundance is likely higher. However, the amount of feldspar has the highest abundance in the Djupvarp Member (Borgen, avg. 7.9%; Fig. 6.25, Åsaveien, avg. 10.7%; Fig. 6.33 and Toverud, avg. 7,9%; Fig. 6.40), but this might also be due to the larger grain size as this would make it more easily to differentiate between feldspar and quartz grains. The quartz/feldspar relationship (Q/F-ratio) is connected to the amount of the reworking of the sediments. Due to abrasion of the sediments mechanically weak or soft grains are shattered during transport (Boggs Jr., 2009). In all localities a variation in the relationship is recognized, where a higher ratio indicate totally a longer distance of transportation and abrasion of the sand population. When comparing the different localities a trend is visible. Higher abundance of siliciclastic sediments is represented with a higher Q/F-ratio, suggesting a higher rate of reworking of the sediments. The Sylling Member and the Djupvarp Member in the Ringerike and Modum districts display a higher Q/F-ratio than the rest of the Sælabonn Formation, suggesting a higher rate of reworking of the beds (Table 7.1). Table 7.1 show an upward decrease in the ratio, whereas the values for the Djupvarp Member are decreasing from the Modum District towards the Ringerike District, suggesting a relative shorter distance of transport for the sediments in the Ringerike District. No other clear trends are prominent, other than higher abundance of sand correlates with higher Q/F-ratio. Due to the data

uncertainty it's difficult to interpret the data. If the source is feldspar-poor the Q/F-ratio would be deceptively high (Pettijohn, 1975), as it might be in this case.

Table 7.1: Average Q/F-ratio from the members. Few samples may cause uncertainty.

	Ringerike District	Modum District
Limovnstangen Mbr.	5	5
Djupvarp Mbr.	7	8
Store Svartøya/Sylling Mbr.	-	8

The porosity and permeability were most likely better before final burial, as fractured mica between grains and corroded quartz and feldspar are recognized (Fig. 6.27). This indicates both a chemical and mechanical compaction of the rocks. The samples show both interconnection and non-interconnection between the pore spaces, which have been filled by calcite cement. The source of the calcite cement is very likely dissolved fossil fragments, and the corrosion of quartz and feldspar is associated with the presence of calcite cement in the rocks, as also shown by Turner and Whitaker (1976).

The limonite in the sample is secondary and is a result of weathering or oxidation of the rock (Kerr, 1959). The highest abundance occurs at Toverud, Åsaveien and Borgen, which also are the localities where the intensity of weathering are the highest.

7.2.1 Provenance

An indicator for the source material coming from the advancing nappe would have been presence of the antiperthite ("Jotunperthite" from the Jotun Thrust Sheets) found and described in the Ringerike Group (Turner and Whitaker, 1976). However, no antiperthites were observed during the study of the thin sections. The high abundance of quartz in the sandstone indicates that the source area was rich in quartz, where the source material could have derived from a land area to the northwest (Telemark Land) or the Valdres Thrust Sheets. The Valdres Thrust Sheets contain slices of Precambrian basement, Precambrian and Vendian immature sedimentary rocks and Cambro-Ordovician quartzites and slates (Nickelsen et al., 1985). The land area to the northwest is suggested to be an important source area for siliciclastic material (Bruton et al., 2010). The presence of polycrystalline and undulatory quartz grains suggest a partly source from metamorphic rocks (Boggs Jr., 2009). The large polycrystalline quartz grains (Fig. 6.40) from the lag layer (facies association FA3) on top of the Ordovician-Silurian surface suggest the same.

Braithwaite et al. (1995) favoured a sediment source from the aulacogen sequence in the Hedmark Basin to the north and the crystalline basement for the Hadeland District (Fig. 2.1), which were uplifted by the movement of the developing nappe pile in the NW. Baarli (1985) suggested that the siliciclastic source for the Oslo and Asker districts was situated in the W to SSW. Braithwaite et al. (1995) also suggested the sandstone to be a second generation sandstone, at the Hadeland District, as it displayed a mineralogical maturity. The Sælabonn Formation at the Ringerike District does not show the same high maturity, as the feldspar content of the sandstone is more likely higher than 10 %. Further research should be performed to confirm this.

The lateral extent of the Sælabonn Formation suggests a source area NW to SW of Ringerike, as it gets gradually thinner towards the south (Ringerike and Skien) and north (Mjøsa) of Hadeland. As the palaeoshoreline was situated to the NW, parallel to the Caledonian Thrust Front a siliciclastic source to the NW is favoured. The sediments from the source area could have been rerouted to the south or north, where the alongshore currents have been the main transport agent for the siliciclastic material on the shelf, once it reached the sea. The primary source is however something that need to be looked further in to, as sufficient data is not available in the data set of the present work.

7.3 Fossil fauna

The sample from the uppermost part of the Langøyene Formation shows a different composition in fossil fauna, compared to the samples from Sælabonn Formation. The presence of ooids, oncoids and algae fragment, suggests a shallow high energy environment (Flügel, 2004) for the uppermost of Langøyene Formation at Grunntjern.

The fossil fragments from the bioclastic beds in the Sælabonn Formation reflects, as presented in Chapter 6.3 (Fig. 6.44, Fig. 6.47, Fig. 6.48, Fig. 6.51, Fig. 6.53, Fig. 6.55), a mixture of infaunal and epifaunal elements (e.g. brachiopods, crinoids, bryozoans, trilobites, corals and gastropods). This was also observed by Thomsen (1982). All fossils observed in the Sælabonn Formation display reworking, which occurred during winnowing of the material during storms. Corals, crinoids and bryozoans need a hard substrate to grow and thrive. Their habitat might have been carbonate shoals on the shelf. The size of the corals might have been a limiting factor on the abundance as high energy is needed to transport them, which only occurred during the larger storms. The other groups (e.g. brachiopods and trilobites) tolerate the muddy substrate. The size of e.g. bryozoans and crinoids are not big which might have

been caused by the environment, as frequent storms would have prevented them from growing larger. The micrite observed in the samples from Grunntjern and Toverud occur as clasts and bioturbation. The occurrence of clasts is due to erosion of sea-bed during storms while as bioturbation is due to burrowing, as they appear as rounded shapes in cross-section (Fig. 6.56). Gastropods in general are abundant in all environments (Flügel, 2004), they are however here only observed in two samples representing storm layer and slumping.

The brachiopod shells have a random orientation which is common for event-beds as tempestites (Kreisa, 1981). The larger shells, where the majority seem to have a convex-up orientation, were affected to a greater extent by the currents, as this is a hydro dynamical more stable position. A statistical analysis should be performed on the brachiopod shells to see if there is a correlation between the size and orientation.

7.4 Depositional Environment

As suggested in Chapter 7.1 the Ringerike District displays a more proximal position to the shoreline than the Modum District. The general trend displays an increase in siliciclastic content in the Djupvarp Member, with a following decrease. Thomsen (1982) has suggested a correlation between the different outcrops for the Sælabonn Formation, in the Ringerike District. Two attributes are recognized for correlation purposes between the localities; however, an exact correlation is difficult to determine. The first one is the increased presence of siliciclastic material in the Djupvarp Member which is recognized at Åsaveien, Borgen and Toverud, but represents different facies associations. The second is the underlying and overlying formations, which are characteristic in appearance. The abrupt change in lithology from the underlying Langøyene Formation and the transitional change from dominance of siliciclastic material to dominance of carbonate material in the overlying Rytteråker Formation.

Store Svartøya and Sylling Member

The Store Svartøya and Sylling members are dominated by facies association FA1a, which represents a calmer environment where tempestites occasionally were deposited. The Store Svartøya Member is thinner than the Sylling Member which was most likely due to differences in the distance to the shoreline (Fig. 7.1). At the lower part of Sylling Member a unit (c. 4.5 m – c. 13 m) of sub-facies associations FA1b and FA1c is recognized together with FA1a, which indicates an increase in energy. This illustrates a slight shallowing which causes an increased input of siliciclastic sediments and deposition of frequent storm layers.
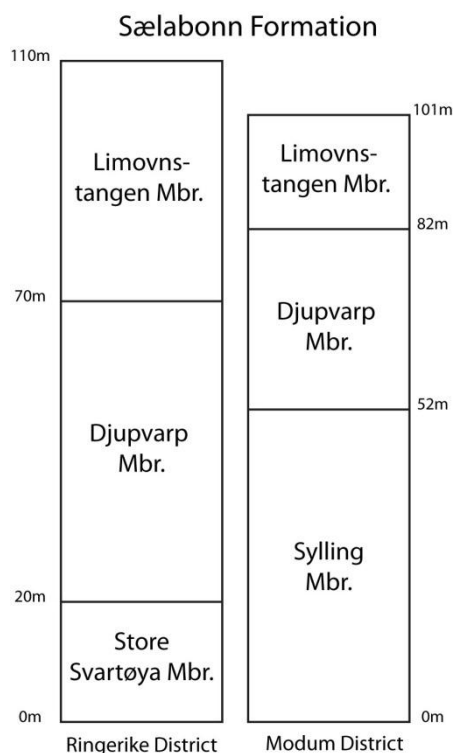
Figure 7.1: Overview of the thicknesses of the members in the Sælabonn Formation in the Ringerike District and the Modum District. The thickness of the members in the Ringerike District is from Thomsen (1982), as the current work lacks the sufficient data to make an estimate.

This unit is followed by a long section of sub-facies association FA1a, which illustrates deeper conditions, as only the strongest storms were able to reach the bottom of the sea-bed. The forming of nodular limestone is an indication of the deeper position of the shelf in this area (Möller and Kvingan, 1988). A turn around point, with increasing siliciclastic sediments, is observed at c. 30 m (Fig. 6.39). Infilling of the accommodation space leads to a shallowing event, with a maximum in the Djupvarp Member. This implies a shallowing in the upper part of Sylling Member into the Djupvarp Member, also suggested by Baarli (1988). The Store Svartøya Member at Grunntjern is characterized by a higher abundance of sand beds closer to the base than the Sylling Member at Toverud, where the beds closer to the base are mostly calcareous. This indicates that Grunntjern was situated more proximal to the siliciclastic source than Toverud. This implies that the lower members of the Sælabonn Formation display a transgressive setting before a turn-around, with in-filling of the accommodation space causing a slight shallowing.

The presence of the various sub-facies associations suggests a position in the offshore-transition area (Fig. 7.2A).

Djupvarp Member

The Djupvarp Member in the Ringerike District displays a shoal environment where the Åsaveien succession displays a more inner position on the shoal, while the Borgen strata display a more distal position. In the Modum District the Djupvarp Member is dominated by the deposition of tempestites. Possible causes for the rhythmicity in the Ringerike District could be (i) eustatic sea-level changes or (ii) regional sea-level changes. The presence of Facies IIIc on top of Facies IIb indicates an abrupt lack of the siliciclastic component, which suggests a retreat of the shoreline.

The Sælabonn Formation sediments were deposited on a large shallow shelf, where a slight increase in sea-level would push the shore further inland, which would diminish the supply of

siliciclastic material. Regional sea-level changes are usually influenced by tectonic movements. Cyclicity due to tectonic movement is difficult to prove, however, the cyclicity has most likely a time span of 100 000's years and not millions of years. A possible cause for this rhythmicity could be the Milankovitch eccentricity cycles, which are of 100.000 and 400.000 years intervals. However, this is a hypothesis which needs more attention. The slightly oblique transport of the sand dunes on the palaeoshoreline suggests transport controlled by oscillatory flow. The tempestites at Toverud are in average thicker than the tempestites observed in the other members; according to Swift and Parsons (1999) tempestites increase in thickness when they are closer to the shore. The access of sand is also greater in the Djupvarp Member which also needs to be taken into account. At the Ringerike District (Borgen and Åsaveien) facies association FA2 reflects the middle member, while at the Modum District (Toverud) sub-facies association FA1b dominates.

A possible origin of the sand shoals would be an overstepping of barriers, formed during transgression by reworking of fluvial sediments deposited on the exposed shelf during previous sea-level lowstand. The water column advances over the sand and erodes it from the substrate; therefore, the sand does not find its way to the shelf, instead it is already situated there (Swift and Parsons, 1999). The barrier sand would eventually evolve and become detached from the shoreface, forming isolated sand bodies on the shelf as the transgression progressed. Thomsen (1982) suggested that Djupvarp Member reflected submerged bars, however the extent of the sand beds suggests otherwise. She also saw indications of tidal influence; this is however not observed at Borgen and Åsaveien, which suggests that the member was positioned deeper than she postulated. The tidal influence might also have been from the remnants of the barrier complex, as she has a more extensive coverage of the Djupvarp Member at Ringerike.

As the transgression progressed the sediments were reworked, due to erosion of the shoreface before the finer sediments are transported offshore where they are deposited (Swift and Parsons, 1999). A progradation of the coastline is favoured for the Djupvarp Member as the tripartite splitting of the formation occurs in several areas from north to south in the Oslo Region (Worsley et al., 1983, Braithwaite et al., 1995). This suggests a regional event with increase of net sediment supply, rather than an overstepping of a barrier complex during transgression.
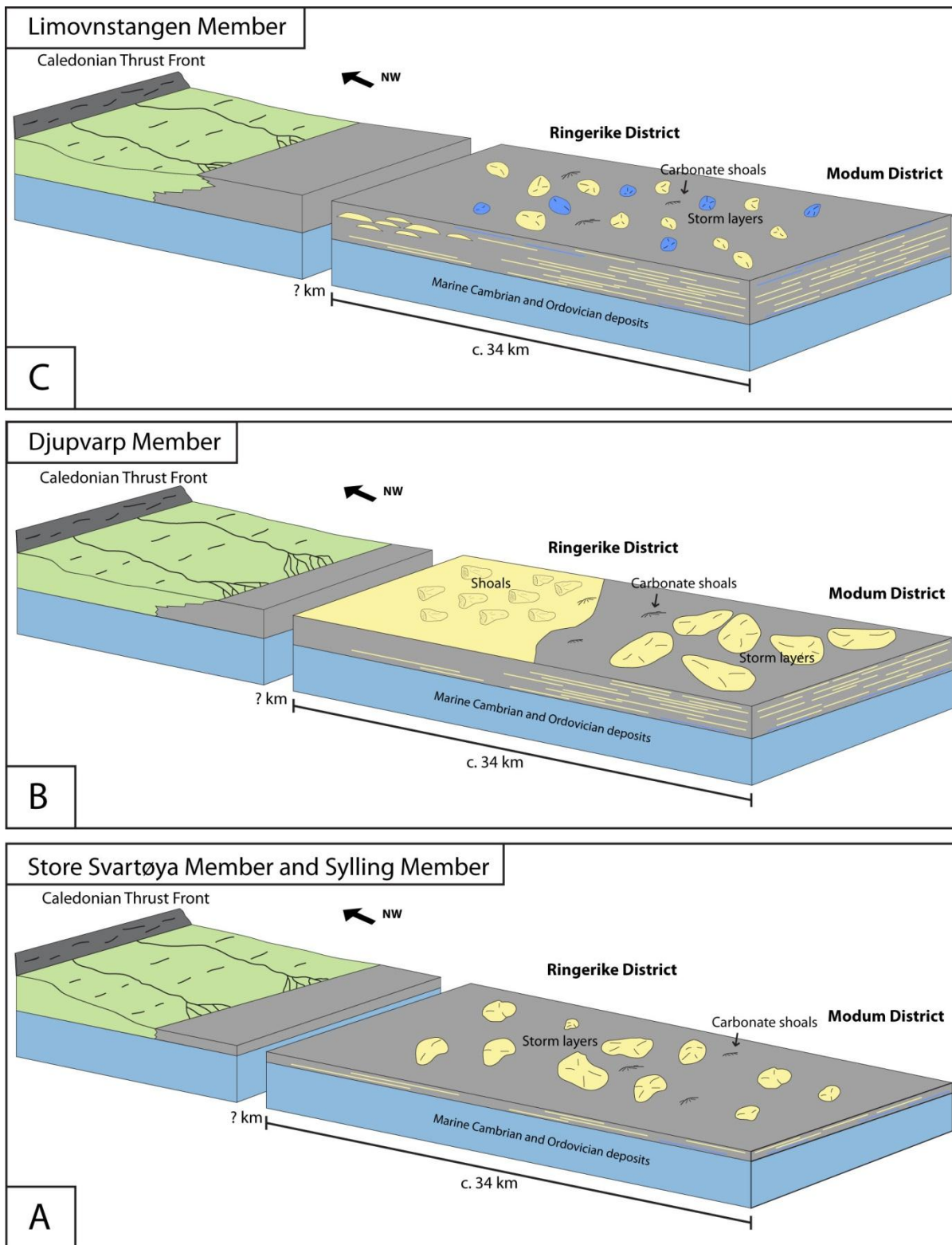
Figure 7.2: Schematic illustration of the depositional environment during deposition of the Sælabonn Formation at Ringerike and Modum districts. A) Store Svartøya and Sylling Member; a transgressive setting where deposition of mud is dominant, where tempestites are deposited during sudden events. B) Djupvarp Member; progradation of the coastline with development of sandy shoals at the Ringerike District and more extensive and thicker tempestites deposited in the Modum District. C) Limovnstangen Member; continued transgression with decrease in siliciclastic material where both deposition of sandy and bioclastic tempestites in mudstone. All four members indicate an inner shelf position. Palinspastic reconstruction suggests that the Grunntjern locality was situated 34 km closer to the palaeoshoreline than the Toverud locality (Chapter 7.5).

84

Braithwaite et al. (1995) observed that the Sælabonn Formation was only represented by the Djupvarp Member in the eastern part of the Hadeland District, suggesting a progradation of the coastline from the NW.

Trace fossils recognized at Toverud, Borgen and Åsaveien have been classified as *Palaeophycus* and *Chondrites*. *Chondrites* is a facies breaker where the occurrence is related to chemically reducing conditions in the sediments, which makes it indirectly dependent on the sea-floor conditions (Bromley and Ekdale, 1984). *Palaeophycus* represents dwelling burrow and are also facies-crossing, occurring in all environments (Benton and Gray, 1981, Buatois and Mángano, 2011).

A progradation of the coastline is suggested for the Djupvarp Member, which explains the formation of shoals in the Ringerike District and increased abundance of thicker tempestites in the Modum District (Fig. 7.2B). Due to low stratigraphic resolution, geometry and extent of the shoal system is difficult to determine, but the Djupvarp Member might represent an isolated shallow marine sandbody in the offshore-transition area on the shelf.

Limovnstangen Member

The Limovnstangen Member reflects a time interval of reduced supply of siliciclastic material, in contrast to depositional time of the Djupvarp Member, as well as a general upward decrease of the siliciclastic material in the member (Fig. 6.15). Both at Toverud and Limovnstangen the same environment is reflected, with slightly thinner beds at Toverud. The decrease of bioclastic material (Chapter 6.2.1) in the Limovnstangen Member is interpreted to have been caused by a transgression. The storms have not been strong enough to wash out the bioclastic material, suggesting a deeper position. The following increase of bioclastic material coincides with the decrease in siliciclastic material, suggesting a lower supply of siliciclastic material and possibly a shallowing. Pulses of siliciclastic material (Fig. 6.15) can be caused by sea-level variations, as their volume and frequency is directly related to sediment supply by nearshore erosion and redeposition (Einsele, 1996). The cause is, however, uncertain, but a connection to the Milankovitch periodicity might be an explanation, or the pulses might reflect events in tectonic activity in the advancing Caledonian Thrust Front. The formation of gutter casts indicate a presence of alongshore currents, which have transported material into the area. Baarli (1985) suggested an oblique transport of the siliciclastic sediments on the shelf for the Solvik Formation, due to geostrophic counter currents set up by storms.

Palaeophycus, *Chondrites*, escape structure, vertical burrows and horizontal burrows are observed in the Limovnstangen Member, where *Palaeophycus* has the highest abundance. The escape structures suggest an episodic deposition of the sandstone beds (Facies IIa). As both the *Palaeophycus* and *Chondrites* are facies-crossing, environmental signals are difficult to interpret based on these observations.

Whitaker (1977) suggested a depth of 200 meters for the Limovnstangen Member at the Ringerike District. This is unlikely as, according to Dumas and Arnott (2006), hummocky cross-stratification only forms in the depth ranges of 13 m to 50 m. An offshore-transition position on the inner shelf is suggested for the Limovnstangen Member (Fig. 7.2C).

7.5 Back-Bulge Depozone

To understand the stratigraphical development of the Sælabonn Formation the distance and the direction of the tectonic shortening should be perceived. To clarify this is a difficult subject, as little shortening is needed to form folds and the amplitude of the folds differs, overthrusting is a problem in itself. Both Fjærtoft (1987) and Morley (1986a) concluded that shortening is difficult to calculate, as there is both lateral and vertical differences in strain of the Lower Palaeozoic succession in the Oslo Region. Morley (1986a) suggested a shortening of 50 % for the Lower Ordovician in the northern part of Ringerike. A 50% shortening of Lower Silurian in the Ringerike District might be a reasonable estimate; however this is just an assumption and further work need to be done to confirm this estimate (Bjørn Tore Larsen, pers. comm., 2012). As previously mentioned the general direction of the shortening was most likely from the NW. Palinspastic reconstruction, with a 50% shortening, suggests an initial distance of 34 km at the time of deposition, from the present 17 km, where Grunntjern would have been situated 34 km closer to the palaeoshore than Toverud (Fig. 7.2).

The Sælabonn Formation is in contrast to the overlying Rytteråker Formation (Chapter 4.2), dominated by siliciclastic sediments. The palaeogeographical position of the Sælabonn Formation has been suggested by Thomsen (1982) to be on an epicontinental shelf; however, the position of the formation in relation to the developing Caledonian foreland basin has been vaguely defined.

The exposure of the shelf sediments, Langøyene Formation, has been suggested to be tectonic and eustatic; where Spjeldnæs (1957) was in favour for folding, while Brenchley and Newall (1975) suggested eustatic sea-level fluctuations and local adjustments of the basement blocks.

Bjørlykke (1974) suggested that the relative subsidence of the Oslo Region in the Early Silurian was not only influenced by a eustatic sea-level rise, but also had a strong tectonic component. The missing part of the Upper Ordovician at the Mjøsa districts was, according to Bjørlykke (1983), caused by uplift and exposure in this period and was synchronous with the subsidence further south in the Oslo Region. Bjørlykke (1983) thought that the most likely cause was the adjustment of the craton related to subduction further west. The evidence of an angular unconformity, which was suggested by Spjeldnæs (1957), is difficult to prove (Bjørlykke, 1983). Spjeldnæs (1957) suggested that the base of Silurian gets younger further north which was supported by Thomsen (1982), who observed kart surface inclined towards the south. Karst surfaces were also observed at Mjøsa, where also a significant age gap is present, where the whole Ashgillian is missing (Skjeseth, 1963, Worsley et al., 1983, Owen et al., 1990). Skjeseth (1963) referred to the Helgøya Formation, which is the lowermost Silurian deposits in the Mjøsa districts, as sub-Stage 6c, which correspond to the Limovnstangen Member in the Ringerike District. The biostratigraphical resolution of conodonts is too low to date the gap between the Ordovician and Silurian strata, but the occurrence of *Oulodus kentuckyensis* and *Icriodella discreta* suggests a Silurian age for the Solvik Formation and Sælabonn Formation in the Asker and Ringerike districts (Aldridge and Mohamed, 1982). Work done on graptolites suggests the same, but data from the Ringerike District is not presented in the paper by Howe (1982).

Palaeo-water depth analysis of graptolites done by Baarli (1985) suggest an overall upwards shallowing for the Asker and Oslo districts. Baarli et al. (2003) performed work on graptolites in the Helgøya Formation (named the Sælabonn Formation in that paper), which suggested a slight deepening of the Helgøya Formation. A cross section from Toten in the NW to Malmøya in the SE suggests a gradual deeper position of the lowermost Silurian towards the SE (Baarli et al., 2003). Comparing the global eustatic curve (Fig. 4.3) by Johnson et al. (1998) with the relative sea-level curves for the Oslo Region given by Baarli et al. (2003), no comparable trend is evident. Differences in the relative sea-level in the districts suggest that the eustatic influence in sea-level has been very little. The different palaeo-water depth-trends from NW to SE suggest tectonic influences as dominant on the region, rather than the eustatic sea-level changes.

The increasing age gap from SE to NW in the Oslo Region suggests an uplift of the northern area. The development of a peripheral bulge would explain the relative decrease and increase in sea-level and creation of accommodation space, together with the eustatic fluctuations in

the sea-level. A tectonic influence caused by the peripheral bulge does not necessarily need to results in an angular unconformity. As the continental crust of Baltica is old and thick (Garfunkel and Greiling, 1998) the bulge would have had a large wavelength. This would cause the Silurian strata to lie disconformably on top of the Ordovician strata.

The transgressional development of the Sælabonn Formation, which also was suggested by Bruton et al. (2010), might have been influenced both by the retrogradation of the peripheral bulge and eustatic sea-level rise. The deepening close to the base of the Solvik Formation was suggested by Baarli (1985) to be caused by a eustatic sea-level rise. Hendriks and Redfield (2005) argued that the Caledonian foreland basin was not a large basin. If this is the case the depression in front of the thrust wedge was not of great proportions, and therefore could "easily" be filled causing spill over of sediments to the forebulge/back-bulge area (Fig. 7.3).

The increase in sea-level and creation of accommodation space at Ringerike may be due to retrogradation of a foreland bulge, whereas the progradation in the Djupvarp Member may be due to a response of filling of the foredeep. Retrograding of a foreland bulge takes place when the thrusting slows down and subsidence is the dominant process in the thrust wedge as sediments fill the basin (Sinclair et al., 1991, Bertog, 2010). The start-up of thrusting will cut off the siliciclastic source and movement of the peripheral bulge will start to move towards the SE. With the decreasing siliciclastic input the bioclastic material starts to dominate, leading to the formation of the Rytteråker Formation. The overall upward shallowing of the Solvik Formation in the central Oslo Districts suggests that the sediment supply was higher than the creation of accommodation space. Therefore a position in the back-bulge depozone might be reasonable to assume for the Sælabonn Formation and the Solvik Formation (Fig. 7.3).
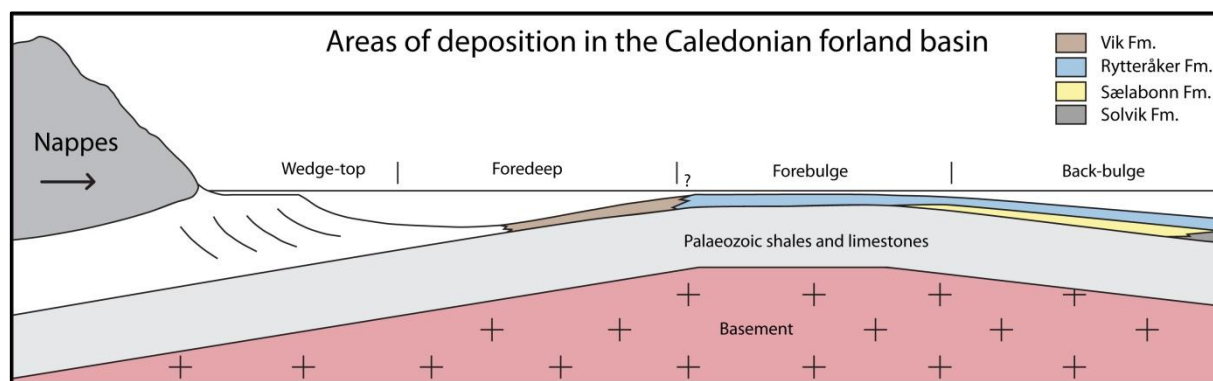

Figure 7.3: Suggested areas of deposition in the Caledonian foreland basin. The horizontal and vertical scale is not representative for the actual distance or thickness. Modified from Baarli (1990a).

The Ordovician-Silurian boundary

The lowermost Silurian sediments, facies association FA3, in-fills the karst surface of the uppermost Ordovician Langøyene Formation, as has been recognized by others (e.g. Skjeseth, 1963, Thomsen, 1982, Braithwaite et al., 1995) in the Ringerike, Hadeland and Toten districts. In this study two localities were studied, where the boundary is exposed. At Grunntjern the massive limestone, uppermost Langøyene Formation, is succeeded by facies association FA1a, of the Sælabonn Formation. These two formations are separated by a wavy surface, the Ordovician-Silurian boundary. At Toverud the same massive limestone is present but with karst structures on top, in-filled by the lag deposit of facies association FA3 (Chapter 6.1.2) and succeeded by facies association FA1a. Karst structures are produced by fresh water running on exposed carbonate rocks (Collinson et al., 2006). Thomsen (1982) and Braithwaite et al. (1995) also described these karst structures at Store Svartøya in the Tyrifjord and in Hadeland, respectively. At Store Svartøya the structures are much larger with a width of 1-2 meters and depth of 0.5 meter, where they are inclined towards the south (Thomsen, 1982).

The wavy surface at Grunntjern might have been caused by topographic differences on the exposed shelf as the flowing water eroded. The in-filling of the karst surfaces was, according to Braithwaite et al. (1995), caused by a minor transgression during the overall regression. Braithwaite et al. (1995) regarded the top Ordovician as a type one sequence boundary. Larsen and Olaussen (2005) recognized the top Ordovician as a second-order sequence boundary. The granule quartz grains could have been transported into the depositional area either through the development of a fluvial environment on the exposed shelf, or as erosional remnants from the underlying Langøyene Formation. A development of fluvial environment would also suggest a development of channels in the Oslo Region. The Ordovician-Silurian boundary is interpreted as a ravinement surface.

7.6 Sedimentological development of the Oslo Region

To understand the regional development of the stratigraphy of the Oslo Region we must first recognize that there have been allocyclic mechanisms influencing the Oslo Region, which eventually has led to structural shortening of the Lower Palaeozoic succession of the region. This means that the localities were separated further apart during the time of deposition than the distance they reflect today.

The sedimentary rocks in the Oslo Region are varied, with wide facies belts displaying different depositional characters. Størmer (1967) recognized a development of NNE-SSW trending facies belts from the Late Ordovician Caradoc, with shallow environments in the north and south progressing into more distal muddy environments to the east. Halvorsen (2003) proposed a new basin model for the Silurian stratigraphy. He also implied that the Sælabonn Formation might have been one of the first clastic derivate from the Caledonian fold-and-thrust belt. Illustration of the Upper Ordovician and Silurian stratigraphy of the Oslo Region is presented in Figure 7.4

1. **Upper Ordovician**

   The channel structures and the infill in the Oslo District have been suggested to be caused by a sea-level low-stand and movements in the basement (Brenchley and Newall, 1975, 1980) as well as an uplift of the western margins of the Oslo District (Spjeldnæs, 1957). The following transgression, where base Silurian gets younger further north, suggests a tilt of the platform and regional uplift of the western margins of the Oslo Region, where at Mjøsa the Upper Ordovician is missing. In Valdres and Gausdal, turbidite deposits of Middle Ordovician age are recognized, belonging to the Strondafjord and Gausdal formations (Nickelsen et al., 1985). These deposits suggest that a foredeep (Fig. 3.4) already existed north of the Oslo Region in the Middle Ordovician.

2. **Llandovery, Rhuddanian/Aeronian Stage**

   The Sælabonn and Solvik formations are siliciclastic units which show a NW to SE deepening, displaying a more distal development to the SE with a possible source to the W to NW. Both the Helgøya and Sælabonn formations display an overall transgressive development in the western and northern parts, whereas the Solvik Formation displays an upward shallowing development in the eastern parts. The creation of accommodation space in the western and northern parts of the Oslo region are possibly caused by the retrogradation of a peripheral bulge. With decreasing movements of nappes, accommodation space will be created at the margins of the orogeny due to subsidence. This allows the carbonate material to dominate the environment, which is represented by the Rytteråker Formation.

   Möller (1989) suggested a migration of a bar system with a reversal in the early Telychian for the Rytteråker Formation. This however, was not in agreement with Baarli

(1990a), as a shallowing occurred in the Ringerike, Asker and Oslo districts. Baarli (1990a) however recognized a reversal of the bottom slope in the Aeronian and Early Telychian with a high south of the Ringerike District. This is likely due to the movement of the peripheral bulge. This is advocated by the formation of the deep graptolite basin or trough in the north postulated by Worsley et al. (1983) and Bjørlykke (1983). The deposition of the Sælabonn and Rytteråker Formation is most likely controlled by the movement of the peripheral bulge. As postulated by Baarli (1985) the fluctuations of the sea-level could also have been caused by eustatic sea-level changes. This is more likely to have caused minor variations in sea-level; where Baarli (1985) observed minor deepening's in the Solvik Formation.

3. **Llandovery, Telychian Stage**

The upper part of the Vik Formation has been regarded as a distal development (Oslo District) of the Bruflat Formation, and the siliciclastic input is recognized as diachronous with the late Aeronian deposits in the Ringerike District and earliest Telychian deposits in the central Oslo Region (Fig. 7.4) (Baarli, 1990a). The west to east dipping palaeoslope previously recorded in the Llandovery was re-established in the mid-Telychian, between the Ringerike and Oslo districts (Baarli, 1990a). The progressively deeper position of the northern Ek Formation compared to the southern Vik Formation (Fig. 7.4) (Worsley et al., 1983, Baarli et al., 2003), suggests a position in the foredeep of the foreland basin (Fig. 7.3). The palaeodepth proposed by Worsley et al. (1983) was revised by Baarli (1990a), with very little difference in depth between the Vik Formation and Rytteråker Formation. The Bruflat Formation has been hypothesised to consist of either coastal deposits or prograding delta deposits. Worsley et al. (2011) interpreted the Bruflat Formation to be submarine fans, and to be the first clastic infill of the Caledonian front. However, the turbidite deposits in the Strondafjord and Gausdal formations suggest otherwise. The deposits could also represent tempestites, not necessarily turbidite deposits, as the foreland basin might have been shallow (Hendriks and Redfield, 2005) which is also in agreement with Worsley et al. (2011). Worsley et al. (2011) suggested a single source for the immature sediment at Ringerike, where Bjørlykke (1983) suggested the Osen-Røa nappe as the source.

4. Wenlock Epoch

In the transition from the Telychian to the Wenlock carbonate sequences of the Braksøya and Steinsfjorden formations display a lack of siliciclastic material (Fig. 7.4) (Worsley et al., 2011). These formations display a marginal marine to subtidal environment, with small regressive and transgressive events in the Steinsfjorden Formation (Worsley et al., 1983). The Malmøya Formation in the central districts (Fig. 7.4) gets progressively shallower with formation of shoals. The shallowing and shoal development might reflect the movement of a bulge. The upper part of the Steinsfjorden Formation is marked with a large scale transgressive episode, which is recognized in all districts (Worsley et al., 1983). This was followed by a regional regression which ended with the deposition of the Ringerike Group (Worsley et al., 1983).

5. Ludlow and Pridoli epochs

The Silurian succession terminates with the deposition of the Ringerike Group; Sundvollen, Stubdal, Store Arøya and Holmestrand formations. Halvorsen (2003) suggested that the Sundvollen Formation developed in a piggy-back basin, where the Stubdal thrust sheet was emplaced on top of the Sundvollen piggy-back basin. Both the Stubdal and Store Arøya formations were deposited by braided rivers in the Caledonian foreland basin (Davies et al., 2005a). Davies et al. (2005a) noticed a north-south difference in the source area between the Stubdal and Store Arøya (named Skien Formation in that paper) formations (Fig. 7.4). Sediments in the Stubdal Formation derived from the Jotunheimen source area whereas sediments from the Store Arøya Formation derived from a mixed Jotunheimen/Sparagmite/local Precambrian source area. They explain this by overfilling of the northern piggyback basin allowing new transport pathways to become available over a topographic high, situated north of the Skien area.
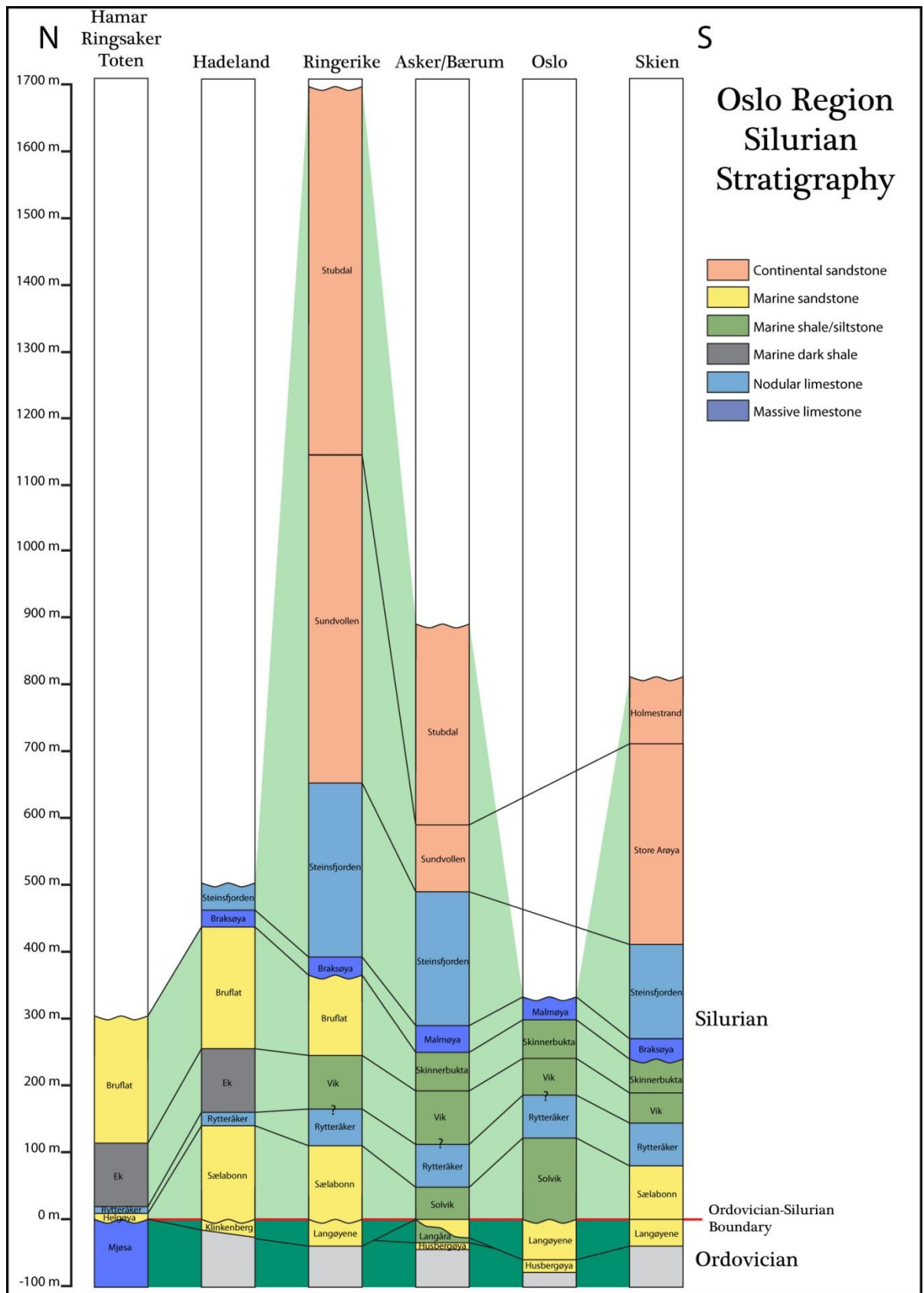
Figure 7.4: The stratigraphy of the Upper Ordovician and Silurian at the different areas with their respective formations in the Oslo Region. The formations only represented with their thickness and not age, as some of the formations are diachronous. Information compiled from Baarli (1985, 1990a), Braithwaite et al. (1995), Davies et al. (2005b), Larsen and Olaussen (2005), Möller (1989), Owen et al. (1990), Thomsen (1982), Worsley et al. (1983) and Worsley et al. (2011).

8 Conclusion

At the time of deposition of the Sælabonn Formation the palaeoshoreline had a SW to NE strike, which is close to parallel with the advancing Caledonian orogeny from the NW. The lowermost Silurian shows a deepening from NW to SE. The mineral content suggests a quartz rich source, most likely from the Valdres Thrust Sheet or the "Telemark land". The bioclastic material indicates a presence of carbonate shoals on the shelf. The deposition of the Sælabonn Formation was most likely under a tectonic influence, which is recorded by the regional sea-level differences; where the central Oslo districts show a general shallowing while the Ringerike and Toten districts displays a transgressive phase. This was likely caused by retrogradation of a peripheral bulge to the NW due to subsidence in the orogenic wedge, as the epicontinental slope was inclined towards the SE. The increased input of siliciclastic material in the Djupvarp Member is caused by a progradation, due to tectonic response in the foreland basin.

1. The Sylling and Store Svartøya members display an upward increase in siliciclastic sediments with a maximum in the Djupvarp Member, and were formed in the offshore-transition environment.

2. Djupvarp Member reflects a sandy shoal complex in the Ringerike District, whereas the Modum District displays a more distal deposit with tempestites. The increase in sand is due to a progradation of the shoreline, where the Ringerike and Modum districts are still situated in the offshore-transitional environment.

3. The Limovnstangen Member has a decrease in the siliciclastic input, from the underlying Djupvarp Member. The formation is dominated by deposition of tempestites of bioclastic and siliciclastic material, due to storms. A turn-around point is recognized, where there is an increase in carbonate material and a general decrease in siliciclastic material. A shallowing is suggested with the development of the Rytteråker Formation taking place.

The Sælabonn Formation was most likely situated in the back-bulge depozone of the Caledonian foreland basin. Further study is needed to solve some of the unanswered questions like:

- The extent of the shoal complex in the Djupvarp Member.
- The source of the siliciclastic material.

9 References

Aldridge, R.J. and Mohamed, I. 1982. Conodont biostratigraphy of the early Silurian of the Oslo region. *Paleontological Contributions from the University of Oslo* 278, 109-119.

Allen, P.A. and Allen, J.R. 2005. *Basin analysis: principles and applications*, Malden, Mass.: Blackwell. 549 pp.

Ashley, G.M. 1990. Classification of large-scale subaqueous bedforms; a new look at an old problem. *Journal of Sedimentary Petrology* 60, 160-172.

Baarli, B.G. 1985. The stratigraphy and sedimentology of the early Llandovery Solvik Formation in the central Oslo region, Norway. *Norwegian Journal of Geology* 65, 255-275.

Baarli, B.G. 1988. Bathymetric co-ordination of proximality trends and level-bottom communities; a case study from the Lower Silurian of Norway. *Palaios* 3, 577-587.

Baarli, B.G. 1990a. Depositional environments in the Telychian Stage (Silurian) of the central Oslo region, Norway. *Geological Journal* 25, 65-79.

Baarli, B.G. 1990b. Peripheral bulge of a foreland basin in the Oslo region during the Early Silurian. *Palaeogeography Palaeoclimatology Palaeoecology* 7-8, 149-161.

Baarli, B.G., Johnson, M.E. and Antoshkina, A.I. 2003. Silurian stratigraphy and paleogeography of Baltica. *In* Landing, E. and Johnson, M.E. (eds). *Silurian Lands and Seas; Paleogeography Outside of Laurentia*. New York: Bulletin New York State Museum, 493, 3-34.

Benton, M.J. and Gray, D.I. 1981. Lower Silurian distal shelf storm-induced turbidites in the Welsh Borders; sediments, tool marks and trace fossils. *Journal of the Geological Society of London* 138, Part 6, 675-694.

Bertog, J. 2010. Stratigraphy of the Lower Pierre Shale (Campanian): Implications for the Tectonic and Eustatic Controls on Facies Distributions. *Journal of Geological Research* 2010.

Bjørlykke, K. 1974. Depositional History and Geochemical Composition of Lower Palaezoic Epicontinental Sediments from the Oslo Region *Geological Survey of Norway* 305, 81 pp.

Bjørlykke, K. 1983. Subsidence and tectonics in late Precambrian and Palaeozoic sedimentary basins of Southern Norway. *Geological Survey of Norway* 380, 159-172.

Bockelie, J.F. and Nystuen, J.P. 1985. The southeastern part of the Scandinavian Caledonides. *In* Gee, D.G. and Sturt, B.A. (eds). *The Caledonian Orogen - Scandinavia and Related Areas; Part 1*: John Wiley & Sons Chichester United Kingdom., 69-88.

Boggs Jr., S. 2009. *Petrology of sedimentary rocks*, Cambridge: Cambridge University Press. 600 pp.

Boyd, R., Dalrymple, R. and Zaitlin, B.A. 1992. Classification of clastic coastal depositional environments. *Sedimentary Geology* 80, 139-150.

Braithwaite, C.J.R., Owen, A.W. and Heath, R.A. 1995. Sedimentological changes across the Ordovician-Silurian boundary in Hadeland and their implications for regional patterns of deposition in the Oslo region. *Norwegian Journal of Geology* 75, 199-218.

Brenchley, P.J. and Newall, G. 1975. The stratigraphy of the upper Ordovician Stage 5 in the Oslo-Asker District, Norway. *Norwegian Journal of Geology Supplement* 55, 243-275.

Brenchley, P.J. and Newall, G. 1980. A facies analysis of upper Ordovician regressive sequences in the Oslo Region, Norway — A record of glacio-eustatic changes. *Palaeogeography, Palaeoclimatology, Palaeoecology* 31, 1-38.

Brenchley, P.J., Newall, G. and Stanistreet, I.G. 1979. A storm surge origin for sandstone beds in an epicontinental platform sequence, Ordovician, Norway. *Sedimentary Geology* 22, 185-217.

Broadhurst, F.M. 1968. Large scale ripples in Silurian limestones. *Lethaia* 1, 28-38.

Bromley, R.G. and Ekdale, A.A. 1984. Chondrites: A Trace Fossil Indicator of Anoxia in Sediments. *Science* 224, 872-874.

Bruton, D.L., Gabrielsen, R.H. and Larsen, B.T. 2010. The Caledonides of the Oslo Region, Norway - stratigraphy and structural elements. *Norwegian Journal of Geology* 90, 93-121.

Buatois, L.A. and Mángano, M.G. 2011. *Ichnology: Organism-Substrate Interactions in Space and Time*, Cambridge: Cambridge University Press. 358 pp.

Collinson, J.D., Thompson, D.B. and Mountney, N. 2006. *Sedimentary structures*, Harpenden: Terra Publishing. 292 pp.

Crampton, S.L. and Allen, P.A. 1995. Recognition of forebulge unconformities associated with early stage foreland basin development; example from the North Alpine foreland basin. *AAPG Bulletin* 79, 1495-1514.

Dattilo, B.F., Brett, C.E., Tsujita, C.J. and Fairhurst, R. 2008. Sediment supply versus storm winnowing in the development of muddy and shelly interbeds from the Upper Ordovician of the Cincinnati region, USA. *Canadian Journal of Earth Sciences* 45, 243-265.

Davies, N.S., Turner, P. and Sansom, I.J. 2005a. Caledonide influences on the Old Red Sandstone fluvial systems of the Oslo Region, Norway. *Geological Journal* 40, 83-101.

Davies, N.S., Turner, P. and Sansom, I.J. 2005b. A revised stratigraphy for the Ringerike Group (Upper Silurian, Oslo region). *Norwegian Journal of Geology* 85, 193-202.

DeCelles, P.G. 1994. Late Cretaceous-Paleocene synorogenic sedimentation and kinematic history of the Sevier thrust belt, Northeast Utah and Southwest Wyoming. *Geological Society of America Bulletin* 106, 32-56.

DeCelles, P.G. and Giles, K.A. 1996. Foreland basin systems. *Basin Research* 8, 105-123.

DeCelles, P.G. and Hertel, F. 1989. Petrology of fluvial sands from the Amazonian foreland basin, Peru and Bolivia. *Geological Society of America Bulletin* 101, 1552-1562.

Dickinson, W.R. 1974. Plate tectonics and sedimentation. *Society of Economic Paleontologists and Mineralogists Special Publication* 22, 1-27.

Dott, R.H., Jr. and Bourgeois, J. 1982. Hummocky stratification; significance of its variable bedding sequences. *Geological Society of America Bulletin* 93, 663-680.

Drummond, C. and Sheets, H. 2001. Taphonomic reworking and stratal organization of tempestite deposition: Ordovician Kope Formation, northern Kentucky, U.S.A. *Journal of Sedimentary Research* 71, 621-627.

Duke, W.L. 1990. Geostrophic circulation or shallow marine turbidity currents? The dilemma of paleoflow patterns in storm-influenced prograding shoreline systems. *Journal of Sedimentary Petrology* 60, 870-883.

Dumas, S. and Arnott, R.W.C. 2006. Origin of hummocky and swaley cross-stratification; the controlling influence of unidirectional current strength and aggradation rate. *Geology Boulder* 34, 1073-1076.

Einsele, G. 1996. Event deposits: the role of sediment supply and relative sea-level changes - overview. *Sedimentary Geology* 104, 11-37.

Evans, O.F. 1941. The classification of wave-formed ripple marks. *Journal of Sedimentary Petrology* 11, 37-41.

Finnegan, S., Bergmann, K., Eiler, J.M., Jones, D.S., Fike, D.A., Eisenman, I., Hughes, N.C., Tripati, A.K. and Fischer, W.W. 2011. The magnitude and duration of Late Ordovician-Early Silurian glaciation. *Science* 331, 903-906.

Fjærtoft, I. 1987. *Strukturgeologisk analyse av tverrsnittet Kalvøya-Borøya-Ostøya gjennom den kambro-siluriske lagrekken, i den vestlige delen av indre Oslofjord*, Department of Geology, University of Oslo, Oslo. 177 pp.

Flügel, E. 2004. *Microfacies of Carbonate Rocks - Analysis, Interpretation and Application* Springer Berlin, Federal Republic of Germany. 976 pp.

Folk, R.L. 1962. Spectral subdivision of limestone types. *American Association of Petroleum Geologists Memoir*, 62-85.

Garfunkel, Z. and Greiling, R.O. 1998. A thin orogenic wedge upon thick foreland lithosphere and the missing foreland basin. *Geologische Rundschau* 87, 314-325.

Gaynor, G.C. and Swift, D.J.P. 1988. Shannon Sandstone depositional model; sand ridge dynamics on the Campanian Western Interior Shelf. *Journal of Sedimentary Petrology* 58, 868-880.

Giles, K.A. and Dickinson, W.R. 1995. The interplay of eustasy and lithospheric flexure in forming stratigraphic sequences in foreland settings; an example from the Antler foreland, Nevada and Utah. *Society for Sedimentary Geology Special Publication* 52, 187-211.

Gradstein, F.M., Ogg, J.G., Schmitz, M. and Ogg, G. 2012. *The Geological Time Scale 2012*.

Halvorsen, T. 2003. *Sediment infill dynamics of a foreland basin: the Silurian Ringerike Group, Oslo Region, Norway*, Department of Geology, University of Oslo, Oslo. 167 pp.

Hendriks, B.W.H. and Redfield, T.F. 2005. Apatite fission track and (U-Th)/He data from Fennoscandia; an example of underestimation of fission track annealing in apatite. *Earth and Planetary Science Letters* 236, 443-458.

Hjelseth, E.v.d.F. 2010. *Caledonian structuring of the Silurian succession at Sundvollen, Ringerike, southern Norway*, Department of Geosciences, University of Oslo, Oslo. 156 pp.

Holt, W.E. and Stern, T.A. 1994. Subduction, platform subsidence, and foreland thrust loading; the late Tertiary development of Taranaki Basin, New Zealand. *Tectonics* 13, 1068-1092.

Howe, M.P.A. 1982. The Lower Silurian graptolites of the Oslo region. *Paleontological Contributions from the University of Oslo* 278, 21-32.

Huff, W.D., Bergström, S.M. and Kolata, D.R. 2010. Ordovician explosive volcanism. *Geological Society of America Special Paper* 466, 13-28.

Jacobi, R.D. 1981. Peripheral bulge - a causal mechanism for the Lower/Middle Ordovician unconformity along the western margin of the Northern Appalachians. *Earth and Planetary Science Letters* 56, 245-251.

Johnson, M.E., Rong, J.-Y. and Yang, X.-C. 1985. Intercontinental correlation by sea-level events in the Early Silurian of North American and China (Yangtze Platform). *Geological Society of America Bulletin* 96, 1384-1397.

Johnson, M.E., Rong, J. and Kershaw, S. 1998. Calibrating Silurian eustasy against the erosion and burial of coastal paleotopography. *In* Landing, E. and Johnson, M.E. (eds). *Silurian Cycles; Linkages of Dynamic Stratigraphy with Atmospheric, Oceanic, and Tectonic Changes*. New York: Bulletin New York State Museum, 491, 3-13.

Jordan, T.A. and Watts, A.B. 2005. Gravity anomalies, flexure and the elastic thickness structure of the India-Eurasia collisional system. *Earth and Planetary Science Letters* 236, 732-750.

Kearey, P., Vine, F.J. and Klepeis, K.A. 2009. *Global tectonics*, Chichester: Wiley-Blackwell. 482 pp.

Kerr, P.F. 1959. *Optical Mineralogy*. 3 ed, New York: McGraw-Hill Book Company. 442 pp.

Kiær, J. 1908. *Das Obersilur im Kristianiagebiete: eine stratigraphisch-faunistische Untersuchung*, Christiania: i kommisjon hos Jacob Dybwad.

Kleven, M.K.H. 2010. *Caledonian (Silurian) out-of-sequence thrusting at Sønsterud, Holsfjorden, Ringerike*, Department of Geosciences, Univeristy of Oslo, Oslo. 130 pp.

Kreisa, R.D. 1981. Storm-generated sedimentary structures in subtidal marine facies with examples from the Middle and Upper Ordovician of southwestern Virginia. *Journal of Sedimentary Petrology* 51, 823-848.

Krumbein, W.C. 1941. The Effects of Abrasion on the Size, Shape and Roundness of Rock Fragments. *The Journal of Geology* 49, 482-520.

Larsen, B.T. and Olaussen, S. 2005. *The Oslo region: a study in classical palaeozoic geology*, Stabekk, Oslo: Geological Society of Norway. 88 pp.

Larsen, B.T., Olaussen, S., Sundvoll, B. and Heeremans, M. 2007. Volcanoes and faulting in an arid climate; The Oslo Rift and North Sea in the Carboniferous and Permian, 359-251 million years ago. *In* Ramberg, I.B., Bryhni, I. and Nøttvedt, A. (eds). *The Making of a Land - Geology of Norway*. Trondheim: Geological Society of Norway, 284-327.

Larsen, B.T., Olaussen, S., Sundvoll, B. and Heeremans, M. 2008. The Permo-Carboniferous Oslo Rift through six stages and 65 million years. *Episodes* 31, 52-58.

Li, M.Z. and King, E.L. 2007. Multibeam bathymetric investigations of the morphology of sand ridges and associated bedforms and their relation to storm processes, Sable Island Bank, Scotian Shelf. *Marine Geology* 243, 200-228.

MacEachern, J.A. and Bann, K.L. 2008. The role of ichnology in refining shallow marine facies models. *Society for Sedimentary Geology Special Publication* 90, 73-116.

Morley, C.K. 1986a. The Caledonian thrust front and palinspastic restorations in the southern Norwegian Caledonides. *Journal of Structural Geology* 8, 753-765.

Morley, C.K. 1986b. Vertical strain variations in the Osen-Røa thrust sheet, North-western Oslo Fjord, Norway. *Journal of Structural Geology* 8, 621-632.

Myrow, P.M. 1992a. Bypass-zone tempestite facies model and proximality trends for an ancient muddy shoreline and shelf. *Journal of Sedimentary Petrology* 62, 99-115.

Myrow, P.M. 1992b. Pot and gutter casts from the Chapel Island Formation, Southeast Newfoundland. *Journal of Sedimentary Petrology* 62, 992-1007.

Myrow, P.M. and Southard, J.B. 1996. Tempestite deposition. *Journal of Sedimentary Research* 66, 875-887.

Möller, N.K. 1986. Evidence of synsedimentary tectonics in the Lower Silurian (Llandovery) strata of Brumunddalen, Ringsaker, Norway. *Norwegian Journal of Geology* 66, 1-15.

Möller, N.K. 1987. A lower silurian transgressive carbonate succession in Ringerike (Oslo Region, Norway). *Sedimentary Geology* 51, 215-247.

Möller, N.K. 1989. Facies analysis and palaeogeography of the Rytteråker Formation (lower Silurian, Oslo region, Norway). *Palaeogeography, Palaeoclimatology, Palaeoecology* 69, 167-192.

Möller, N.K. and Kvingan, K. 1988. The genesis of nodular limestones in the Ordovician and Silurian of the Oslo region (Norway). *Sedimentology* 35, 405-420.

NGU, G.S.o.N. 2012. *Database for Geological Units* Geological Survey of Norway 2012 [Accessed: 28.08 2012]. Available at http://aps.ngu.no/pls/oradb/geoenhet_SokiDb.Startapp?

Nickelsen, R.P., Hossack, J.R., Garton, M. and Repetsky, J. 1985. Late Precambrian to Ordovician stratigraphy and correlation in the Valdres and Synnfjell thrust sheets of the Valdres area, southern Norwegian Caledonides; with some comments on sedimentation. *In* Gee, D.G. and Sturt, B.A. (eds). *The Caledonian Orogen - Scandinavia and Related Areas; Part 1*: John Wiley & Sons Chichester United Kingdom., 369-378.

Nystuen, J.P. 1981. The Late Precambrian "Sparagmites" of Southern Norway: A Major Caledonian Allochthon - The Osen-Røa Nappe Complex. *American Journal of Science* 281, 69-94.

Olaussen, S. 1981. Formation of celestite in the Wenlock, Oslo region, Norway; evidence for evaporitic depositional environments. *Journal of Sedimentary Petrology* 51, 37-46.

Owen, A.W., Bruton, D.L., Bockelie, J.F. and Bockelie, T.G. 1990. The Ordovician successions of the Oslo region, Norway. *Geological Survey of Norway Special Publication* 4, 54 pp.

Patton, T.L. and O'Connor, S.J. 1988. Cretaceous flexural history of northern Oman Mountain foredeep, United Arab Emirates. *AAPG Bulletin* 72, 797-809.

Pedersen, R.B., Bruton, D.L. and Furnes, H. 1992. Ordovician faunas, island arcs and ophiolites in the Scandinavian Caledonides. *Terra Nova* 4, 217-222.

Pedersen, R.B., Furnes, H. and Dunning, G.R. 1988. Some Norwegian ophiolite complexes reconsidered. *Geological Survey of Norway Special Publication* 3, 80-85.

Penland, S., Suter, J.R., McBride, R.A., Williams, S.J., Kindinger, J.L. and Boyd, R. 1989. Holocene sand shoals offshore of the Mississippi River delta plain. *Transactions Gulf Coast Association of Geological Societies* 39, 471-480.

Pérez-López, A. and Pérez-Valera, F. 2012. Tempestite facies models for the epicontinental Triassic carbonates of the Betic Cordillera (southern Spain). *Sedimentology* 59, 646-678.

Pettijohn, F.J. 1975. *Sedimentary rocks*, New York: Harper & Row. 628 pp.

Plint, A.G. 1996. Marine and nonmarine systems tracts in fourth-order sequences in the early-middle Cenomanian, Dunvegan alloformation, northeastern British Columbia, Canada. *Geological Society Special Publications* 104, 159-191.

Reading, H.G. and Collinson, J.D. 1996. Clastic coasts. *In* Reading, H.G. (ed). *Sedimentary environments; processes, facies and stratigraphy*. United Kingdom: Blackwell Science Oxford, United Kingdom, 154-231.

Roberts, D. 2003. The Scandinavian Caledonides; event chronology, palaeogeographic settings and likely modern analogues. *Tectonophysics* 365, 283-299.

Royden, L.H. 1993. The tectonic expression slab pull at continental convergent boundaries. *Tectonics* 12, 303-325.

S.K. 2012. *Norge Digitalt - Nasjonal geografisk infrastruktur* Statens Kartverk 2012 [Accessed: 27.09 2012]. Available at http://www.statkart.no/?_to=914.

Sinclair, H.D. 1997. Tectonostratigraphic model for underfilled peripheral foreland basins; an Alpine perspective. *Geological Society of America Bulletin* 109, 324-346.

Sinclair, H.D. and Allen, P.A. 1992. Vertical versus horizontal motions in the Alpine orogenic wedge; stratigraphic response in the foreland basin. *Basin Research* 4, 215-232.

Sinclair, H.D., Coakley, B.J., Allen, P.A. and Watts, A.B. 1991. Simulation of foreland basin stratigraphy using a diffusion model of mountain belt uplift and erosion; an example from the Central Alps, Switzerland. *Tectonics* 10, 599-620.

Skjeseth, S. 1963. Contributions to the geology of the Mjøsa districts and the classical sparagmite area in southern Norway. *Geological Survey of Norway* 220, 126 pp.

Skuce, A.G., Goody, N.P. and Maloney, J. 1992. Passive-roof duplexes under the Rocky Mountain foreland basin, Alberta. *AAPG Bulletin* 76, 67-80.

Southard, J.B. and Boguchwal, L.A. 1990. Bed configurations in steady unidirectional water flows; part 2, synthesis of flume data. *Journal of Sedimentary Petrology* 60, 658-679.

Spjeldnæs, N. 1957. The Silurian/Ordovician border in the Oslo District. *Norwegian Journal of Geology* 37, 355-371.

Stow, D.A.V. 2005. *Sedimentary rocks in the field: a colour guide*, London: Manson Publishing. 320 pp.

Størmer, L. 1967. Some aspects of the Caledonian geosyncline and the foreland west of the Baltic Shield. *Quarterly Journal of the Geological Society* 123, 183-214.

Størmer, L., Heintz, A., Henningsmoen, G., Skjeseth, S. and Spjeldnæs, N. 1953. The middle Ordovician of the Oslo region, Norway; 1, Introduction to stratigraphy. *Norwegian Journal of Geology* 31, 37-141.

Sundvoll, B. and Larsen, B.T. 1994. Architecture and early evolution of the Oslo Rift. *Tectonophysics* 240, 173-189.

Swift, D.J.P. and Parsons, B.S. 1999. Shannon Sandstone of the Powder River Basin; Orthodoxy and Revisionism in Stratigraphic Thought. *Society for Sedimentary Geology Special Publication* 64, 55-84.

Thomsen, E. 1982. Sælabonn Formation (nedre Silur) i Ringerike, Norge. *Dansk Geologisk Forening, Årsskrift for 1981*, 1-11.

Thomsen, E. and Baarli, B.G. 1982. Brachiopods of the lower Llandovery Sælabonn and Solvik formations of the Ringerike, Asker and Oslo districts. *Paleontological Contributions from the University of Oslo* 278, 63-78.

Thomsen, E., Jin, J. and Harper Davis, A.T. 2006. Early Silurian brachiopods (Rhynchonellata) from the Sælabonn Formation of the Ringerike District, Norway. *Bulletin of the Geological Society of Denmark* 53, 111-126.

Thorne, J.A., Grace, E., Swift, D.J.P. and Niedoroda, A. 1991. Sedimentation on continental margins; III, The depositional fabric; an analytical approach to stratification and facies identification. *International Association of Sedimentologists Special Publication* 14, 59-87.

Turner, P. and Whitaker, J.H.M. 1976. Petrology and provenance of late Silurian fluviatile sandstones from the Ringerike Group of Norway. *Sedimentary Geology* 16, 45-68.

Varban, B.L. and Plint, A.G. 2008. Palaeoenvironments, palaeogeography, and physiogeography of a large, shallow, muddy ramp; late Cenomanian-Turonian Kaskapau Formation, Western Canada foreland basin. *Sedimentology* 55, 201-233.

Wentworth, C.K. 1922. A scale of grade and class terms for clastic sediments. *Journal of Geology* 30, 377-392.

Whitaker, J.H.M. 1973. "Gutter casts", a new name for scour-and-fill structures; with examples from Llandoverian of Ringerike and Malmoya, southern Norway. *Norwegian Journal of Geology Supplement* 53, 403-417.

Whitaker, J.H.M. 1977. *A Guide to the Geology around Steinsfjord, Ringerike*, Oslo, Norway: Universitetsforlaget 56 pp.

Worsley, D. 1982. *Field meeting Oslo Region 1982*. Palaeontological contributions from the University of Oslo. 278, Oslo: University of Oslo. 175 pp.

Worsley, D., Aarhus, N., Bassett, M.G., Howe, M.P.A., Mørk, A. and Olaussen, S. 1983. The Silurian succession of the Oslo Region. *Geological Survey of Norway Bulletin* 72, 57 pp.

Worsley, D., Baarli, B.G., Howe, M.P.A., Hjaltason, F. and Alm, D. 2011. New data on the Bruflat Formation and the Llandovery/Wenlock transition in the Oslo region, Norway. *Norwegian Journal of Geology* 91, 101-120.

Worsley, D., Baarli, B.G. and Johnson, M.E. 1982. An excursion guide to the Lower Silurian sequences of the Asker, Ringerike and Oslo districts of the Oslo region. *Paleontological Contributions from the University of Oslo* 1982, 161-175.

Yang, W. 2007. Transgressive wave ravinement on an epicontinental shelf as recorded by an Upper Pennsylvanian soil-nodule conglomerate-sandstone unit, Kansas and Oklahoma, U.S.A. *Sedimentary Geology* 197, 189-205.

Yeats, R.S. and Lillie, R.J. 1991. Contemporary tectonics of the Himalayan frontal fault system; folds, blind thrusts and the 1905 Kangra earthquake. *Journal of Structural Geology* 13, 215-225.

Zwaan, K.B. and Larsen, B.T. 2003. *Berggrunnskart HØNEFOSS 1815 III, M 1:50.000, foreløpig utgave*. Geological Survey of Norway.

Appendix A

Legend to the Sedimentological Logs

Lithology

Sandstone

Siltstone

Sandy limestone

Limestone

Mudstone

Sedimentary structures

Symmetrical ripple

Parallel lamination

Loading

Trough cross-bedding

Gutter cast

Folded lamination

HCS Hummocky cross-stratification

Sand clasts

Cross-bedding

Cut-and-fill

Asymmetric ripple

Loaded ripple

Water escape
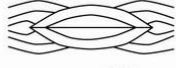
Paleocurrent directions

Unidirectional current

Bidirectional current

Gutter cast

Other notes

: Break in outcrop

: Thin section

: Acetate peels

PMO-number : Numbers refer to the museum collection numbers

R (#) : Refrence layer; to correlate logs from the same locality.

: Fault

Biogenic structures

Brachiopod

Crinoid

Rugose coral

Tabulate coral

Vertical bioturbation

Horizontal bioturbation

Cephalopod

Trilobite

Brachiopod in concreasion

Lim01-11

PMO-number	Thickness (m)	Lithology	Grain size, paleocurrent direction and sedimentary structures	Strike/dip	Facies	Facies associations

III

Lim01-11

PMO-number	Thickness (m)	Lithology	Grain size, paleocurrent direction and sedimentary structures	Strike/dip	Facies	Facies associations

Facies column entries (top to bottom):
i.a
ii.a/i.a
i.a
ii.a
iii.b/i.a
i.a/ii.a
iii.b/i.a
ii.a/i.a
i.b
iii.b/i.a
ii.a
iii.b
i.a/ii.a
ii.a
i.a/ii.a
ii.a
iii.b
i.a/ii.a
ii.a
i.a/ii.a
ii.a
i.a/ii.a
ii.a
iii.b
i.a/ii.a
i.a/iii.b/ii.a

Facies associations: FA1a, FA1c, FA1a

Grain size scale: Clay | Silt | VF | F | M | C | VC | G | PEB.

HCS

IV

Lim02-11

32V 0569127
UTM 6658756

PMO-number	Thickness (m)	Lithology	Grain size, paleocurrent direction and sedimentary structures	Strike/dip	Facies	Facies associations

221.417

5 m

ii.a
iii.b — FA1b

HCS
HCS — i.a/ii.a

i.a/ii.b
i.a/ii.a
i.a/iii.b
i.a/ii.a — FA1a

iii.b/ii.a — FA1c

i.a/ii.a — FA1a

i.a/iii.b — FA1c

4 m

ii.a —
i.a/ii.a — FA1a

R. 1

ii.a
i.a

221.443

iii.b/ii.a/i.a — FA1c

HCS

i.a/ii.a
ii.a — FA1b

HCS

i.a/ii.a
iii.b — FA1a
i.a/ii.a

3 m

ii.a
ii.a/i.a — FA1b

iii.b/i.a
ii.a — FA1c
ii.a
iii.c

221.442

i.a/ii.a

i.a/ii.a
i.a/iii.b
iii.b/ii.a
i.a
ii.a — FA1a

i.a/ii.a

HCS
i.a/iii.b
ii.a
i.a/ii.a

2 m

ii.a/i.a — FA1b

i.a/ii.a/iii.b — FA1a

ii.a
iii.b
ii.a
ii.a
i.a — FA1b
ii.a
i.a/ii.a/iii.b

i.a/ii.a
iii.b/i.a — FA1a
ii.a/i.a

iii.c — FA1c

221.441

1 m

i.a

221.416

ii.a
iii.b
i.b/i.a — FA1b
ii.a
iii.b/i.a
ii.a/i.a
ii.a
iii.b

HCS

i.b — FA1a

0 m

i.a/ii.a

Clay | Silt | VF | F | M | C | VC | G | PEB.

V

Lim02-11

PMO-number	Thickness (m)	Lithology	Grain size, paleocurrent direction and sedimentary structures	Strike/dip	Facies	Facies associations

Lim02-11

PMO-number	Thickness (m)	Lithology	Grain size, paleocurrent direction and sedimentary structures	Strike/dip	Facies	Facies associations

Legend: Clay | Silt | VF | F | M | C | VC | G | PEB.

Lim02-11

PMO-number	Thickness (m)	Lithology	Grain size, paleocurrent direction and sedimentary structures	Strike/dip	Facies	Facies associations

VIII

Lim02-11

PMO–number	Thickness (m)	Lithology	Grain size, paleocurrent direction and sedimentary structures	Strike/dip	Facies	Facies associations

Facies column (top to bottom):

- ii.a
- iii.b
- i.a — FA1a
- iii.b/ii.a
- ii.a/i.a
- ii.a
- i.a/i.a
- ii.a/i.a
- iii.b — FA1b
- i.a/ii.a
- iii.b/ii.a
- ii.a/i.a
- iii.b
- ii.a/i.a
- i.a
- ii.a — FA1a
- i.a
- iii.b — FA1c
- i.a
- i.a/ii.a
- ii.a — FA1b
- iii.b — FA1c
- i.a/ii.a — FA1b
- i.a/iii.b
- i.a/ii.a — FA1a
- ii.a/iii.b — FA1b
- i.a/ii.a
- ii.a/iii.b
- iii.b
- i.a/ii.a
- iii.b — FA1c
- ii.a/iii.b
- iii.b
- i.a
- iii.b/ii.a
- i.a/ii.a — FA1a
- ii.a — FA1b
- i.a/ii.a

PMO-number: 221.450

Scale marks: 25 m, 24 m, 23 m, 22 m, 21 m, 20 m

Grain size scale: Clay | Silt | VF | F | M | C | VC | G | PEB.

IX

Lim02-11

PMO-number	Thickness (m)	Lithology	Grain size, paleocurrent direction and sedimentary structures	Strike/dip	Facies	Facies associations

Grain size scale: Clay | Silt | VF | F | M | C | VC | G | PEB.

Thickness markings: 30 m, 29 m, 28 m, 27 m, 26 m, 25 m

PMO-numbers: 221.422, 221.451

R. 4

R. 3

Facies labels: iii.c/ii.d, i.a, ii.d/iii.c, ii.d/iii.c, i.a, ii.d/iii.c, i.a, iii.c, iii.b/ii.a, ii.a/i.a, i.a/iii.b, i.a, iii.b, i.a, ii.a, i.a, ii.a, ii.a/i.a, i.a/ii.a, ii.b, i.a/ii.a, iii.b, i.a/ii.a, i.a/ii.a, ii.a

Facies associations: FA1c, FA1b, FA1a, FA1a, FA1b, FA1a, FA1b

X

Lim02-11

PMO-number	Thickness (m)	Lithology	Grain size, paleocurrent direction and sedimentary structures	Strike/dip	Facies	Facies associations
	35 m					
	34 m					
	33 m					
	32 m					
						FA1c
					i.a/iii.b	
						FA1a
					i.a/ii.a	
					i.a/iii.b	
	31 m				ii.a	
					i.a/iii.b	FA1c
					ii.a	
					i.a/iii.b	
						FA1c
					i.a/iii.b	
						FA1a
	30 m				ii.a	

Clay | Silt | VF | F | M | C | VC | G | PEB.

XI

Lim03-11

32V   0569048
UTM 6658823

PMO-number	Thickness (m)	Lithology	Grain size, paleocurrent direction and sedimentary structures	Strike/dip	Facies	Facies associations

Grain size scale: Clay | Silt | VF | F | M | C | VC | G | PEB.

Annotations within column: HCS, R. 4, R. 3

Facies labels (top to bottom): ii.a/i.a, iii.b, i.a, ii.a/i.a, i.a/ii.a, iii.b, ii.a, i.a/iii.b, i.a/ii.a, i.a/ii.a/iii.b, i.a/iii.b, iii.b, i.a/ii.a, iii.c, i.a/ii.a, ii.a, iii.b/i.a, i.a, iii.b, i.a/ii.a, iii.b/ii.a, i.a/ii.a, iii.b, i.a/ii.a, ii.a, i.a/ii.a/iii.b, i.a/ii.a, i.a/iii.b, ii.a, i.a/ii.a, i.a/iii.b/i.a, i.a/ii.a, ii.a/iii.b, i.a, ii.a/iii.b, i.a, ii.a/iii.b, i.a, ii.a, i.a/iii.b, i.a/ii.a, i.a/iii.b, ii.a, i.a, i.a, i.a/ii.a, ii.a, i.a/ii.a, i.a/ii.a, ii.a, i.a, iii.b

Facies associations (top to bottom): FA1b, FA1a, FA1c, FA1a, FA1c, FA1b, FA1a, FA1b, FA1a, FA1b, FA1a

XII

Lim03-11

32V 0569048
UTM 6658823

PMO-number	Thickness (m)	Lithology	Grain size, paleocurrent direction and sedimentary structures	Strike/dip	Facies	Facies associations

10 m

iii.b/i.a

9 m

ii.a

iii.b/i.a

iii.c

FA1c

iii.b/i.a

8 m

iii.c
iii.b/i.a
i.a/ii.a

iii.b/i.a

iii.b

i.a/iii.b
i.a
i.a/iii.b
i.a
iii.b

7 m

i.a/iii.b

i.a
iii.c
i.a/iii.b
i.a

i.a/iii.b

ii.a
i.a/ii.a
ii.a
iii.b
i.a
ii.b
i.a
iii.b

FA1b

6 m

HCS

i.a/ii.a

i.a/iii.b
i.a/ii.a
i.a/iii.b

i.a/ii.a
ii.a
i.a/ii.a
iii.b
i.a/ii.a
ii.a

FA1a

HCS

FA1b

5 m

Clay | Silt | VF | F | M | C | VC | G | PEB.

XIII

Bor01-11

32V 0569709
UTM 6660340

PMO-number	Thickness (m)	Lithology	Grain size, paleocurrent direction and sedimentary structures	Strike/dip	Facies	Facies associations
					ii.b	
221.453					i.a/ii.a	
					ii.a	
					iii.c	
					i.a/ii.a	
221.425					ii.a	
					i.a	
					ii.a	
					i.a/ii.a	
					ii.a	
					iii.c	
					i.a/ii.a	
					ii.a	
					ii.b	
					ii.a	
					i.b	
221.424				013/08		FA2
					ii.b	
					i.b	
					ii.b	
221.452					i.a	
					iii.c	
					ii.b	
					i.b	
					ii.a	
					i.a	
221.423					ii.b	
					ii.b	

Clay | Silt | VF | F | M | C | VC | G | PEB.

XIV

Bor01-11

PMO-number	Thickness (m)	Lithology	Grain size, paleocurrent direction and sedimentary structures	Strike/dip	Facies	Facies associations
	10 m					
	9 m				ii.b	
221.426						
221.455					i.a / ii.a	
221.454	8 m				iii.c	
	7 m				ii.b	FA2
	6 m				ii.b	
221.427					ii.a	
	5 m				ii.b	

Clay Silt VF F M C VC G PEB.

XV

Bor02-11

PMO-number	Thickness (m)	Lithology	Grain size, paleocurrent direction and sedimentary structures	Strike/dip	Facies	Facies associations
	5 m				ii.b	
					iii.c	
					ii.b	
	4 m					
					i.a	
221.457					iii.c	
	3 m				ii.b	FA2
					ii.a	
	2 m				ii.b	
221.456	1 m			013/12	i.a	
					iii.c	
					ii.b	
					i.a/ii.a	
	0 m				ii.b	

Clay | Silt | VF | F | M | C | VC | G | PEB.

XVI
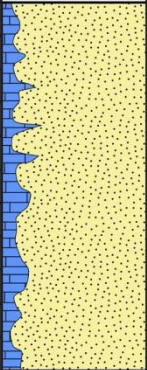
Bor02-11

PMO-number	Thickness (m)	Lithology	Grain size, paleocurrent direction and sedimentary structures	Strike/dip	Facies	Facies associations
	10 m					
	9 m					
	8 m					
	7 m					
	6 m					
					ii.b	FA2
	5 m					

Clay | Silt | VF | F | M | C | VC | G | PEB.

Åsa-11

32V   0572783
UTM   6667092

PMO-number	Thickness (m)	Lithology	Grain size, paleocurrent direction and sedimentary structures	Strike/dip	Facies	Facies associations
	5 m				ii.b	
					ii.a	
					ii.a	
					ii.a	
221.430					ii.a	
					ii.a	
					i.a	
	4 m				ii.b	
					ii.a/i.a	
	3 m			030/13	ii.b	
221.429						FA2
	2 m				ii.b/i.a	
221.428						
	1 m				ii.c	
221.458						
					ii.a	
					i.a/ii.a	
					ii.a	
					i.a/ii.a	
	0 m				ii.a/i.a	

Clay | Silt | VF | F | M | C | VC | G | PEB.

XVIII

Åsa-11

PMO-number	Thickness (m)	Lithology	Grain size, paleocurrent direction and sedimentary structures	Strike/dip	Facies	Facies associations
	10 m					
221.459	9 m			004/11	ii.b	
	8 m				ii.b	
				025/19	ii.a	
					ii.a/i.a	
221.431	7 m					FA2
	6 m				ii.b	
	5 m				ii.b	

Clay | Silt | VF | F | M | C | VC | G | PEB.

Grunn-11

PMO-number	Thickness (m)	Lithology	Grain size, paleocurrent direction and sedimentary structures	Strike/dip	Facies	Facies associations
	4 m					
	3 m					
	2 m					
	1 m					
221.440			HCS	052/35	ii.a	
					i.a/ii.a	
					i.a/ii.a	
					ii.a	
					i.a	FA1a
221.460					iii.b/ii.a	
					ii.a	
					i.a	
					i.a/ii.a	
221.439	0 m			043/45		

Clay | Silt | VF | F | M | C | VC | G | PEB.

XX

Tov-11

PMO-number	Thickness (m)	Lithology	Grain size, paleocurrent direction and sedimentary structures	Strike/dip Fault dis.	Facies	Facies associations

Sedimentary log showing lithology, grain size, paleocurrent, facies and facies associations for Tov-11.

Facies values from top to bottom: i.a/ii.a/iii.b (FA1b), i.a/iii.b, i.a/ii.a (FA1a), i.a/ii.a/iii.b (FA1c), i.a/ii.a, i.a/ii.a/iii.b, i.a/iii.b (FA1b), i.a/ii.a/iii.b, i.a/ii.a, i.a/iii.b/ii.d (FA1a)

Strike/dip: 240/64, 1m?

PMO-numbers: 221.564, 221.563, 221.561, 221.560, 221.562, 221.432

Facies associations: FA1b, FA1a, FA1c, FA1b, FA1a, FA3

Grain size scale: Clay, Silt, VF, F, M, C, VC, G, PEB.

XXI

Tov-11

PMO-number	Thickness (m)	Lithology	Grain size, paleocurrent direction and sedimentary structures	Strike/dip Fault dis.	Facies	Facies associations

Facies column (top to bottom):
- ii.a/i.a — FA1b
- i.a/ii.a
- i.a/iii.a
- ii.a
- i.a
- iii.b
- i.a
- iii.b
- ii.a/i.a
- i.a — FA1a
- ii.a
- i.a
- ii.a
- i.a/ii.a
- ii.a
- iii.b
- ii.a
- i.a/ii.a
- ii.a
- i.a/ii.a
- iii.b
- ii.a
- i.a/iii.b
- ii.a
- i.a/iii.b
- i.a/ii.a
- i.a/iii.b
- i.a/ii.a
- i.a/iii.b
- i.a/ii.a
- i.b
- ii.a
- i.a/iii.b
- ii.a/iii.b
- ii.a/i.a — FA1b
- ii.a/iii.b
- i.a/iii.b
- i.a/ii.a
- ii.a/iii.b
- i.a/ii.a

Strike/dip Fault dis.: ?

PMO-number: 221.433 (at 16 m)

Grain size scale: Clay | Silt | VF | F | M | C | VC | G | PEB.

Sedimentary structures labels: HCS

XXII

Tov-11

PMO-number	Thickness (m)	Lithology	Grain size, paleocurrent direction and sedimentary structures	Strike/dip Fault dis.	Facies	Facies associations
	35 m				ii.a	
					i.a/iii.b	
	34 m		HCS		i.a/ii.a	
	33 m				i.a/iii.a	
					i.a/ii.a	
	32 m			243/66	i.a/iii.a	
	31 m				ii.a	
	30 m				i.a/iii.a/ii.a	
	29 m					FA1a
					i.a/ii.a	
	28 m		HCS		ii.a	
					i.a	
	27 m				i.a/iii.a	
	26 m					
	25 m				i.a/ii.a	
	24 m					
	23 m					

Clay | Silt | VF | F | M | C | VC | G | PEB.

XXIII

Tov-11

PMO-number	Thickness (m)	Lithology	Grain size, paleocurrent direction and sedimentary structures	Strike/dip Fault dis.	Facies	Facies associations
					i.a	
					i.a/ii.a	
221.462	45 m				i.a/iii.b	
			Bryozo HCS		ii.a	
					i.a/ii.b	
					ii.b	
					i.a/ii.b	
					i.a/iii.b	
					i.a/ii.a	
					i.a/iii.b	
					i.a/ii.a	FA1a
					ii.a	
					i.a/ii.a	
221.464					i.a/iii.b	
221.461			HCS	1,7m	i.a/ii.a	
					i.a/ii.a	
					i.a/iii.b	
					i.a/ii.a	
	38 m				i.a/ii.a	
					i.a	
221.434					i.a/ii.a	
	36 m				i.a/iii.b	
					ii.a	
					i.a/iii.b	
	35 m				i.a/ii.a	

Clay | Silt | VF | F | M | C | VC | G | PEB.

XXIV

Tov-11

PMO-number	Thickness (m)	Lithology	Grain size, paleocurrent direction and sedimentary structures	Strike/dip Fault dis.	Facies	Facies associations

Grain size scale: Clay | Silt | VF | F | M | C | VC | G | PEB.

Facies column entries (top to bottom):
- ii.a/i.a
- ii.a/i.a
- ii.a
- ii.a/i.a
- i.a
- ii.a
- ii.a/i.a
- i.a/ii.a
- ii.a/i.a
- i.a/ii.a
- ii.a
- i.a/ii.a

Sedimentary structures: HCS

Strike/dip Fault dis.: 0,5m ; 240/80

Facies associations: FA1b ; FA1a

XXV

Tov-11

PMO-number	Thickness (m)	Lithology	Grain size, paleocurrent direction and sedimentary structures	Strike/dip Fault dis.	Facies	Facies associations

71 m

i.a/ii.a

i.a/ii.a

FA1a

70 m

ii.a/i.a

FA1b

69 m

68 m

ii.a/i.a

i.a/ii.a

ii.a/i.a

67 m

i.a/ii.a

ii.a

66 m

i.a/ii.a

65 m

i.a/ii.a

64 m

ii.a/i.a

221.436

ii.a/i.a

63 m

ii.a/i.a

62 m

ii.a/i.a

FA1b

61 m

ii.a/i.a

60 m

221.435

ii.a/i.a

59 m

ii.a

ii.a/i.a

FA1a

Clay | Silt | VF | F | M | C | VC | G | PEB.

XXVI

Tov-11

PMO-number	Thickness (m)	Lithology	Grain size, paleocurrent direction and sedimentary structures	Strike/dip Fault dis.	Facies	Facies associations

XXVII

Tov-11

PMO-number	Thickness (m)	Lithology	Grain size, paleocurrent direction and sedimentary structures	Strike/dip Fault dis.	Facies	Facies associations
					i.a/ii.a	
	95 m				i.a/iii.b	
			HCS		i.a/ii.a	
					i.a/iii.b	
221.567	94 m				i.a/ii.a	
					i.a/iii.b	
					i.a/ii.a	
					i.a/iii.b	
	93 m					
					i.a/ii.a	
	92 m			250/72	i.a/ii.b	
			~		i.a/ii.a	
	91 m					
					i.a/iii.b/ii.a	
	90 m					
						FA1a
	89 m			268/79	ii.a/i.a	
					i.a/ii.a	
	88 m				ii.a/i.a	
	87 m					
	86 m					
	85 m				ii.a	
					ii.a/i.a	
	84 m		~		i.a/ii.a	
					ii.a/i.a	
	83 m		≡		i.a/ii.a	

Clay | Silt | VF | F | M | C | VC | G | PEB.

XXVIII

Tov-11

32V 0574657
UTM 6643517

PMO-number	Thickness (m)	Lithology	Grain size, paleocurrent direction and sedimentary structures	Strike/dip Fault dis.	Facies	Facies associations

107 m

106 m

105 m

104 m

103 m

102 m

101 m — i.a/iii.b — FA1c

221.438 100 m — HCS — i.a/ii.a/iii.b — i.a/iii.b

HCS — i.a/ii.a — i.a/iii.b — i.a/ii.a

99 m — i.a/iii.b — i.a/ii.a

i.a/iii.b

98 m — i.a/ii.a — i.a/iii.b — i.a/ii.a — FA1a

221.465 — i.a/iii.b — i.a/ii.a — i.a/iii.b

97 m — i.a/ii.a — 0,8m — 251/55 — i.a/iii.b — i.a/ii.a/iii.b

HCS — i.a/iii.b — i.a/ii.a — i.a/iii.b

96 m — i.a/ii.a/iii.b

221.463 — HCS — HCS — i.a/ii.a/iii.b — i.a/ii.a

HCS — i.a/iii.b — i.a/ii.a

95 m — HCS

Clay | Silt | VF | F | M | C | VC | G | PEB.

XXIX

XXX

Appendix B

Log number:	Lim01-11, Lim02-11 and Lim03-11
Locality:	Limovnstangen
Geographical position:	Lim01-11; 0569121-6658770 to 0569121-6658770
	Lim02-11; 0569127-6658756 to 0569195-6658681
	Lim03-11; 0569048-6658823 to 0569048-6658823

Description of the outcrop: Three outcrops were logged at this locality which is located in an anticline fold. Log Lim01-11 (7,8m) was logged from a nearly vertical outcrop by the beach, where the log starts at the beach and ends were the vegetation covers the remaining outcrop. Log Lim02-11(31,7m) was logged by walking along the beach towards east. From 0m to 20m the rocks crop out from a cliff, the remaining part of the log was logged on the beach hence the holes in the log due to cover by beach rocks. Log Lim03-11 (10,1m) was logged on the west part of Limovnstangen, where rocks crop out from a small cliff. Sedimentary structures were easily recognizable at Lim01-11 and lower part of Lim02-11. The upper part of Lim02-11 is exposed to weathering and is covered by beach rock which made it harder to observe any structures. Due to moss sedimentary structures was harder to observe at Lim03-11.

Log number:	Bor01-11 and Bor02-11
Locality:	Borgen
Geographical position:	Bor01-11; 0569709-6660340
	Bor02-11; 0569714-6660317

Description of the outcrop: Two outcrops were logged at this locality which is a vertical cliff situated by the beach. Both of the logs (Bor01-11; 9,2m and Bor02-11; 6,1m) were logged by climbing up the outcrop. Sedimentary structures and lithology was easily observable at this locality.

Log number:	Åsa-11
Locality:	Åsaveien
Geographical position:	Åsa-11; 0572783-6667092 to 0572768-6667124

Description of the outcrop: The outcrop is situated along a road, where Åsa-11 (9,3m) was logged by walking alongside the road. Sedimentary structures were hard to observe due to weathering of the rocks.

Log number:	Grunn-11
Locality:	Grunntjern
Geographical position:	Grunn-11; 0573695-6668853

Description of the outcrop: The outcrop is located in a forest not far from a dirt road. The bedding of the outcrop has a 35-45 degrees dip. Log Grunn-11 (1,5m) was easily logged but

sedimentary structures were hard to observe due to growth of moss and weathering of the outcrop.

Log number:	Tov-11
Locality:	Toverud
Geographical position:	Tov-11; 0574669-6643419 to 0574657-6643517

Description of the outcrop: The rocks crop out along a dirt road, were the bedding is almost vertically. Log Tov-11 (102,2m) was logged by walking along the road. Several faults were observed in the outcrop and displacement of the faults was noted when possible. Sedimentary structures were difficult to observe due to growth of moss and algae, and weathering of the outcrop. Some of the outcrop was also covered by rocks due to rockslide from the area above.

XXXIV

Appendix C

Appendix C: Paleocurrent measurements of symmetric ripples, asymmetric ripples, cross-bedding, trough cross-bedding, gutter casts and cephalopods.

Log	Lim01 - 11			
Height (m)	**Type**	**Paleocurrent**	**Wavelength (cm)**	**Amplitude (cm)**
0,2	Symmetrical ripple	110-290	N/A	N/A
2,6	Symmetrical ripple	148-328	N/A	N/A
2,65	Symmetrical ripple	150-330	N/A	N/A
3,95	Gutter cast	34-214	(-)	(-)
4,05	Symmetrical ripple	131-311	N/A	N/A
4,53	Symmetrical ripple	180-0	N/A	N/A
4,55	Symmetrical ripple	185-5	N/A	N/A
5,3	Asymmetric ripple	318	(-)	(-)
6,08	Symmetrical ripple	200-20	N/A	N/A
6,4	Symmetrical ripple	195-15	N/A	N/A
6,45	Symmetrical ripple	210-30	N/A	N/A

Log	Lim02 - 11			
Height (m)	**Type**	**Paleocurrent**	**Wavelength (cm)**	**Amplitude (cm)**
0,8	Gutter cast	50-230	(-)	(-)
1,05	Cross -bedding	50	(-)	(-)
1,15	Cross –bedding	221	(-)	(-)
1,45	Gutter cast	106-286	(-)	(-)
1,65	Symmetrical ripple	184-4	12	1,5
1,85	Symmetrical ripple	110-290	13,5	1
2,05	Gutter cast	268-88	(-)	(-)
2,85	Symmetrical ripple	109-289	42	2,5
3,9	Symmetrical ripple	111-291	N/A	N/A
3,9	Gutter cast	27-207	(-)	(-)
5,35	Symmetrical ripple	110-290	N/A	N/A
5,6	Symmetrical ripple	97-277	N/A	N/A
5,7	Symmetrical ripple	141-321	N/A	N/A
6,4	Symmetrical ripple	125-305	110	35
6,58	Symmetrical ripple	131-311	15	0,8
7,45	Symmetrical ripple	92-272	17	0,8
7,75	Symmetrical ripple	141-321	20	0,9
7,9	Symmetrical ripple	103-283	32	1
8,23	Symmetrical ripple	123-303	N/A	N/A
8,7	Symmetrical ripple	146-326	16	1,4
8,9	Symmetrical ripple	110-290	14	1
9,68	Symmetrical ripple	137-317	N/A	N/A
9,8	Gutter cast	81-261	(-)	(-)
10,43	Asymmetrical ripple	303	10	0,9
10,7	Gutter cast	63-243	(-)	(-)
10,9	Symmetrical ripple	94-274	N/A	N/A
11,2	Symmetrical ripple	137-317	14	1

Height (m)	Type	Paleocurrent	Wavelength (cm)	Amplitude (cm)
11,65	Gutter cast	81-261	(-)	(-)
11,75	Symmetrical ripple	129-309	14	0,8
12,05	Symmetrical ripple	161-341	N/A	N/A
12,4	Symmetrical ripple	112-292	77	3,1
12,6	Symmetrical ripple	112-292	60	2,9

Log		Lim03 - 11		
Height (m)	Type	Paleocurrent	Wavelength (cm)	Amplitude (cm)
1,9	Symmetrical ripple	152-332	74	4,5
2,2	Gutter cast	29-209	(-)	(-)
4,65	Symmetrical ripple	111-291	54	3
4,8	Symmetrical ripple	148-328	12	0,9

Log		Bor01-11		
Height (m)	Type	Paleocurrent	Wavelength (cm)	Amplitude (cm)
0,9	Symmetrical ripple	161-341	15	0,8
1	Trough cross-bedding	281	(-)	(-)
1,5	Trough cross-bedding	288	(-)	(-)
1,78	Symmetrical ripple	138-318	16	0,8
2,2	Trough cross-bedding	310	(-)	(-)
3,18	Symmetrical ripple	187-367	80	14
3,4	Trough cross-bedding	311	(-)	(-)
3,52	Symmetrical ripple	129-309	19	1,2
4,05	Symmetrical ripple	148-328	16	1
4,35	Symmetrical ripple	155-335	15	1
4,6	Symmetrical ripple	126-306	11	0,8
4,8	Trough cross-bedding	321	(-)	(-)
6	Trough cross-bedding	272	(-)	(-)
7,1	Trough cross-bedding	313	(-)	(-)
8,15	Symmetrical ripple	125-305	8	0,6

Log		Bor02-11		
Height (m)	Type	Paleocurrent	Wavelength (cm)	Amplitude (cm)
0,35	Symmetrical ripple	144-324	13	2,5
1	Symmetrical ripple	123-303	N/A	N/A
1,05	Symmetrical ripple	80-260	N/A	N/A
1,18	Symmetrical ripple	121-301	N/A	N/A
1,6	Trough cross-bedding	309	(-)	(-)
3	Trough cross-bedding	339	(-)	(-)
3,7	Gutter cast	112-292	(-)	(-)
4,9	Cephalopod	270	(-)	(-)
4,91	Cephalopod	287	(-)	(-)
5,4	Trough cross-bedding	288	(-)	(-)

Log	Åsa-11			
Height (m)	**Type**	**Paleocurrent**	**Wavelength (cm)**	**Amplitude (cm)**
1,7	Trough cross-bedding	260	(-)	(-)
2,2	Trough cross-bedding	345	(-)	(-)
2,4	Trough cross-bedding	186	(-)	(-)
9,2	Trough cross-bedding	290	(-)	(-)

Log	Tov-11			
Height (m)	**Type**	**Paleocurrent**	**Wavelength (cm)**	**Amplitude (cm)**
64,2	Gutter cast	55	(-)	(-)
66	Symmetrical ripple	307	N/A	N/A
96,9	Symmetrical ripple	311	N/A	N/A

Appendix D

Appendix D: Results from point counting of thin sections. Lim. Mbr. = Limovnstangen Member, Djup. Mbr. = Djupvarp Member, S.S. Mbr. = Store Svartøya Member, S. Mbr. = Sylling Member, Lang. Fm. = Langøyene Formation. The polycrystalline/undulating quartz is enclosed in brackets in the Quartz-column.

Loc.	PMO-number	Level (m)	Fm./Mbr.	Quartz (%)	Calcite (%)	K-feldspar (%)	Mica (%)	Plagioclase (%)	Fossil fragments (%)	Pyrite (%)	Limonite (%)	Opaque minerals (%)
Limovnstangen	221.416	0,85	Lim. Mbr.	54,0 (8,0)	37,5	5,8	1,8	0,5	0,0	0,0	0,0	0,5
	221.417	4,95	Lim. Mbr.	36,0 (6,5)	57,0	6,8	0,0	0,3	0,0	0,0	0,0	0,0
	221.418	7,55	Lim. Mbr.	15,0 (1,3)	80,5	2,5	0,5	0,3	0,0	0,0	0,8	0,5
	221.419	12,9	Lim. Mbr.	30,3 (3,0)	60,3	6,3	0,0	0,5	1,8	0,0	0,0	1,0
	221.420	17,8	Lim. Mbr.	26,8 (3,3)	67,5	5,0	0,3	0,3	0,3	0,0	0,0	0,0
	221.421	19,9	Lim. Mbr.	55,0 (1,8)	32,0	9,5	1,5	1,3	0,3	0,0	0,3	0,3
	221.422	27,8	Lim. Mbr.	24,8 (3,3)	68,8	4,8	0,0	0,3	1,0	0,5	0,0	0,0
Borgen	221.423	0,7	Djup. Mbr.	54,4 (2,5)	32,2	7,6	0,0	0,3	5,1	0,0	0,5	0,0
	221.424	2,58	Djup. Mbr.	71,8 (4,3)	18,0	8,3	0,0	0,3	0,0	0,0	0,5	1,3
	221.425	3,98	Djup. Mbr.	61,9 (2,8)	26,8	6,0	0,5	0,0	0,0	0,0	4,0	0,8
	221.426	8,6	Djup. Mbr.	62,6 (4,0)	28,7	5,7	0,5	0,5	0,2	0,0	0,5	1,2
	221.427	5,5	Djup. Mbr.	65,3 (6,8)	18,3	10,3	0,0	0,5	0,0	0,3	3,0	2,5
Åsaveien	221.428	1,35	Djup. Mbr.	63,3 (4,3)	20,0	11,8	0,3	1,3	0,0	0,0	0,0	3,5
	221.429	2,55	Djup. Mbr.	69,8 (6,5)	2,0	16,0	0,3	0,5	0,3	0,0	2,5	8,8
	221.430	4,45	Djup. Mbr.	58,0 (4,0)	30,0	6,8	1,3	1,0	0,0	0,3	0,0	2,8
	221.431	7,2	Djup. Mbr.	37,3 (2,0)	49,0	4,3	0,3	1,0	2,8	0,0	3,3	2,3
Toverud	221.432	0	S. Mbr.	29,3 (5,8)	52,5	2,8	0,0	0,3	0,3	14,8	0,0	0,3
	221.433	15,9	S. Mbr.	36,3 (2,0)	59,3	3,5	0,5	0,0	0,0	0,3	0,0	0,3

XL

	221.434	36,5	S. Mbr.	55 (5,5)	32,8	9,8	0,3	0,3	0,0	0,5	0,0	1,5
	221.435	59,9	Djup. Mbr.	69,5 (3,0)	6,5	9,5	0,5	0,0	0,0	0,0	8,8	5,3
	221.436	63,4	Djup. Mbr.	70,1 (4,5)	13,4	8,5	0,0	0,2	0,2	0,0	6,2	1,2
	221.437	79,4	Lim. Mbr.	50,5 (4,5)	40,0	4,8	0,3	0,8	0,3	0,3	0,5	2,8
	221.438	100,2	Lim. Mbr.	5,8 (0,3)	84,5	1,0	0,0	0,3	4,0	1,0	4,0	0,0
Grunn-tjern	221.439	-0,25	Lang. Fm	2,3 (0,0)	91,5	0,0	0,0	0,0	6,3	0,0	0,0	0,0
	221.440	1,48	S.S. Mbr.	8,0 (0,0)	83,5	0,3	0,0	0,0	5,5	0,0	1,8	1,0

XLII

Appendix E

Appendix E: Results of the quartz/feldspar ratio of thin sections. Lim. Mbr. = Limovnstangen Member, Djup. Mbr. = Djupvarp Member, S. Mbr. = Sylling Member.

Loc.	PMO-number	Level (m)	Fm./Mbr.	Q/F-ratio
Limovnstangen	221.416	0,85	Lim. Mbr.	9
	221.417	4,95	Lim. Mbr.	5
	221.418	7,55	Lim. Mbr.	5
	221.419	12,9	Lim. Mbr.	4
	221.420	17,8	Lim. Mbr.	5
	221.421	19,9	Lim. Mbr.	5
	221.422	27,8	Lim. Mbr.	5
Borgen	221.423	0,7	Djup. Mbr.	7
	221.424	2,58	Djup. Mbr.	8
	221.425	3,98	Djup. Mbr.	10
	221.426	8,6	Djup. Mbr.	10
	221.427	5,5	Djup. Mbr.	6
Åsaveien	221.428	1,35	Djup. Mbr.	5
	221.429	2,55	Djup. Mbr.	4
	221.430	4,45	Djup. Mbr.	7
	221.431	7,2	Djup. Mbr.	7
Toverud	221.432	0	S. Mbr.	10
	221.433	15,9	S. Mbr.	10
	221.434	36,5	S. Mbr.	6
	221.435	59,9	Djup. Mbr.	7
	221.436	63,4	Djup. Mbr.	8
	221.437	79,4	Lim. Mbr.	9
	221.438	100,2	Lim. Mbr.	5

Appendix F

Appendix F: Results from point counting of acetate peels. Lim. Mbr. = Limovnstangen Member, Djup. Mbr. = Djupvarp Member, S.S. Mbr. = Store Svartøya Member.

Loc.	PMO-number	Level (m)	Mbr.	Unidentified grains (%)	Calcite matrix (%)	Brachiopod Spines (%)	Brachiopods (%)	Bryozoans (%)	Trilobites (%)	Crinoids (%)	Undetermined Bioclasts (%)	Corals (%)	Micrite (%)	Gastropods (%)	Intraclasts (%)
Limovnstangen	221.441	1,15	Lim. Mbr.	0,8	69,0	0,5	5,5	11,6	5,3	4,1	3,0	0,0	0,0	0,0	0,2
	221.442	2,7	Lim. Mbr.	3,4	75,9	0,2	5,6	9,9	1,2	2,0	1,5	0,0	0,0	0,0	0,2
	221.443	3,6	Lim. Mbr.	58,5	27,9	0,0	6,2	3,5	1,2	2,3	0,5	0,0	0,0	0,0	0,0
	221.444	6,4	Lim. Mbr.	1,0	75,0	0,0	6,4	8,1	3,1	3,6	1,0	0,0	0,0	0,0	1,7
	221.445	7,6	Lim. Mbr.	23,2	55,2	0,0	2,5	7,9	3,3	6,2	1,7	0,0	0,0	0,0	0,0
	221.446	10,2	Lim. Mbr.	38,1	51,2	0,4	1,6	3,5	2,4	2,2	0,4	0,0	0,0	0,0	0,0
	221.447	11,7	Lim. Mbr.	26,0	55,4	0,2	1,0	15,7	1,0	0,5	0,0	0,0	0,0	0,0	0,0
	221.448	12,5	Lim. Mbr.	13,7	60,2	0,4	5,1	14,3	2,8	2,4	1,1	0,0	0,0	0,0	0,0
	221.449	16,45	Lim. Mbr.	23,4	44,6	0,0	11,2	9,5	1,3	0,0	0,5	2,8	0,0	0,0	6,7
	221.450	20,4	Lim. Mbr.	51,4	31,6	0,1	8,1	4,2	2,5	2,0	0,0	0,0	0,0	0,0	0,0
	221.451	26,9	Lim. Mbr.	0,6	74,5	0,3	12,5	8,4	0,9	2,3	0,3	0,0	0,0	0,0	0,3
Åsaveien	221.458	0,7	Djup. Mbr.	50,3	37,8	0,0	3,0	2,7	1,2	0,0	0,3	0,0	0,0	4,0	0,6
	221.459	9,15	Djup. Mbr.	68,7	18,7	0,0	4,4	4,4	0,3	1,7	0,4	0,3	0,0	0,0	1,2
Toverud	221.562	6,5	S.S. Mbr.	14,3	46	0,5	8,2	0,0	0,0	0,5	1,8	1,5	27,1	0,0	0,0
	221.560	6,7	S.S. Mbr.	6,0	67,8	3,1	6,7	3,4	0,0	2,5	1,3	0,9	8,3	0,0	0,0
	221.561	7,1	S.S. Mbr.	25,3	39,8	0,5	5,0	0,3	0,0	0,6	0,1	0,6	27,8	0,0	0,0

XLVI

	221.563	7,2	S.S. Mbr.	17,3	67,3	0,5	2,9	0,0	0,0	0,6	0,0	0,0	10,8	0,0	0,4
	221.564	7,3	S.S. Mbr.	18,7	69,6	0,3	5,3	0,1	0,0	0,0	0,9	0,0	4,2	0,0	1,0
	221.461	39,25	S.S. Mbr.	9,5	43,4	0,0	5,0	6,3	0,0	8,0	2,0	0,0	25,9	0,0	0,0
	221.464	39,5	S.S. Mbr.	21,4	32,6	0,0	3,1	5,5	0,0	1,8	2,2	0,0	33,3	0,0	0,0
	221.462	45,2	S.S. Mbr.	9,7	61,9	0,3	3,3	4,5	0,6	1,8	0,9	0,0	16,9	0,0	0,0
	221.566	79,55	Lim. Mbr	14,2	76,5	0,0	0,9	0,9	0,0	0,0	0,3	0,0	7,1	0,0	0,0
	221.565	82,25	Lim. Mbr	1,2	77,2	0,0	11,3	4,0	3,1	1,5	0,4	0,0	1,3	0,0	0,0
	221.567	94,1	Lim. Mbr	37,7	50,1	0,0	1,9	1,2	0,0	0,0	0,5	0,0	2,9	0,2	5,4
	221.463	95,6	Lim. Mbr	3,7	57,4	0,9	4,3	3,9	0,7	12,6	1,3	0,0	14,8	0,0	0,4
	221.465	97,4	Lim. Mbr	11,6	59,9	1,2	4,1	5,1	0,5	10,1	1,2	0,0	6,3	0,0	0,0
Grunn-tjern	**221.460**	0,3	S.S. Mbr.	19,2	25,1	0,0	4,6	4,6	0,0	6,7	1,0	0,0	38,7	0,0	0,0
Borgen	**221.452**	1,12	Djup. Mbr.	14,1	56,6	0,0	4,3	15,8	0,3	6,6	0,3	0,0	1,7	0,0	0,3
	221.453	4,3	Djup. Mbr.	7,9	66,6	0,0	1,3	20,9	0,1	0,1	0,3	0,0	1,9	0,0	0,7
	221.454	8	Djup. Mbr.	54,5	24,2	0,0	6,7	2,9	0,0	0,1	0,6	8,6	1,6	0,0	0,7
	221.455	8,2	Djup. Mbr.	55,7	17,1	0,0	0,2	1,7	0,0	0,2	0,0	0,0	24,9	0,0	0,0
	221.456	1,05	Djup. Mbr.	14,6	45,9	0,0	2,5	20,1	0,0	13,8	0,1	0,0	1,6	0,0	1,3
	221.457	3,55	Djup. Mbr.	26,7	37,9	0,0	6,5	16,2	0,0	11,4	0,6	0,1	0,4	0,0	0,2

Appendix G

Appendix G: Overview of the observed trace fossils from field.

| Locality	Log	Depth (m)	Plate	Orientation
Limovnstangen	Lim01-11	2,6	1A	Top of bed
	Lim01-11	3,05	1B	Base of bed
	Lim01-11	3,12	1C	Base of bed
	Lim02-11	0,9	2A	Cross section of bed
	Lim02-11	3,46	2B	Top of bed
	Lim02-11	11,75	2C	Base of bed
	Lim02-11	11,75	2D	Base of bed
	Lim02-11	18,5	3A	Base of bed
	Lim02-11	19,9	3B	Base of bed
	Lim02-11	19,9	3C	Top of bed
	Lim02-11	20,93	3D	Top of bed
	Lim02-11	21,12	4A	Top of bed
	Lim02-11	28,55	4B	Top of bed
	Lim02-11	0 - 13	4C	Top of bed
	Lim02-11	0 - 13	4D	Top of bed
	Lim02-11	0 - 13	5A	Top of bed
	Lim02-11	0 - 13	5B	Top of bed
	Lim02-11	0 - 13	5C	Top of bed
	Lim02-11	0 - 13	5D	Top of bed
	Lim02-11	0 - 13	6A	Cross section of bed
	Lim02-11	0 - 13	6B	Top of bed
	Lim02-11	0 - 13	6C	Top of bed
	Lim02-11	0 - 13	6D	Top of bed
	Lim02-11	0 - 13	6E	Top of bed
Borgen	Bor01-11	0,25	7A	Base of bed
Åsaveien	Åsa-11	0,08	7B	Base of bed
Toverud	Tov-11	57,8	7C	Base of bed
	Tov-11	57,8	7D	Top of bed
	Tov-11	67,5	8A	Top of bed
	Tov-11	72,3	8B	Top of bed

L
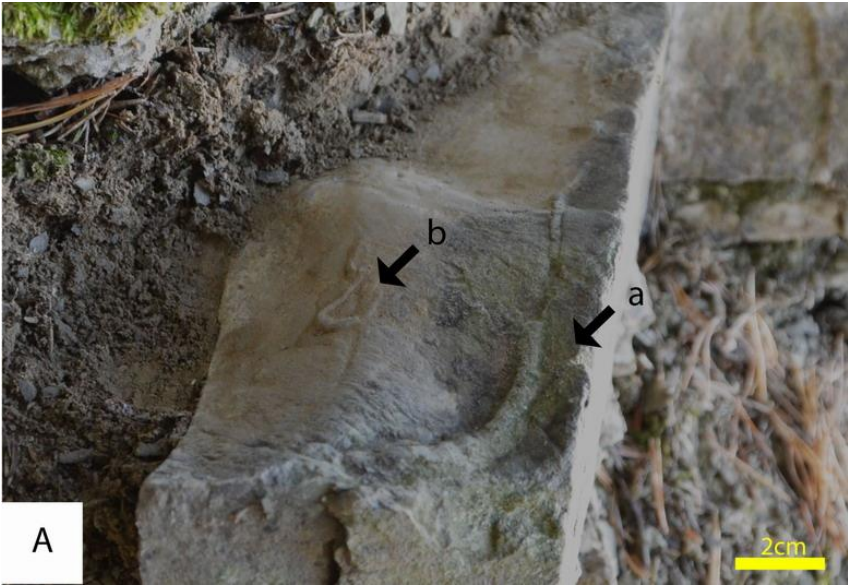
Plate 1

Plate 1A:
a) Palaeophycus
b) Palaeophycus

Plate 1B:
a) Palaeophycus
b) Palaeophycus

Plate 1C:
a) Palaeophycus

Plate 2

Plate 2A: a) Escape structure

Plate 2C: a) Palaeophycus

Plate 2B: a) Palaeophycus

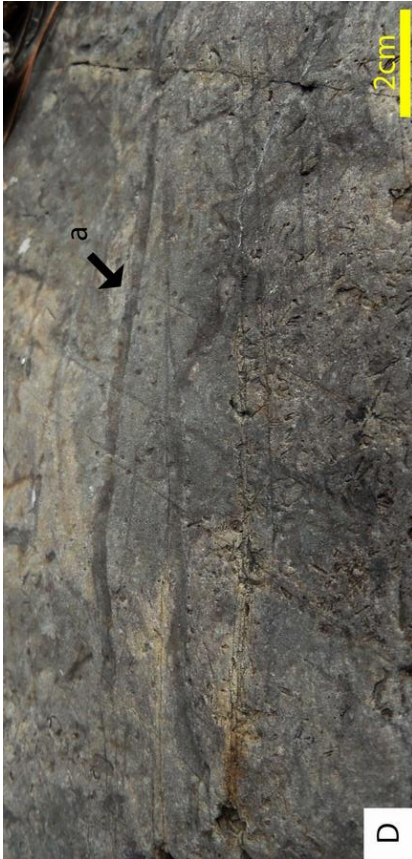Plate 2D: a) Palaeophycus

Plate 3

Plate 3C: a) Palaeophycus

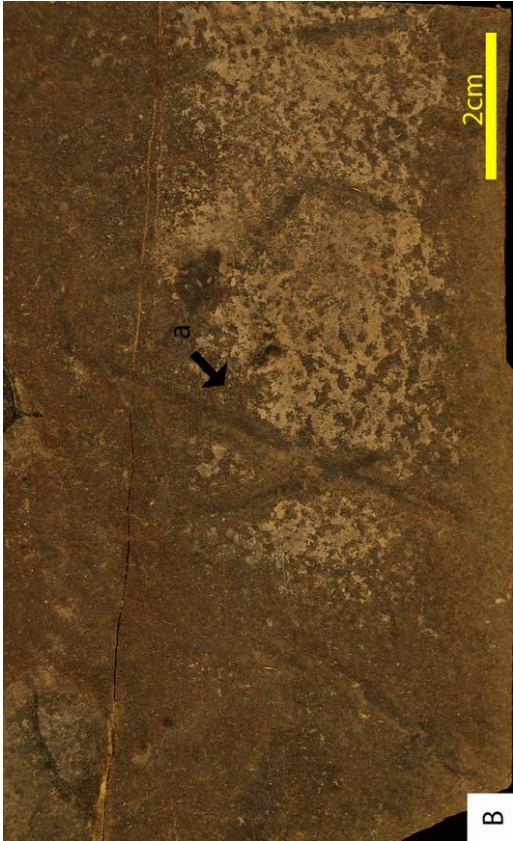Plate 3D: a) Horizontal burrowing

Plate 3A: a) Chondrites, b) Chondrites

Plate 3B: a) Horizontal burrowing

Plate 4

Plate 4C: a) Palaeophycus

Plate 4D: a) Palaeophycus

Plate 4A: a) Vertical burrowing

Plate 4B: a) Chondrites, b) Horizontal burrowing

Plate 5

Plate 5C: a) Palaeophycus

Plate 5D: a) Palaeophycus

Plate 5A: a) Palaeophycus

Plate 5B: a) Palaeophycus

Plate 6

Plate 6A: a) Escape structure

Plate 6B: a) Palaeophycus, b) Vertical burrowing

Plate 6C: a) Palaeophycus

Plate 6D: a) Chondrites

Plate 6E: a) Chondrites

Plate 7

Plate 7A: a) Palaeophycus
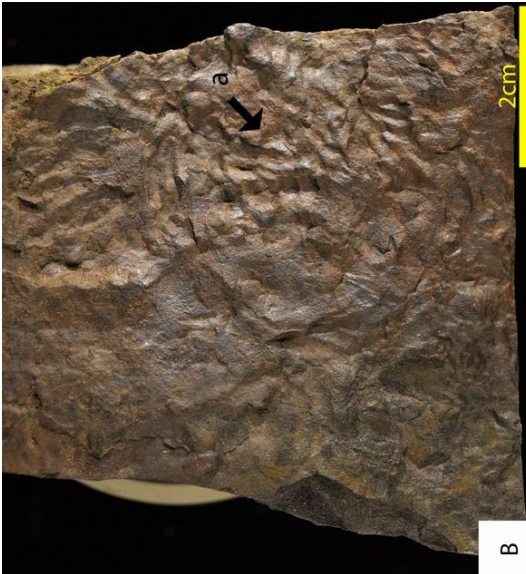
Plate 7B: a) Chondrites

Plate 7C: a) Chondrites

Plate 7D: a) Palaeophycus

Plate 8

Plate 8A: a) Palaeophycus

Plate 8B: a) Palaeophycus, b) Palaeophycus

Appendix H

Terminology of the members in the Sælabonn Formation

Table 1: Overview of the different terminology used for the members in the Sælabonn Formation in Ringerike and Modum districts.

Reference:	Thomsen (1982)	Thomsen et al. (2006)	Baarli (1988)
Districts (Fig.2.1)	*Ringerike District*		*Modum District*
Upper member	Limovnstangen	Steinsåsen	Limovnstangen
Middle member	Djupvarp	Djupvarp	Djupvarp
Lower member	Store Svartøya	Store Svartøya	Sylling

Kiær divided stage 6, which was later defined as the Sælabonn Formation, into three sub-stages (6a, 6b and 6c) (Worsley et al., 1983, Braithwaite et al., 1995). Thomsen (1982) revised this by giving lithostratigraphical names to the sub-stages. Thomsen et al. (2006) erected a new name for the upper member, Steinsåsen Member, but did not give any arguments about why they changed the name from her earlier article (Table 1) (Limovnstangen Member in Thomsen, 1982). According to NGU (2012) Rytteråker and Limovnstangen formations are synonyms, which is the most likely explanation for the change in name of the upper member of the Sælabonn Formation by Thomsen et al. (2006). The Rytteråker Formation is a well-recognized name used in the scientific community for this unit. The terminology used for the upper and middle members by Baarli (1988) in the Modum Districts is the same as used by Thomsen (1982) in the Ringerike District. They have the same characteristics; increased input of siliciclastic material in the middle member and thin to medium thick beds of sandstone and limestone in the upper member. The Sylling Member is however defined as the lower member, as it does not display the same lithological characteristics as the Solvik Formation in the Oslo-Asker District, or the Store Svartøya Member in the Ringerike District (Baarli, 1988). These three members (Djupvarp, Store Svartøya and Sylling) are defined in the database by NGU (2012), but they are, however, not included into the description of the Sælabonn Formation. The database refers only to three informal members; *"possible to divided into three informal members in many areas"*. A revision of the database regarding the information of the Sælabonn Formation is suggested. Regarding the "Limovnstangen Formation", the name should be demoted to the upper member of the Sælabonn Formation. The name "Limovnstangen" will thereby refer to a well exposed and protected locality where a representative outcrop of the upper member of the Sælabonn Formation is present.

LX

Appendix I

| m | LITH | mm φ | SHEET | OF | DATE: | SCALE: |

m	LITH	mm φ ǀ CLAY ǀ Si ǀ VF ǀ F ǀ M ǀ C ǀ VC ǀ G ǀ PEB.
25		

CLAY SILT VF F M C VC G PEB.

LXII